Assessing the Cypress Sandstone for Carbon Dioxide-Enhanced Oil Recovery and Carbon Storage: Part I—Reservoir Characterization of Noble Oil Field, Western Richland County, Illinois

Nathan D. Webb and Nathan P. Grigsby

Illinois State Geological Survey, Prairie Research Institute, University of Illinois at Urbana-Champaign

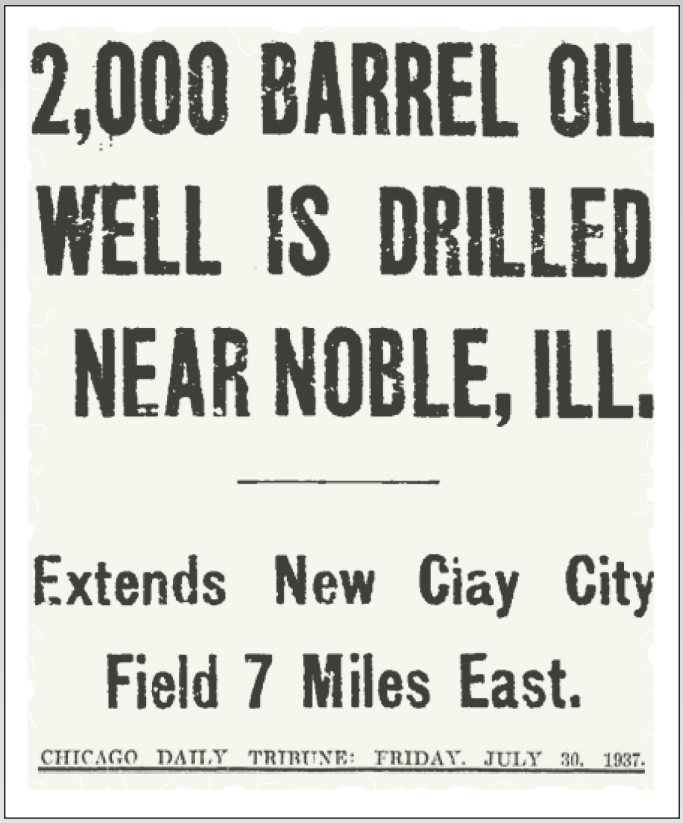

2,000 BARREL OIL WELL IS DRILLED NEAR NOBLE, ILL.

Extends New Clay City Field 7 Miles East.

CHICAGO DAILY TRIBUNE: FRIDAY, JULY 30, 1937.

Circular 601 2020

ILLINOIS STATE GEOLOGICAL SURVEY
Prairie Research Institute
University of Illinois at Urbana-Champaign

ILLINOIS
Illinois State Geological Survey
PRAIRIE RESEARCH INSTITUTE

Front cover: *Headline in the Chicago Daily Tribune, July 30, 1937.*

Assessing the Cypress Sandstone for Carbon Dioxide-Enhanced Oil Recovery and Carbon Storage: Part I—Reservoir Characterization of Noble Oil Field, Western Richland County, Illinois

Nathan D. Webb and Nathan P. Grigsby

Illinois State Geological Survey, Prairie Research Institute, University of Illinois at Urbana-Champaign

Circular 601 2020

ILLINOIS STATE GEOLOGICAL SURVEY
Prairie Research Institute
University of Illinois at Urbana-Champaign
615 E. Peabody Drive
Champaign, Illinois 61820-6918
http://www.isgs.illinois.edu

ILLINOIS
Illinois State Geological Survey
PRAIRIE RESEARCH INSTITUTE

Suggested citation:
Webb, N.D., and N.P. Grigsby, 2020, Assessing the Cypress Sandstone for carbon dioxide-enhanced oil recovery and carbon storage: Part I—Reservoir characterization of Noble Oil Field, western Richland County, Illinois: Illinois State Geological Survey, Circular 601, 53 p.

Contents

Tables

Figures

ABSTRACT

Noble Oil Field, located in southwestern Richland County, Illinois, has a cumulative production of 46 million barrels of oil (MMBO; 257.8 million ft^3, or 7.3 million m^3). Approximately 50% of this production is derived from a relatively thin oil reservoir that occurs in a thick (up to 165 ft, or 50 m), fluvial valley-fill sandstone within the Mississippian Cypress Sandstone. Attempts at production from such reservoirs are susceptible to early onset of high produced water and low recovery efficiencies (25%, in the case of Noble Field). As such, these reservoirs have the potential for nonconventional carbon dioxide (CO_2)-enhanced oil recovery (EOR), meaning EOR that includes geologic storage of CO_2 as a significant component of the process.

Reservoir characterization of the thick valley-fill sandstone within the Cypress Sandstone has shown that it is multistory and fluvial. Where multiple stories amalgamate (as in Noble Field), they create thick, relatively widespread sandstone bodies that have characteristics favorable for CO_2 storage, such as high lateral and vertical permeability, limited compartmentalization, and large pore volumes. More than 75 MMBO (423.8 million ft^3, or 12 million m^3) is estimated to remain in the reservoir, of which 30.7 to 46.2 MMBO (172.3 to 259.6 million ft^3, or 4.88 to 7.35 million m^3) is estimated to be moveable. A residual oil zone may also exist in the field, based on a southwesterly tilted oil–water contact and the occurrence of a persistent, parallel calcite-cemented zone beneath the oil–water contact. A better understanding of these rocks is needed, given the economic importance of the remaining oil resource in the Cypress Sandstone at Noble Field and its potential as a sink for anthropogenic CO_2.

INTRODUCTION

Almost one-third of the more than 3.5 (billion barrels of oil (21.2 billion ft^3, or 0.6 billion m^3) produced in Illinois is from the Chesterian (upper Mississippian) Cypress Sandstone (Huff and Seyler 2010). Most Cypress oil production is from compartmentalized, heterogeneous northeast–southwest-oriented sandstone lenses that have been interpreted as tidal bars (Grube 1992; Whitaker and Finley 1992; Xu and Huff 1995). However, sandstone bodies exceeding 165 ft (50 m) in thickness, interpreted as part of an incised valley-fill system (Nelson et al. 2002), are also a source of oil production. These valley-fill Cypress sandstones, commonly referred to as the "thick," "massive," or "lower" Cypress, as well as eroded older deposits of the Cypress Sandstone and underlying formations, occupy a northeast–southwest-trending fairway that crosses the central part of the Illinois Basin (hereafter, the Basin).

Oil reservoirs in valley-fill Cypress deposits are relatively thin with respect to their host sandstone, and they exhibit low primary oil recovery because of the early onset of water coning (i.e., bottom water infiltration of the perforation zone in the near-wellbore area that reduces oil production) and excessive water management issues. As a result, such reservoirs are presently underproduced oil resources in the Basin. In addition to the relatively thin oil reservoirs developed in their tops, the valley-fill Cypress potentially has residual oil zones (ROZs) underlying the reservoir.

In this study, we focused on characterizing the Cypress Sandstone reservoir at Noble Field in Richland County, Illinois, which is the most productive valley-fill Cypress oil field in the Basin. Approximately half of the cumulative oil production from the field is attributed to the Cypress Sandstone (with the remainder attributed to commingled production from older formations). As part of the reservoir characterization, we examined the geology of the valley-fill Cypress, its historical oil production, and characteristics of the oil reservoir.

This contribution is part of a research project to assess the valley-fill Cypress for the presence of ROZs and the potential for nonconventional carbon dioxide (CO_2)-enhanced oil recovery (EOR), meaning CO_2-EOR that includes geologic storage of CO_2 as a significant component of the process. This study also provides the foundation for future geocellular modeling and reservoir simulations of nonconventional CO_2-EOR within the Cypress Sandstone at Noble Field. Additionally, we have documented the process of using indirect indicators to identify a possible ROZ. These results will serve as an analog for characterizing the geological parameters relevant to improving oil production from similar deposits elsewhere in the Basin.

DISCOVERY OF NOBLE FIELD

In the early 1900s, large oil fields were discovered in southeastern Illinois and were later developed (Blatchley 1913). However, as subsequent exploration moved into the central part of the Basin, brine was encountered at reservoir depths (e.g., in Crawford and Lawrence Counties at depths of 750 to 2,000 ft, or 229 to 609.6 m), and interest in developing the area stagnated (Wasson 1938). Pure Oil Company initiated reconnaissance of the Illinois Basin in 1927, and the company's east–west regional log cross section and subsequent torsion-balance survey in 1930 indicated a structural feature in the area of Noble in western Richland County, Illinois. A seismic reflection survey in 1935–1936 confirmed that this feature was a major anticline (Wasson 1938). In early literature, this structure was referred to as the Noble or Basin anticline, but it is now recognized as the Clay City Anticline (Nelson 1995). The Ohio Oil Company eventually discovered Noble Field in July 1937 (Bell 1938) underlying the village of Noble (Figure 1). Because of continuous development along the Clay City Anticline since the 1940s, Noble Field is now adjoined by oil fields to the northeast and southwest and is considered part of the Clay City Consolidated Oil Field.

The discovery well, Arbuthnot 1 (API 121590012100, NW¼NW¼ sec. 8, T3N, R9E), had an initial oil production of 2,500 barrels (bbl; 14,037.6 ft^3, or 397.5 m^3). Production was from the "McClosky" oolite ("McClosky" being an informal term for oil reservoirs in the Fredonia Limestone Member; Figure 2), which remained the preliminary target in Noble Field and in adjacent fields on the Clay City Anticline. Although the "McClosky" proved to be a prolific oil producer, oil-bearing sandstones were also noted in the "basal Chester" interval, including the Aux Vases and Cypress Sandstones, and deeper test wells indicated viable oil reservoirs in the St. Louis and Salem Limestones.

Pure Oil Company largely developed Noble Field after its discovery, but smaller independent companies undertook concurrent development on the periphery of Pure's operations (Figure 3). Most development drilling targeted reservoirs in the Chesterian Ste. Genevieve

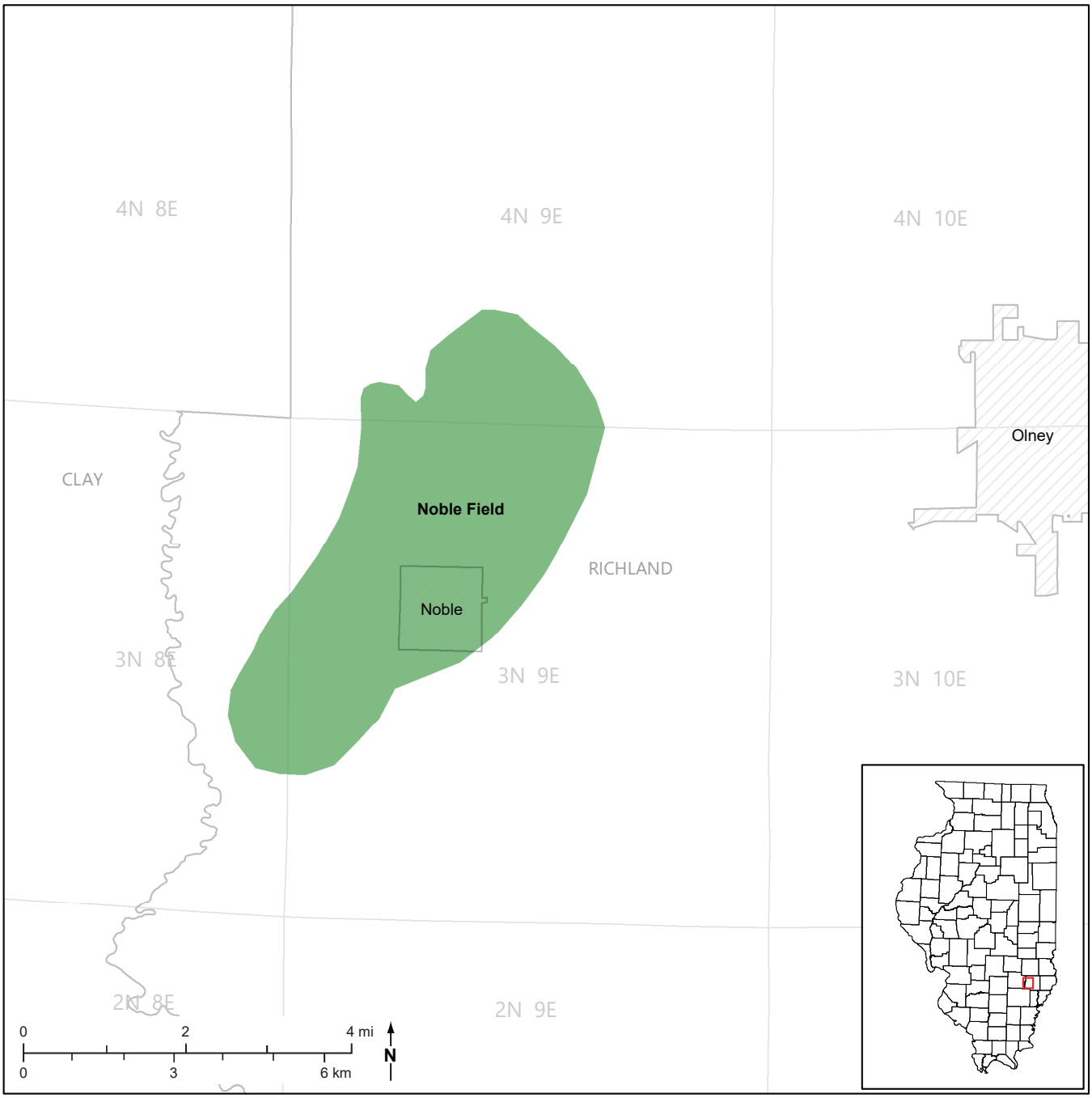

Figure 1 Index map showing the approximate extent of Noble Field (shaded in green) in western Richland County, as estimated from early reports published after discovery of the field. Township lines are shown in gray, and municipalities are shown in gray crosshatch.

Limestone and the Aux Vases and Cypress Sandstones. In the middle 1960s, Union Oil Company of California (UNOCAL) purchased Pure and took over its interests in the field. In the 1960s and again in the 1980s, independent operators were responsible for spikes in drilling activity, mainly in the southern half of the field, in secs. 8, 9, 16, and 17, T3N, R9E. In 1987, UNOCAL undertook infill drilling, targeting deeper reservoirs in the St. Louis and Salem Limestones in secs. 3, 4, 5, and 9, T3N, R9E, over a 10-year period. Elysium Energy, which later became Noble Energy, Inc., was active in the field in the early 2000s and initiated another round of infill drilling in the northern portion of the field. Citation Oil and Gas Corporation purchased Noble Energy's interests in the field in 2010 and, by the mid-2010s had undertaken drilling, primarily targeting Valmeyeran carbonate reservoirs.

Although oil has been produced from numerous formations, Noble Field is notable for having significant oil production from the reservoir in the top of the

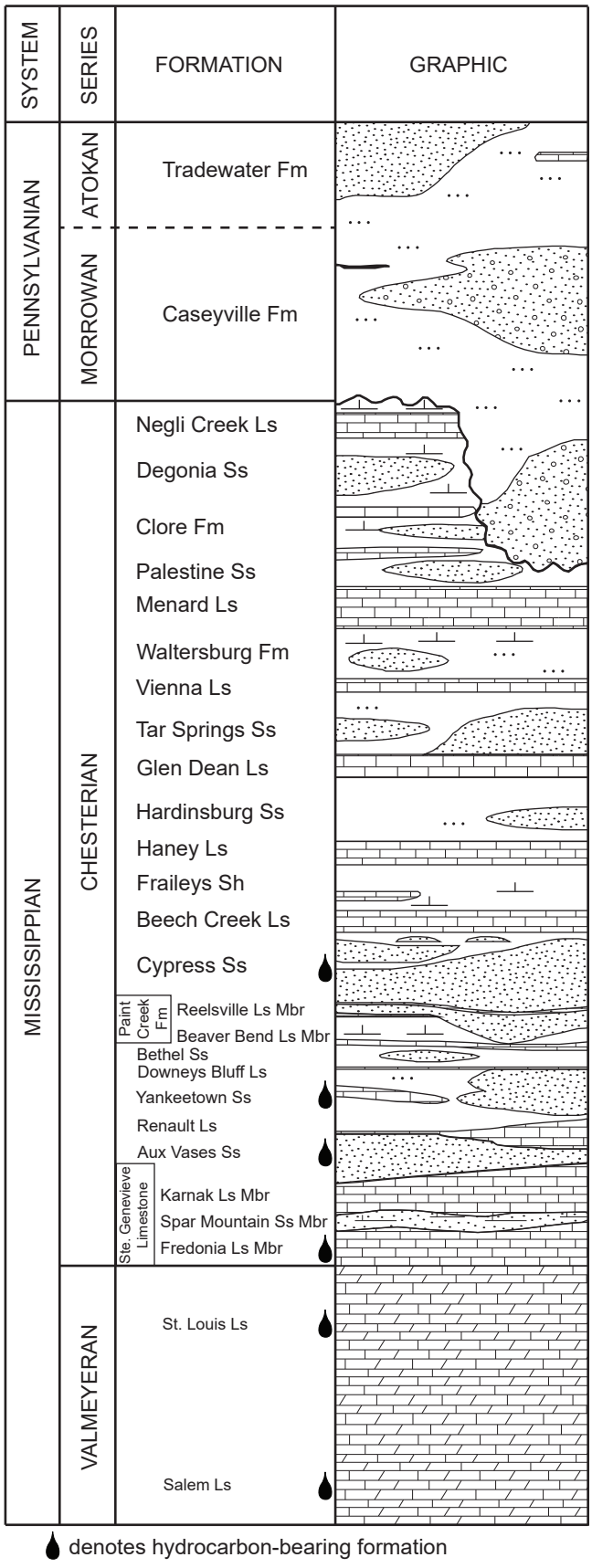

Figure 2 Generalized stratigraphic column of Noble Field showing the principal oil-producing formations. Modified from Cole and Nelson (1995).

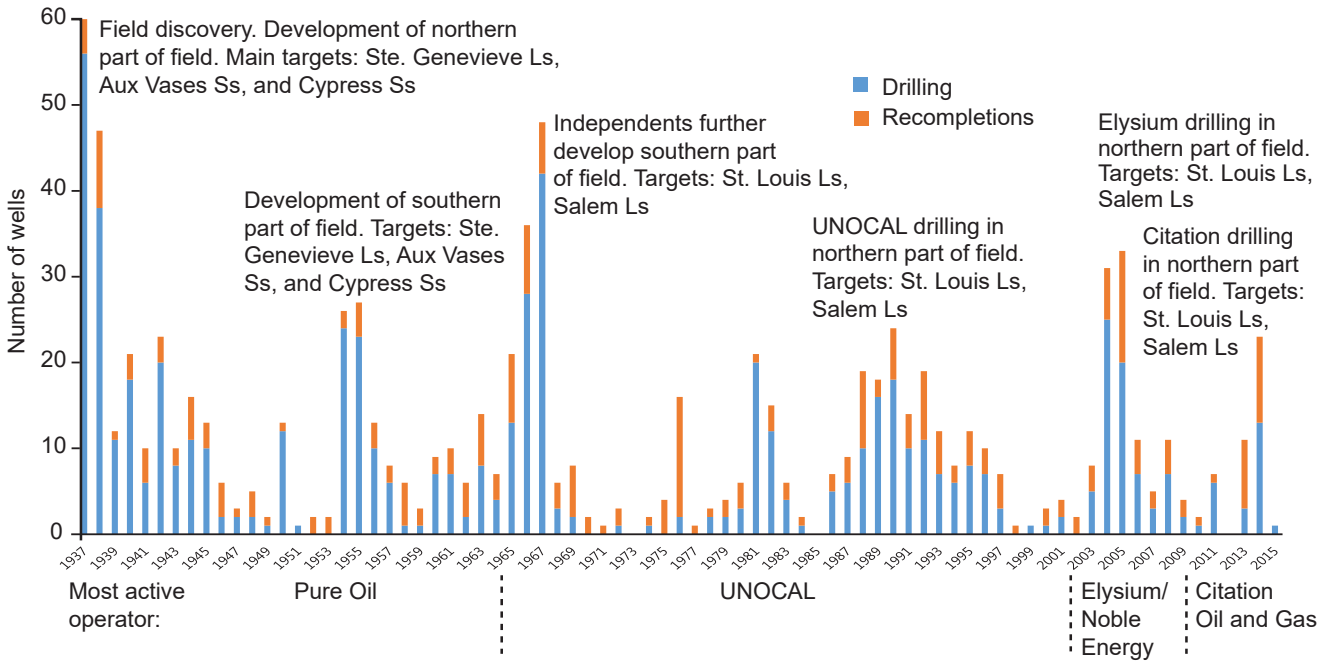

Figure 3 Annotated graph of annual drilling activity and well recompletions in Noble Field. Historical drilling activity provides a context for determining the relative historical productivity of all formations in the field. Data were available up to the first quarter of 2015.

valley-fill Cypress Sandstone. Unlike other areas of the Basin, where production from the Cypress Sandstone is from compartmentalized tidal bar sandstones, the Cypress at Noble Field is a thick, generally homogeneous sandstone typical of the kind found throughout a fairway of valley-fill Cypress Sandstone (Figure 4). Primary production from the Cypress Sandstone began in 1937. Beginning in the early 1940s, the Cypress was used for the disposal of produced water from other formations. In the 1950s, the Cypress served as a source of water for waterflooding (i.e., injection of water into the reservoir formation to displace residual oil) of other formations. In 1954, organized waterflooding of the Cypress began (Witherspoon and Jackson 1955).

STRATIGRAPHY

The stratigraphic nomenclature used here largely follows that of Willman et al. (1975); however, in subsequent revisions, the boundary has been moved between the Chesterian and Valmeyeran Series below the base of the Ste. Genevieve Limestone (Maples and Waters 1987). This stratigraphic column summarizes the middle Mississippian to lower Pennsylvanian strata in Noble Field and indicates hydrocarbon-bearing formations (Figure 2). In this publication, we have listed common oil industry terms on first mention of a given formation. These informal names appear in quotes after the formal name. Whole cores, core chips, and sample sets; core descriptions for cores that are no longer available; and published descriptions were used to detail the lithology of the units described below.

The stratigraphy observed in well logs in Noble Field includes Pennsylvanian strata that overlie and truncate several Chesterian units along the sub-Absaroka unconformity. Many old wells in the field reach their total depth within the Ste. Genevieve Limestone (~2,900 ft, or 883.9 m), whereas wells drilled since the late 1960s generally penetrate deeper Valmeyeran carbonate reservoirs (~3,000 to 3,700 ft, or 914.4 to 1,128 m; Figure 3).

Ordovician to Devonian Systems

Three wells in Noble Field penetrate deeper than the Mississippian System, and relatively little is known about the physical characteristics of the lower Paleozoic strata in the field. The deepest well in the field, the C.T. Montgomery B-18 well (API 121590068100, sec. 4, T3N, R9E), reaches a depth of 6,800 ft (2,073 m) in the Ordovician St. Peter Sandstone. In this well, the Devonian Lingle Formation was encountered with a slight show of oil at 4,608 ft (1,405 m), and the Ordovician Kimmswick ("Trenton") Limestone had an oil show at 5,992 ft (1,826 m). The John O. Coen 99 well (API 121592608600, sec. 9, T3N, R9E) reaches a depth of 4,830 ft (1,472 m) in the Devonian Dutch Creek Sandstone. Records from this well indicate a very slight show of oil in the Ullin ("Warsaw") Limestone, a show of gas in the New Albany Shale, a slight show of oil and a show of gas in the Lingle Formation and Grand Tower Limestone, and a show of oil and a slight show of gas in the Dutch Creek Sandstone.

Mississippian System

Mississippian System strata in Noble Field range in composite thickness from 2,300 to 2,500 ft (701 to 762 m), depending largely on the degree of incision along the sub-Absaroka unconformity at the top of the succession. On the interfluves

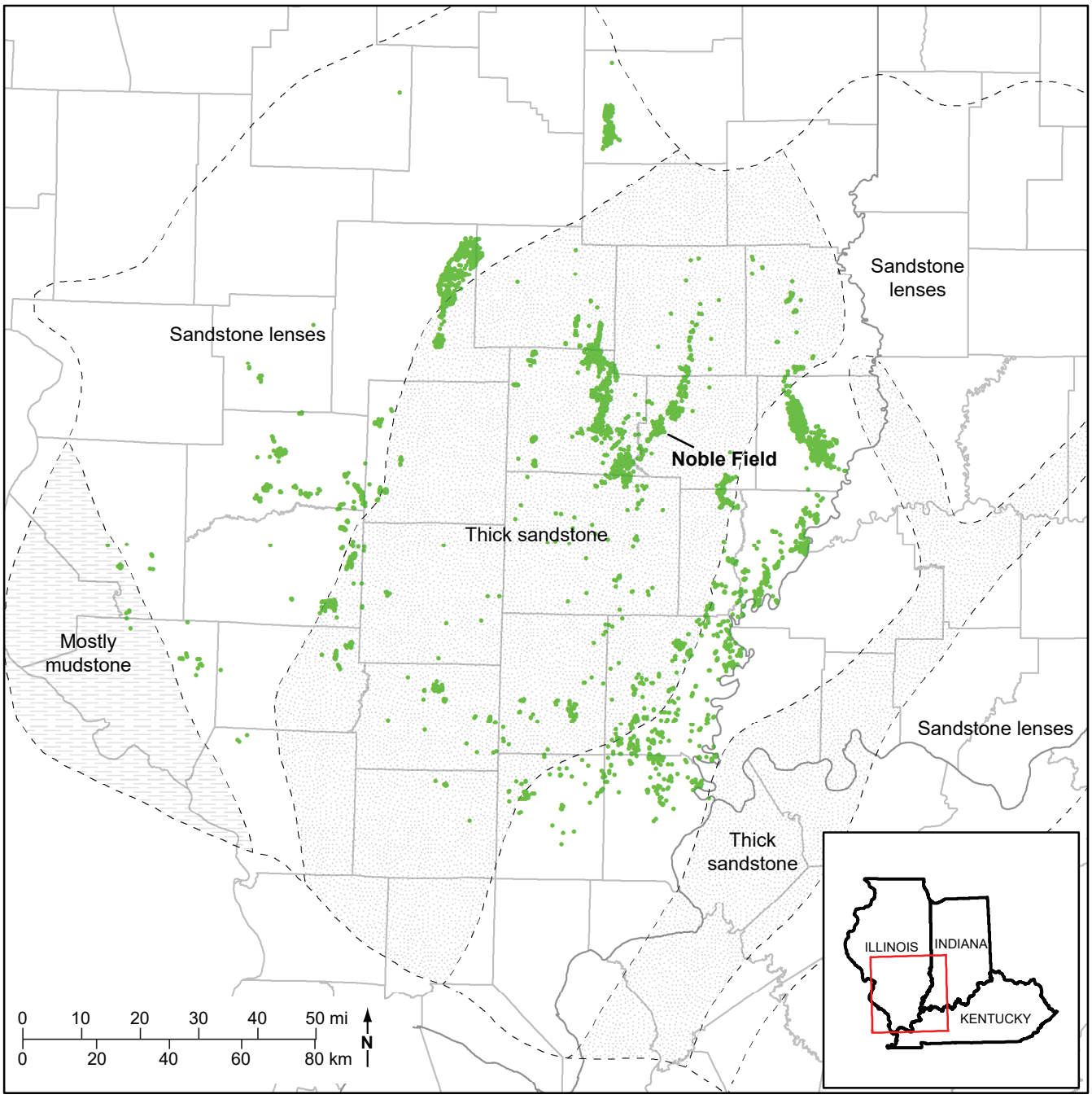

Figure 4 Map showing the generalized distribution of Cypress Sandstone facies across the Illinois Basin. Wells that produce oil from the Cypress Sandstone in Illinois are shown in green. Modified from Nelson et al. (2002).

of the unconformity surface, the youngest Chesterian unit identified is the Negli Creek Limestone (lowermost member of the Kinkaid Limestone; Bristol and Howard 1971). Unconformity paleovalleys can incise approximately 200 ft (61 m) to the level of the Menard Limestone (Bristol and Howard 1971).

Kinderhookian and Valmeyeran Series

Near the base of the Mississippian System is approximately 10 ft (3 m) of Chouteau Limestone representing the Kinderhookian Series. Carbonate strata dominate the roughly 1,500 ft (457.2 m) thick Valmeyeran Series in Noble Field, with some fine-grained siliciclastic deposits at the base of the succession. At the base of the Valmeyeran is 50 ft (15 m) of Springville Shale overlain by 80 ft (24.4 m) of Borden Siltstone. These are overlain by approximately 150 ft (45.7 m) of Fort Payne Formation and 400 ft (121.9 m) of Ullin Limestone. The upper portion of the Valmeyeran Series consists of the Salem

and St. Louis Limestones at thicknesses of approximately 400 ft (121.9 m) and 250 ft (76.2 m), respectively. Both formations contain multiple thin reservoirs. The top of the St. Louis Limestone generally occurs at a depth of approximately 3,000 to 3,100 ft (914.4 to 944.9 m), and the top of the Salem Limestone generally occurs at approximately 3,300 ft (1,006 m).

Chesterian Series

The Chesterian Series is composed of cycles of interlayered siliciclastics with limestones that are thin but laterally continuous and generally traceable on geophysical logs. Numerous Chesterian limestones were correlated on cross sections in Noble Field, including the Renault, Downeys Bluff, Beech Creek ("Barlow"), Glen Dean, and Menard Limestones and the Karnak and Beaver Bend Limestone Members. The Negli Creek Limestone was correlated in the few areas where it was not eroded by the sub-Absaroka unconformity. Descriptions of the Chesterian strata in Noble Field are provided below.

The Fredonia Limestone Member is the basal member of the Ste. Genevieve Limestone and is the lowest Chesterian Series unit in the Basin (Maples and Waters 1987). The unit is commonly light brown to white, medium to coarse oolitic limestone to gray lithographic limestone that can contain very fine grained sand in places. The limestone contains brachiopod fossil fragments and can be calcite cemented. The oolitic limestone facies of the Fredonia, known informally as "McClosky" (Workman and Bell 1937), has ooids of uniform size and is highly porous when not wholly cemented by calcite (Bell and Cohee 1938). "McClosky" oil reservoirs occur as porous lenses that are sporadic in their spatial distribution, leading early developers of the field to encounter approximately 10% dry holes (Lee 1939). Dry holes commonly offset wells with high initial production (Wasson 1938). Oolitic reservoirs occur about 50 ft (15 m) below the top of the Karnak Member of the Ste. Genevieve Limestone (Wasson 1938).

The Spar Mountain Sandstone Member of the Ste. Genevieve Limestone ("Rosiclare" sand or "Rosiclare" lime) overlies the Fredonia Limestone Member. Regionally, the Spar Mountain is lithologically variable, consisting of mixed carbonates and siliciclastics. Maximum thicknesses of 60 to 120 ft (18.3 to 36.6 m) occur west of Richland County in a north–south-trending valley, where the formation is mostly sandstone (Leetaru 2000). In Noble Field, the Spar Mountain is much thinner. It is generally characterized by poorly sorted sand grains and large, dark ooids but can be composed purely of ooids in some places (Lee 1939).

The Karnak Member of the Ste. Genevieve Limestone is a regionally extensive limestone marker bed that occurs at approximately 2,950 ft (899.2 m) in Noble Field. Within the Chesterian Series, the Karnak is one of the last major limestone units deposited before the transition to dominantly clastic with cyclical carbonate deposition. The limestone of the Karnak Member is greenish gray to dark gray argillaceous limestone to dolomite that is very fine to coarsely crystalline and oolitic and is interbedded with dark gray to greenish gray shale.

The Aux Vases Sandstone overlies the Ste. Genevieve at an average depth of 2,850 ft (868.7 m) and represents the first significant pulse of siliciclastic deposition into the Basin following the dominantly carbonate Valmeyeran succession. The Aux Vases is lithologically variable, consisting of a lower calcareous, fine-grained sandstone to fossiliferous limestone or dolomite that can be sandy or oolitic, a middle sandy oolitic limestone, and an upper fine-grained shaley sandstone (Lee 1939). On a regional scale, the Aux Vases Sandstone thickens considerably and becomes largely sandstone to the west, whereas to the east it becomes largely shale and limestone (Seyler 1986; Leetaru 2000). The Aux Vases in Noble Field is lithologically transitional between these two regional provinces. The Renault Limestone directly overlies the Aux Vases Sandstone and is typically 3 to 6 ft (~1 to 2 m) thick.

The Yankeetown ("Benoist") Sandstone overlies the Renault Limestone and occurs at an average depth of 2,780 ft (847.3 m). Geophysical logs indicate 20 to 30 ft (6.1 to 9.1 m) of shaley sandstone. A regional study of the Yankeetown Sandstone indicated that its thickness in Noble Field should average approximately 10 ft (3 m) of net clean sandstone (Leetaru et al. 2005). The Yankeetown interval has a typical lithologic succession throughout the field and tends to be calcareous at both the top and the base of the sandstone. A few feet (<1 m) of shale commonly separate the top of the sandstone from the overlying Downeys Bluff Limestone. The Downeys Bluff Limestone forms a widely traceable marker bed that reaches a maximum thickness of 10 ft (3 m) but is commonly only a few feet (<1 m) thick. Above the Downeys Bluff Limestone, the Bethel Sandstone interval is commonly represented on logs by 20 to 30 ft (6.1 to 9.1 m) of shale. The thickness of the formation is greater when sandy but thinner when shaley.

The Paint Creek Formation overlies the Bethel Sandstone and consists of two limestone benches, the lower Beaver Bend Limestone Member and the upper Reelsville Limestone Member, separated by roughly 10 ft (3 m) of shale. The overall thickness of the Paint Creek Formation is typically 30 to 40 ft (9.1 to 12.2 m) in the field but varies because the overlying Cypress Sandstone eroded into the Paint Creek Formation. In general, the Beaver Bend Limestone Member is traceable across the field. The Reelsville can be identified in some wells where the base of the Cypress Sandstone rests directly on it, but the erosive basal contact of the Cypress Sandstone causes the Reelsville to be truncated in places. In other areas, the valley-fill Cypress Sandstone appears to erode through the intervening shale and lie directly on the Beaver Bend Limestone Member.

The Cypress Sandstone is well developed as a thick, continuous sandstone that generally has a blocky appearance on spontaneous potential (SP) or gamma-ray logs. The shape of the top of the Cypress is generally convex upward, with a flat to slightly undulating base. The thickness of the sandstone can vary from 90 to 175 ft (27.4 to 53.3 m). A comprehensive reservoir characterization of the valley-fill Cypress Sandstone is presented later in this circular. A 20 to 30 ft (6.1 to 9.1 m) thick shaley interval generally occurs between the top of the sandstone and the base of the Beech Creek Limestone. This shaley interval consists of dark gray shale that is generally noncalcareous near the top and bottom. Near the middle of the zone is a variegated dark green and red mudstone that is variably calcareous, containing small calcite nodules and having a blocky appearance. This section

of the shaley interval is interpreted as a paleosol and has been noted in many reports around the Basin (Nelson et al. 2002). The upper portion of the dark gray shale is silty and grades upward into the Beech Creek Limestone.

The Beech Creek Limestone forms a continuous 10 to 15 ft (3 to 4.6 m) thick bench that overlies the Cypress Sandstone and is a regionally reliable marker datum. The Beech Creek Limestone is a dense, argillaceous, medium to very coarsely crystalline limestone that can be oolitic. Overlying the Beech Creek Limestone are approximately 40 ft (12.2 m) of Fraileys Shale, a consistent bench of Haney Limestone, and another 50 to 60 ft (15.2 to 18.3 m) of shale.

The Glen Dean Limestone is a continuous limestone marker bed that overlies the Golconda Formation and, in the Noble area, is usually 20 to 30 ft (6.1 to 9.1 m) thick. The Tar Springs Sandstone is well developed in most areas of Noble Field and can reach a thickness of 80 to 100 ft (24 to 30.5 m) in places. The sandstone appears clean and blocky on SP and gamma-ray log traces in many areas but can also separate into two or more discrete sandstone bodies; the lower sandstone is generally blocky, whereas the upper sandstone has a more lobate appearance on logs. The Vienna Limestone occurs as a thin limestone in the shaley interval approximately 30 ft (9.1 m) above the thickest Tar Springs Sandstone or higher above the top, where the sandstone is thinner and more poorly developed.

The Waltersburg Formation is usually 50 ft or more (15.2 m or more) thick but can thin to less than 20 ft (6.1 m). The sandstone within the Waltersburg Formation is present throughout the field and is part of a southwestward-trending, elongate sandstone belt that has a narrow, sinuous pattern (Potter 1962). The Menard Limestone is composed of three thin limestone benches and is present over most of Noble Field. In some areas of the field, the sub-Absaroka unconformity rests directly on the top or partially truncates the Menard Limestone. The Palestine Sandstone and the Negli Creek Limestone are poorly represented in Noble Field because they have been almost completely eroded, except for a small area on the western flank of the Clay City Anticline.

Pennsylvanian System

The uppermost Paleozoic bedrock in Noble Field consists of Pennsylvanian-aged strata that geophysical logs indicate are approximately 2,000 to 2,200 ft (609.6 to 670.6 m) thick. A thin mantle of Pleistocene glacial sediment caps this succession. Previous mapping has indicated that all the named Pennsylvanian formations in Illinois are present in Noble Field, from the basal Caseyville Formation up to the Mattoon Formation (Willman et al. 1975). Some of the most consistent marker beds identified on geophysical logs in the lower formations were correlated, namely those in the Caseyville and Tradewater Formations.

The base of the Caseyville Formation lies along the surface of the sub-Absaroka unconformity. The Caseyville Formation is made up of sandstones and shales. No distinct marker beds traceable on geophysical logs are present within the Caseyville Formation in Noble Field. The Tradewater Formation directly overlies the Caseyville Formation and cannot be clearly differentiated from the Caseyville on geophysical logs because of the paucity of marker beds. Sandstone bodies in the Caseyville and Tradewater Formations range in thickness from less than 10 ft to nearly 200 ft (3 m to nearly 61 m) and have low resistivity, indicating that they are water saturated. Cady et al. (1951) described the Pennsylvanian strata above the Tradewater Formation in some detail and they are not discussed here.

GEOLOGIC CHARACTERIZATION OF THE CYPRESS SANDSTONE

Facies Analysis

Whole cores from three wells in the northern part of Noble Field (sec. 4, T3N, R9E) and one well to the south and down-structure from the main part of the field (sec. 30, T3N, R9E) were available in the Illinois State Geological Survey (ISGS) samples library (Table 1). The 70 ft (21 m) C.T. Montgomery B-2 core was taken in 1938; this core was later reduced, sampled, or had poor recovery because no more than 50 ft (15 m) remains. The core is heavily oil stained, making identification of sedimentary features other than basic textural descriptions difficult. The C.T. Montgomery B-34 well (Figure 5) was cored in 2004, and the John O. Coen 120 well was cored in 2005. These three cores penetrated the uppermost portion of the valley-fill Cypress Sandstone in their respective wells. The Long 2 well was cored in 2017 as part of this research project. It penetrated through a sandstone lens and a portion of the underlying shale, as well as through 40 ft (12.2 m) of the 70 ft (21.3 m) thick valley-fill sandstone at the base of the formation. Full descriptions of the Coen 120 and Montgomery B-34 cores are provided in Appendix A.

In general, the valley-fill Cypress Sandstone observed in all cores is fine grained to very fine grained, with rare occurrences of medium-grained sandstone. Both the Montgomery B-34 and Coen 120 cores record changes in depositional energy and sedimentary structures near the top of the valley-fill succession (Figure 6). In the Montgomery core, cross-bedded sandstone near the base grades upward into a lower energy ripple-bedded sandstone at 2,588.5 ft (789.0 m) that sharply transitions at 2,584.5 ft (787.8 m) to a heterolithic flaser- to wavy-bedded sandstone, marking another, more abrupt drop in energy. The reduced depositional energy resulted in alternating deposits of sand deposited by bed-load traction, with silts and clays deposited by fallout from suspension. The heterolithic facies grades upward into very fine grained ripple-bedded sandstone that extends to the top of the cored interval. The Coen 120 core shows a similar succession.

The depositional environment, energy, and resulting sedimentary features define the sedimentary facies used in this study. In both cores, sedimentary facies and reservoir quality correlate well with the oil staining of the rock. Reservoir facies exhibit oil staining and include cross-bedded and ripple-bedded sandstone, whereas nonreservoir facies lack oil staining and exhibit wavy- and lenticular-bedded sandstones.

Figure 5 Core from the C.T. Montgomery B-34 well. The top of the core is in the upper left corner and proceeds downhole toward the bottom right. Each box segment is 2 ft (0.6 m) long. The core shows a typical upward change in facies from dominantly cross-bedded and ripple-bedded sandstone to heterolithic strata above. The change in color of the core from light brown to light gray reflects the lack of oil staining in the nonreservoir heterolithic facies. Figure 6 shows a graphical depiction of facies in the Montgomery core.

Table 1 Core wells with whole core of the Cypress Sandstone in Noble Field

Well name and number	API number	ISGS core number	Cored interval, ft (m)
C.T. Montgomery B-2	121590139100	835	2,575–2,645 (784.9–806.2)
C.T. Montgomery B-34	121592606400	15658	2,576–2,606 (785.2–794.3)
John O. Coen 120	121592608300	15659	2,583–2,611 (787.3–795.8)
Long 2	121592648800	15661	2,629–2,649 (801.3–807.4) 2,720–2,761 (829.1–841.6)

Reservoir Facies

Fine-grained, cross-bedded sandstone was the dominant sedimentary facies observed in the cores (Figure 5). Cross-bed sets are visually well defined. The oil staining of the cores exacerbates the contrast. Very fine grained, ripple cross-laminated sandstone can be found at the base of some cross-bed sets. Truncation surfaces or thin sets of ripple bedding mark bedset boundaries and can occur from a few inches (centimeters) to a little more than 1 ft (0.3 m) apart. Portions of the cross-bedded facies exhibit distorted bedding caused by penecontemporaneous soft sediment deformation. The sandstone is commonly slightly calcareous and exhibits dense calcite-cemented zones in some places. Iron oxide mottling is common in the reservoir facies. Light to medium brown oil staining is present in the cross-bedded and ripple-bedded facies, whereas in the portion of the Montgomery B-2 core below the oil–water contact, the sandstone is unstained and remains white. Aside from minor amounts of clay found along cross-bed foresets, the cross-bedded facies is largely composed of clean sandstone that exhibits a high reservoir quality. See the Petrologic Properties section for further discussion of geological controls on the reservoir characteristics.

Nonreservoir Facies

Non-hydrocarbon-bearing facies in the upper portion of the Montgomery B-34 core (Figure 5) exhibit heterolithic strata. Very fine grained wavy-bedded to flaser-bedded sandstones are light orange to white, and they appear to have been altered by iron oxide staining. This staining is generally constrained to sections that are relatively free of shaley lenses or drapes. Some ripple cross laminations occur throughout the heterolithic strata, as do rare horizontal and vertical burrows. Zones of shale-rich, lenticular-bedded sandstones also occur.

Geometry

Geophysical logs available for correlation and mapping included 1940s- to 1970s-era electric logs with SP and resistivity curves (generally long normal, short normal, and lateral resistivity) from approximately 380 wells. About 130 wells had more recent logs, including neutron density porosity, gamma-ray, SP, and induction resistivity.

The geophysical log expression of the valley-fill Cypress Sandstone is characterized by a blocky, aggradational profile on

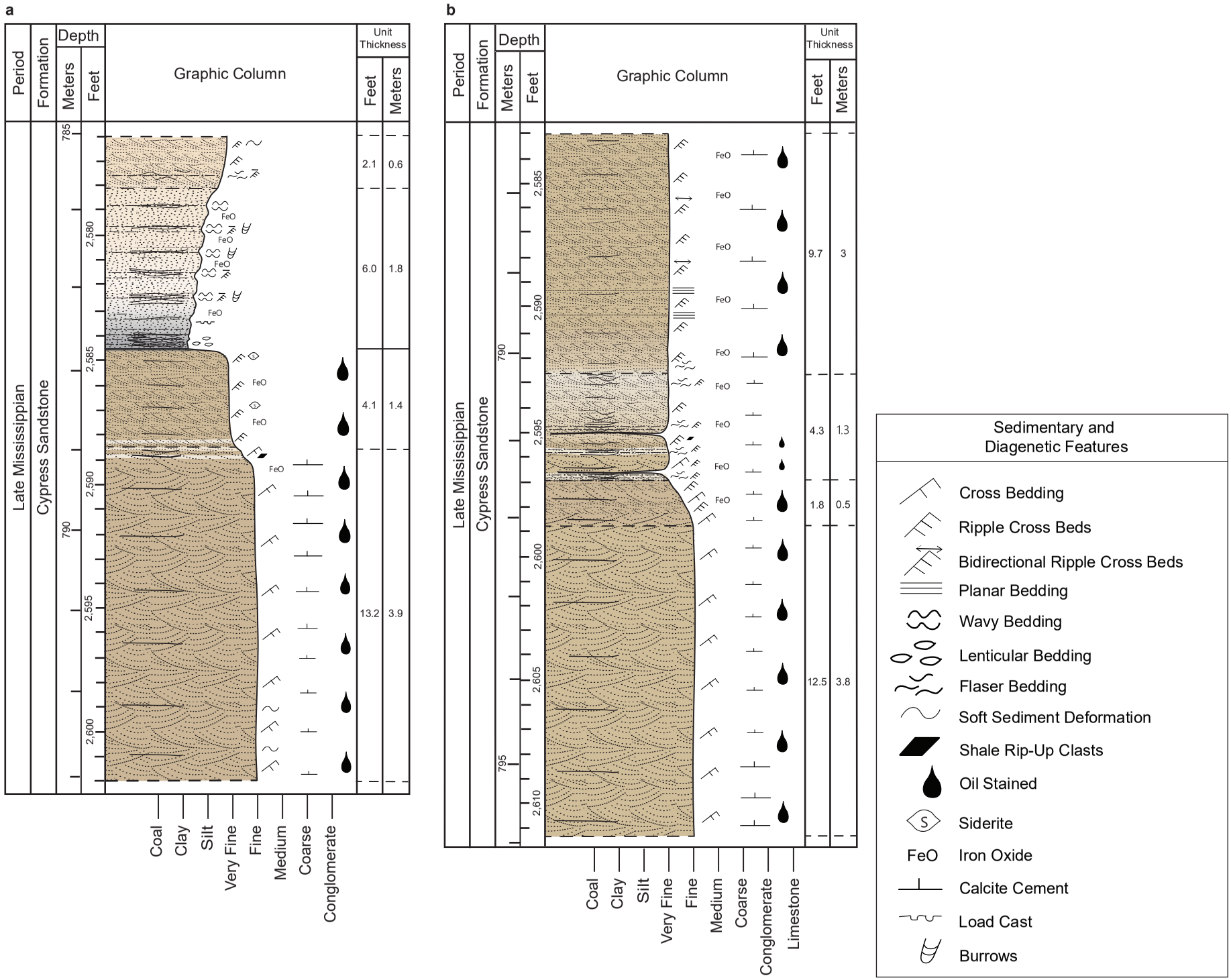

Figure 6 Lithologic logs of (a) the C.T. Montgomery B-34 well (API 121592606400, sec. 4, T3N, R9E) and (b) the John O. Coen 120 well (API 121592608300, sec. 4, T3N, R9E). The sedimentary facies observed in each core controls the reservoir quality.

the SP and gamma-ray logs, with a slight fining-upward trend at the top of the sandstone that transitions into a shalier, retrogradational log profile (Figure 7). The basal contact of the sandstone is generally sharp and well defined (Figure 7). Resistivity curves typically show relatively high resistivity at the top of the sandstone corresponding with the oil reservoir. Resistivity gradually decreases with depth and, in some wells, is punctuated by sharp high-resistivity spikes. The high-resistivity zone is thickest in the older logs, indicating the original thickness of the oil reservoir. Newer logs show a thinner zone of high resistivity that reflects decades of oil production.

Some wells exhibit a spike of high resistivity at the base of the Cypress Sandstone near its contact with the underlying Paint Creek Formation. In such cases, the Cypress is assumed to rest conformably on top of the intact Reelsville Limestone Member and the resistivity spike is interpreted to be the Reelsville. Alternatively, the basal portion of the sandstone may contain an erosional lag of clay clasts or limey fossil fragments and may be calcite cemented as a result (e.g., Morad et al. 2010). Both scenarios have been noted in studies of analogous Cypress outcrops in southern Illinois (Cole and Nelson 1995).

Geophysical log cross sections indicate that the basal contact of the Cypress Sandstone with the underlying strata is erosional (Nelson et al. 2002; Figure 8). The Reelsville Limestone Member is absent and likely eroded over most of the field. A shaley interval is usually present between the base of the Cypress and the underlying Beaver Bend Limestone Member, but the Cypress has eroded through the shale and rests directly on top of the Beaver Bend in many areas. Locally, the Cypress has entirely eroded through the Beaver Bend.

The boundaries at the top and base of the valley-fill Cypress Sandstone were determined, and the resulting gross thickness of the sandstone was mapped (Figure 9). The gross sandstone thickness refers to the thickness between the top and base of the entire valley-fill Cypress Sandstone body and may include thin intercalated shales or shaley sandstone intervals (Figure 7).

Normalized SP logs were used to determine the net thickness of the Cypress Sandstone. The Fraileys Shale was set as the shale baseline, or 0% clean sandstone (Figure 7). The 100% clean sandstone SP response was calibrated by using the lower water-saturated portion of the valley-fill Cypress Sandstone, which had the greatest amount of negative SP deflection from the shale baseline. Net sandstone refers to the cumulative thickness of sandstone above a certain normalized SP value cutoff; 50% has commonly been used in previous Cypress Sandstone studies (Grube 1992; Grube and Frankie 1999). Because of the blocky nature of the valley-fill Cypress on SP logs, the net-to-gross ratio of the sandstone in Noble Field is high: data from 385 normalized SP logs indicated an average of 87% clean sandstone. Thus, for all practical purposes, the gross isopach map shown in Figure 9 represents the net (50% clean) sandstone thickness.

The Cypress Sandstone forms an inverted V-shape of two intersecting sandstone trends in the mapped area: one that trends northwest–southeast and one that trends northeast–southwest. The former dominates and is roughly 7 mi (11 km) long and 2.8 mi (4.4 km) wide, narrowing toward the southeast (Figure 9). The latter, a subordinate northeast–southwest-trending sandstone body, intersects the larger body and is approximately 1.5 mi (2.4 km) wide. The sandstone reaches a maximum thickness of more than 175 ft (53.3 m) just east of the crest of the Clay City Anticline, in secs. 10, 11, 14, and 15 (T3N, R9E). The sandstone reaches a minimum thickness of approximately 30 ft (9.1 m) along the southern border of the mapped area (Figures 9 and 10).

The net sandstone isopach map is a composite of three amalgamated sandstone stories. Areas of the map (Figure 9) where the sandstone thickness drops below approximately 70 ft (21.3 m) indicate one of two things:

1. The upper part of the formation has changed facies to shale, as shown in Figure 10. These shales may represent overbank or floodplain facies, or they may represent an abandoned clay-filled channel. Figure 9 shows a possible arcuate-shaped clay-filled channel in the southern half of the map where the Cypress Sandstone is near its thinnest.
2. The valley-fill Cypress has broken up into multiple sandstone bodies separated by shales as much as 20 to 30 ft (6.1 to 9.1 m) thick. In these areas, the isopach map reflects only the lower sandstone body that has the highest degree of lateral continuity across the field. To the northeast in Noble North Field, the lower, continuous sandstone is overlain by an additional sandstone that can be 30 to 40 ft (9.1 to 12.2 m) thick; above that, thin, lenticular sandstone bodies lie below the base of the Beech Creek Limestone (Figure 11). Lee (1939) and the Midwest Geological Sequestration Consortium (MGSC 2005) have previously described the Cypress in this area.

Depositional Model

In a regional study of lower Chesterian stratigraphy, Nelson et al. (2002) assigned portions of the Cypress Sandstone and its overlying and underlying formations to three unconformity-bounded depositional sequences. The older part of the Cypress that is transitional with underlying Paint Creek Formation deposits is part of Sequence 7 of the scheme by Nelson et al. (2002). The valley-fill Cypress corresponds to Sequence 8, and some of the shaley deposits overlying the flooding surface that transition upward into the Beech Creek Limestone are part of Sequence 9. The mapped geometry of the sandstone bodies, vertical and lateral relationships, geophysical log characteristics, and sedimentary structures observed in cores provided the means to make preliminary interpretations of the depositional environment of the Cypress Sandstone at Noble Field, with some comments on how it fits within the scheme of Nelson et al. (2002). Although the Cypress appears as a mostly homogeneous sandstone on geophysical logs, detailed mapping has shown internal lithologic breaks, which allow the sandstone to be divided into three successive units (Figure 12).

Lower Sandstone

The lower boundary of the sandstone is assumed to be erosional because geophysical log correlations indicate that, in places, it incises through the Reelsville Limestone Member, a member of the underlying Paint Creek Formation (Figure 13). Approximately 26 ft (7.9 m) of erosional relief into the Paint Creek

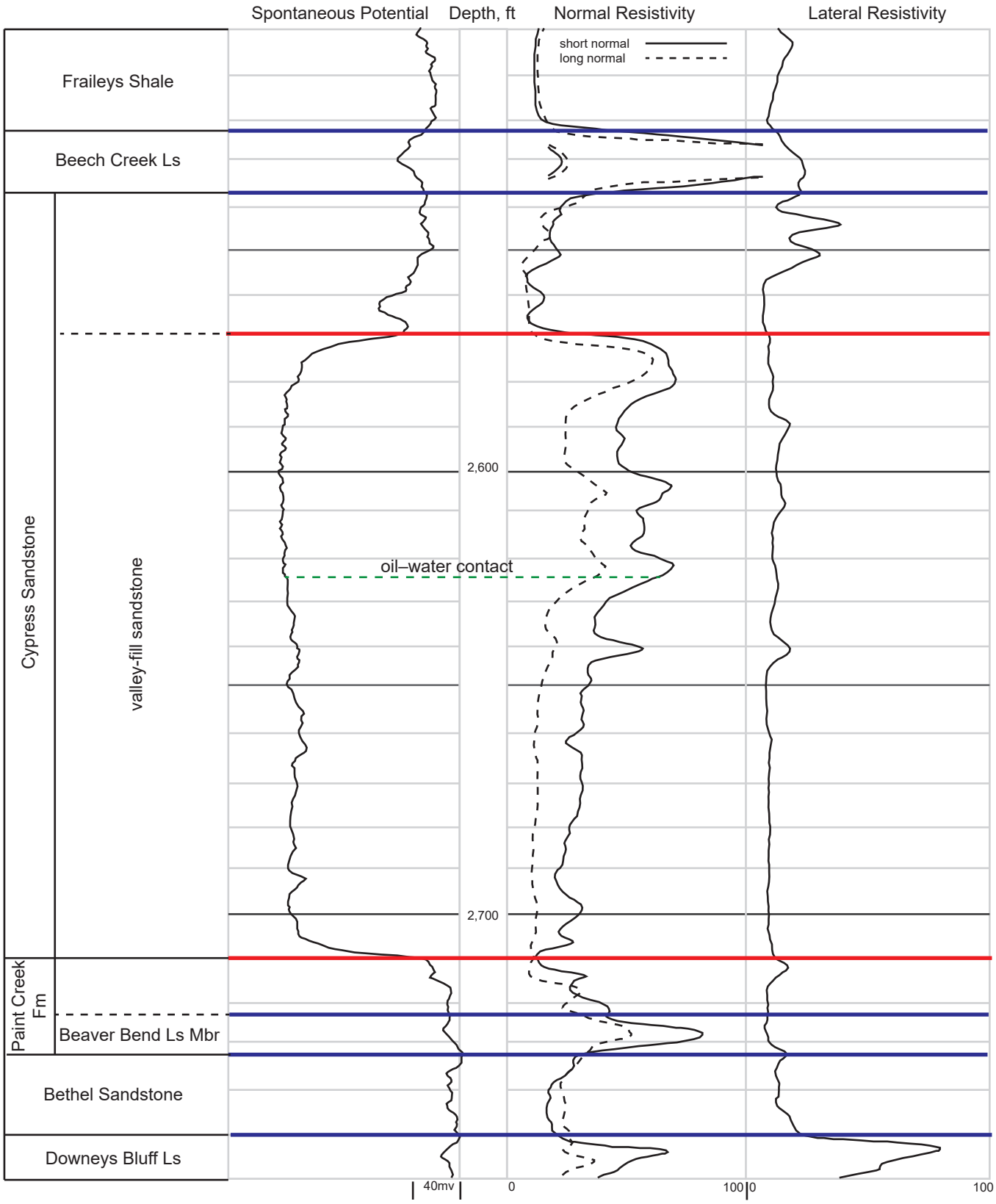

Figure 7 Type electric log of the valley-fill Cypress Sandstone in Noble Field from the C.T. Montgomery B-15 well (API 121590140400, SW¼NW¼ sec. 4, T3N, R9E). The Cypress Sandstone consists of approximately 140 ft (42.7 m) of sandstone overlain by approximately 35 ft (10.7 m) of shale and shaley sandstone. Roughly 53 ft (16.2 m) of oil reservoir is developed in the top of the sandstone, as indicated by the resistivity profile and confirmed by the sample descriptions on file at the ISGS.

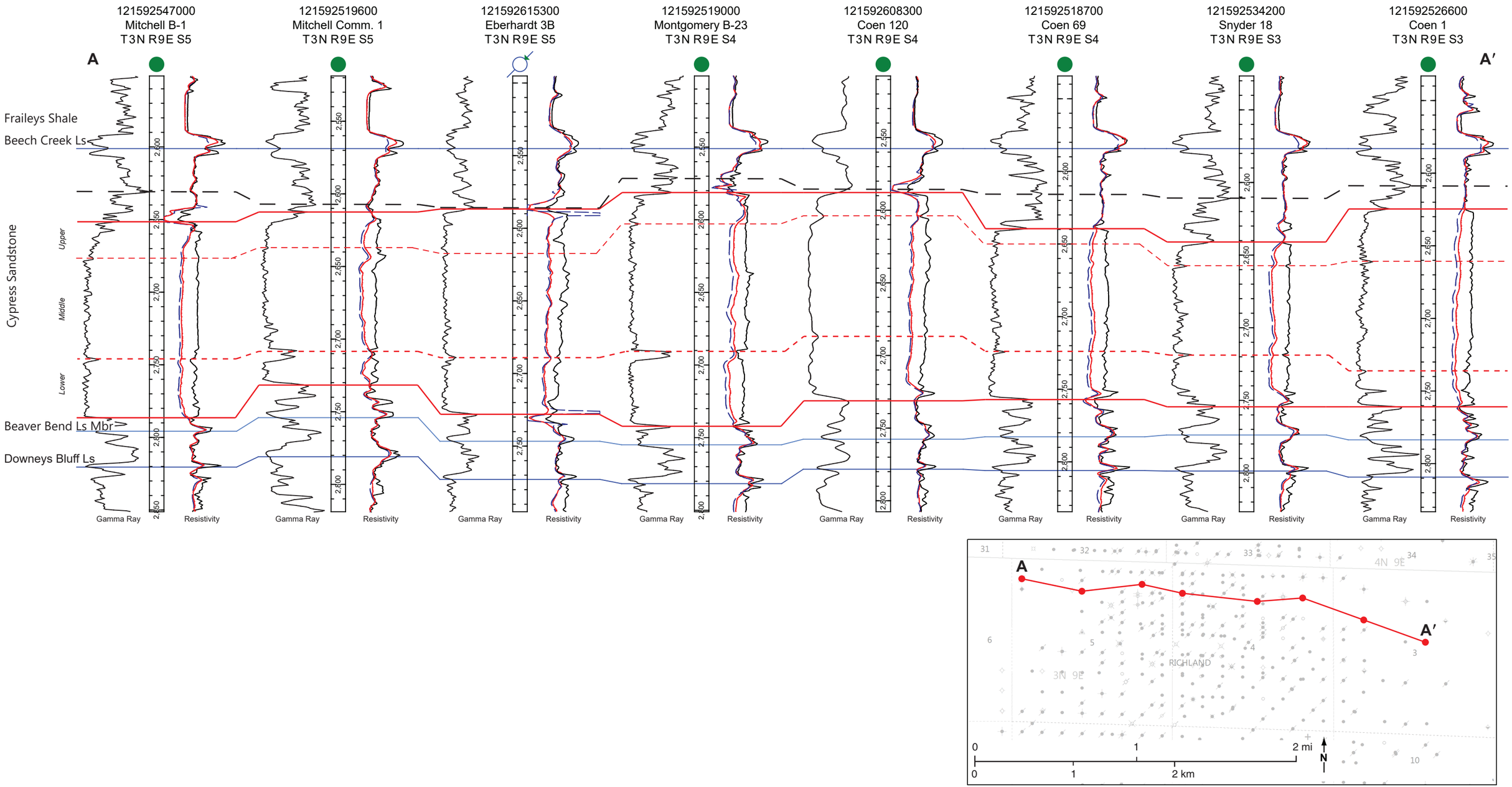

Figure 8 West-to-east cross section showing the log signatures of the valley-fill Cypress Sandstone across Noble Field. The cross section is flattened at the base of the Beech Creek Limestone. The blue lines represent correlations of limestone units. The red lines indicate the correlation of the top and base of the Cypress Sandstone. The dashed red lines indicate correlative markers within the Cypress. The erosional base of the Cypress is indicated by the pinch and swell of the interval between the base of the sandstone and the base of the Beaver Bend Limestone Member. The well log profile through the sandstone is aggradational, showing stacked sandstone stories that can be differentiated most clearly where shale breaks are present (red dashed lines) but may be indistinguishable where sandstone-on-sandstone contacts occur. The retrogradational deposits immediately above the sandstone may be overbank/floodplain or estuarine sediments that fill abandoned channels. Zones of low resistivity above the thick sandstone may indicate areas of patchy coal or carbonaceous shale. A gamma-ray maximum likely marks a significant marine flooding surface (black dashed line), above which transgressive deposits compose the remainder of the formation up to the Beech Creek Limestone.

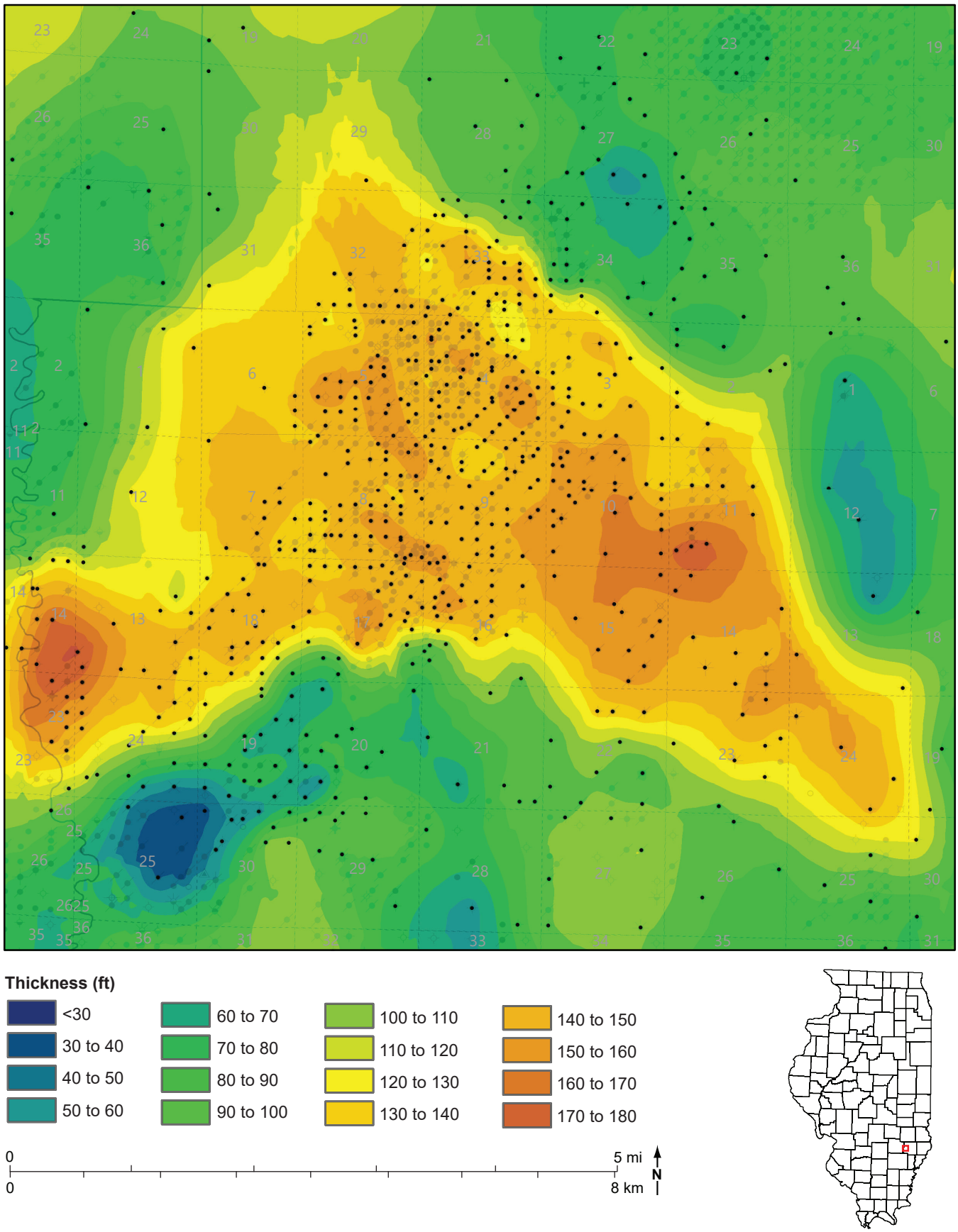

Figure 9 Isopach map of Noble Field showing the valley-fill Cypress Sandstone. The contour interval is 10 ft (3.0 m). The map shows an intersecting northwest–southeast and northeast–southwest trend of maximum thickness, which is oblique to the northeast–southwest trend of the overall valley-fill Cypress Sandstone fairway. Data points are shown on the map as black dots.

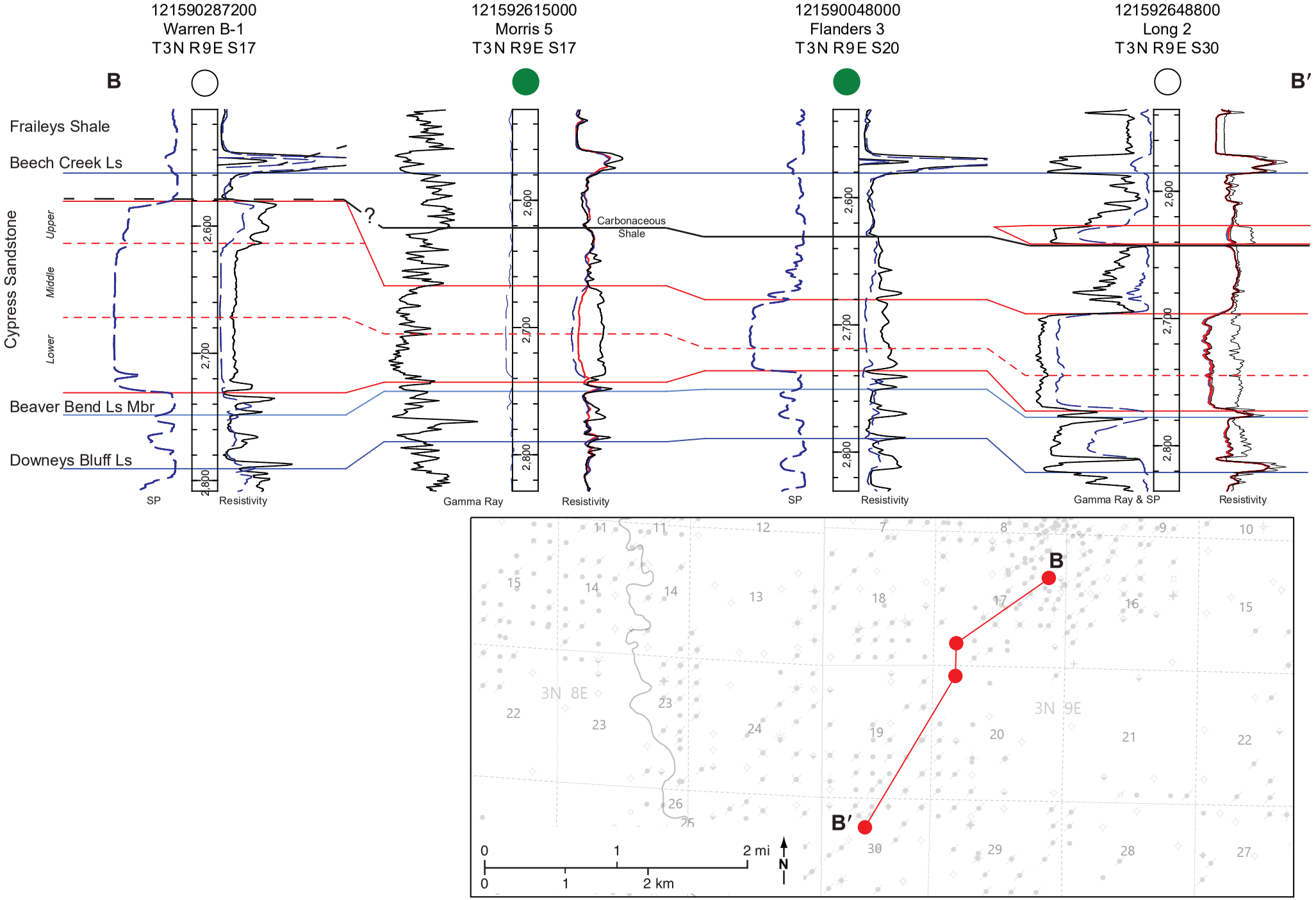

Figure 10 Northeast-to-southwest cross section showing how the Cypress Sandstone thins southwestward from Noble Field. The cross section is flattened at the base of the Beech Creek Limestone. The blue lines represent correlations of limestone units. The red lines indicate the correlation of the top and base of the Cypress Sandstone. The dashed red lines indicate correlative markers within the Cypress. A thin zone of low-density rock correlates with a zone of low resistivity and occurs at roughly the stratigraphic position where a thin coal has previously been described from drill cuttings. Core through this interval in the Long 2 (sec. 30, T3N, R9E) revealed a thin, carbonaceous shale with ubiquitous plant fossils.

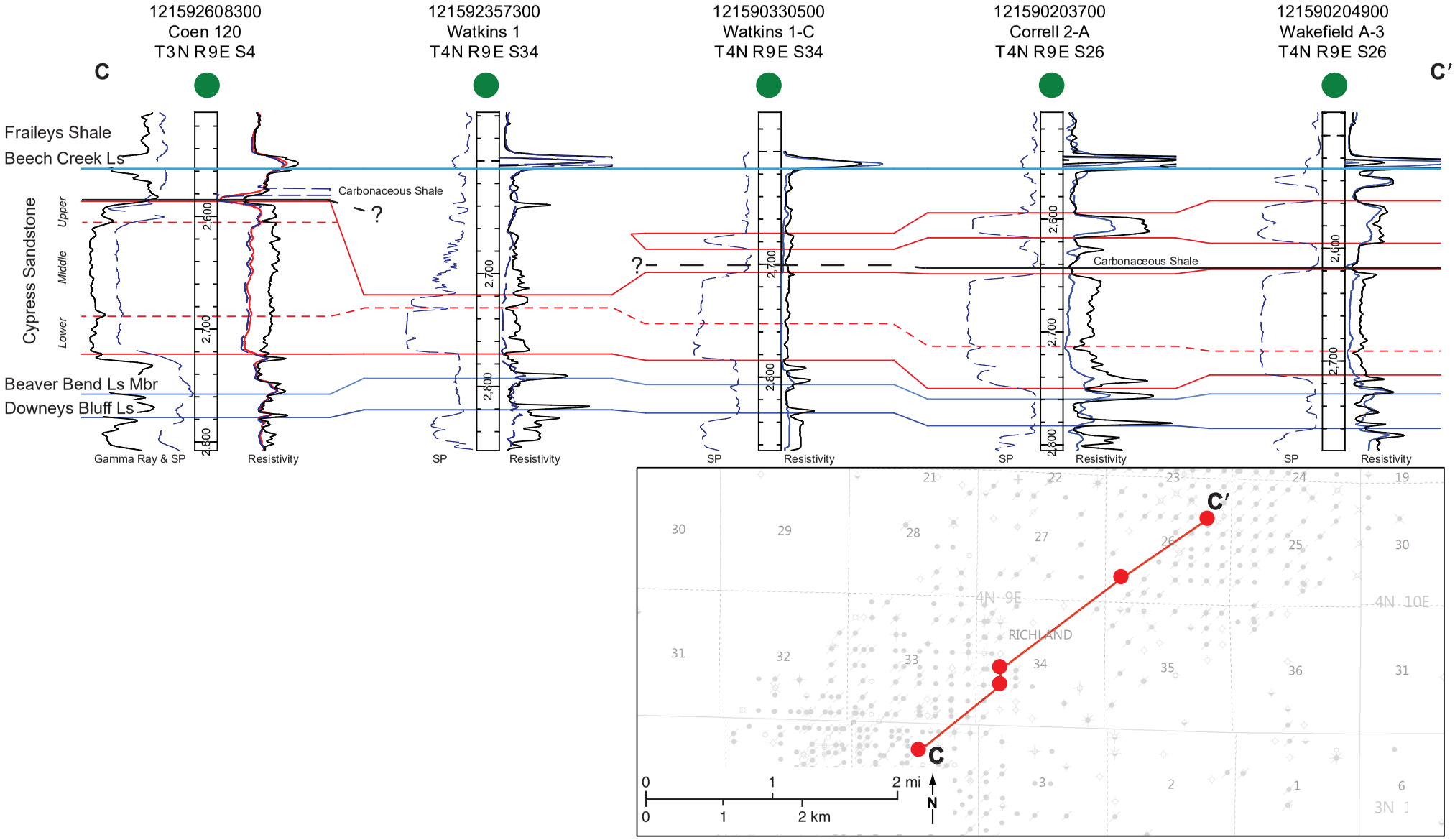

Figure 11 Southwest-to-northeast cross section showing how the Cypress transitions from Noble Field to Noble North Field. The cross section is flattened at the base of the Beech Creek Limestone. The blue lines represent correlations of limestone units. The red lines indicate the correlation of the Cypress Sandstone. The dashed red lines indicate correlative markers within the Cypress. The thick sand body on the left is hydraulically connected with the lower sandstone on the right side of the cross section. A middle sandstone overlies the lower sandstone and thickens to approximately 40 ft (12.2 m). A thin, lenticular sandstone body directly underlies the Beech Creek Limestone in Noble North Field. SP, spontaneous potential.

Formation was observed in this study of Noble Field. Nelson et al. (2002) previously documented the erosional base of the sandstone and noted that, based on geophysical log correlations in Richland County, the incised valleys of the Cypress Sandstone do not cut as deeply into underlying strata as is the case near the outcrop belt, where the Cypress can cut through several underlying formations.

A sandstone 20 to 70 ft (6.1 to 21.3 m) thick rests along the erosional lower contact and is continuous across Noble Field (Figure 8). The Long 2 core penetrates approximately 25 ft (7.6 m) of the lower sandstone in Noble Field. Cross bedding dominates the core, with some sections of convolute bedding. The base of the sandstone was not cored, however, and the interpretation of the base on an accompanying Weatherford Compact microimager log was equivocal, meaning the erosional basal contact of the formation remains speculative.

Phillips (1954) and Chapman (1953) previously noted the lateral persistence of the lower sandstone and described the basal part of the Cypress Sandstone as a discontinuous sheet deposit of fine-grained white quartz sandstone that covers most of Richland and Clay Counties, respectively. Cross-section correlations from this study confirmed the persistence of this sandstone across Richland County. The sandstone generally thins and pinches out against the Charleston Monocline, the steep western flank of the La Salle Anticlinorium.

In a previous regional study of the Cypress Sandstone, Cole and Nelson (1995) interpreted the lower sandstone as having been deposited in a shallow, subtidal environment and cited bidirectional current indicators, clay drapes on ripples, oscillatory ripples, and a normal marine fossil fauna as evidence of its marine origin. Cole and Nelson (1995) asserted that the lower Cypress Sandstone intertongues with shallow marine shales and limestones of the Paint Creek Formation. Later correlations by Nelson et al. (2002) refined this interpretation. In some areas of the Basin, a basal, coarsening-upward marine sandstone grades upward from the underlying Paint Creek Formation deposits as part of Sequence 7. In other areas, apparent lateral intertonguing results from the deposition of Cypress Sandstone in incised valleys along an unconformable contact, where Cypress Sandstone may be laterally juxtaposed to and lap onto the truncated surface of the underlying marine shales and limestones of the Paint Creek Formation as part of Sequence 8. In areas where sandstone of Sequence 7 is unconformably overlain by sandstone of Sequence 8, it may be difficult to differentiate the two. Nelson et al. (2002) favored an estuarine interpretation for the valley-fill portion of the Cypress (Sequence 8) and stated that extensive tidal reworking of lowstand fluvial deposits within a tidal embayment during transgression seemed probable, implying that the incised valley systems were first filled with fluvial sediments before being reworked.

Mud drapes and bidirectional sedimentary structures typical of tidally influenced deposits were not observed, nor was a normal marine fossil fauna pervasive within the Long 2 core. The common cross bedding and presumed erosional lower contact are indicative of fluvial deposition. A fluvial sheet sandstone is thus the favored interpretation for the lower sandstone at Noble Field; in this case, the expected marine portion of the Cypress Sandstone (part of Sequence 7) is assumed to be eroded. Fluvial sheet sandstones are formed through the amalgamation of fluvial channel belts during periods of low aggradation (Wright and Marriott 1993; Shanley and McCabe 1994; Blum et al. 2013). The overextension of rivers over long, low-gradient coastal plains can also form sheet sandstones because of the reduction in stream power and the resultant storage of sand in channels on the coastal plain (Holbrook 1996). Sediment-choked channels cause frequent avulsion, which, over time, leads to the development of a regionally continuous sandstone sheet (Holbrook 1996). Multivalley sandstone sheets thus form where the need for sediment storage exceeds accommodation within a single valley, resulting in lateral reworking (Holbrook et al. 2006). Thus, the lower parts of the valley-fill Cypress Sandstone are probably regressive lowstand deposits composed predominantly of thalweg sandstones. Floodplain deposits were eroded or reworked during lateral channel migration and are not typically preserved. Such sheet sandstones are capable of being deposited by multiple fluvial styles, including sinuous meandering systems, low-sinuosity braided systems, and anastomosing systems.

Middle Sandstone

The most consistent lithologic break within the whole of the valley-fill Cypress succession occurs at the top of the lower sandstone. This change occurs nearly everywhere in the field and manifests as a minor positive deflection to a shale break a few feet (<1 m) thick on gamma-ray logs in different areas of the field (Figure 8). Well cuttings from six wells show that the shale break is generally composed of dark gray to reddish gray shale that contains bryozoan fossil fragments (Figure 14). The middle sandstone overlies this shale break and is the cleanest portion of the valley-fill Cypress Sandstone, based on the highest deflection of the log from the shale baseline and the blocky, aggradational log profile (Figure 12). The middle sandstone is generally 90 to 110 ft (27 to 33.5 m) thick and contains thin shale breaks. Although these breaks may provide some basis for subdividing this unit, the breaks are not laterally persistent and traceable; in many places, the middle sandstone appears continuous on logs.

The middle sandstone is present everywhere in Noble Field, but it pinches out or grades laterally into green shale with thin, nonporous sandy shale partings northeast and southwest of Noble Field (Lee 1939; Figures 10 and 11). Chapman (1953) described this sandstone as being composed of northwest-trending bodies composed of fine-grained, well-sorted, and angular to subangular quartz sandstone that is light gray or greenish gray but is usually white and can contain calcite cement. Available core description records on file at the ISGS corroborate this lithologic description, although some medium-grained sandstone was observed in sample sets (Figure 14). Approximately 15 ft (4.6 m) of the middle sandstone is preserved in the Long 2 core, presenting as uniformly fine-grained cross-bedded sandstone. The contact between the middle and lower sandstones in this core appears erosional, with some small clay chips occurring within the basal portion of the middle sandstone.

It has also been interpreted, based on the limited core data and the cross-section correlations of the middle sandstone, as

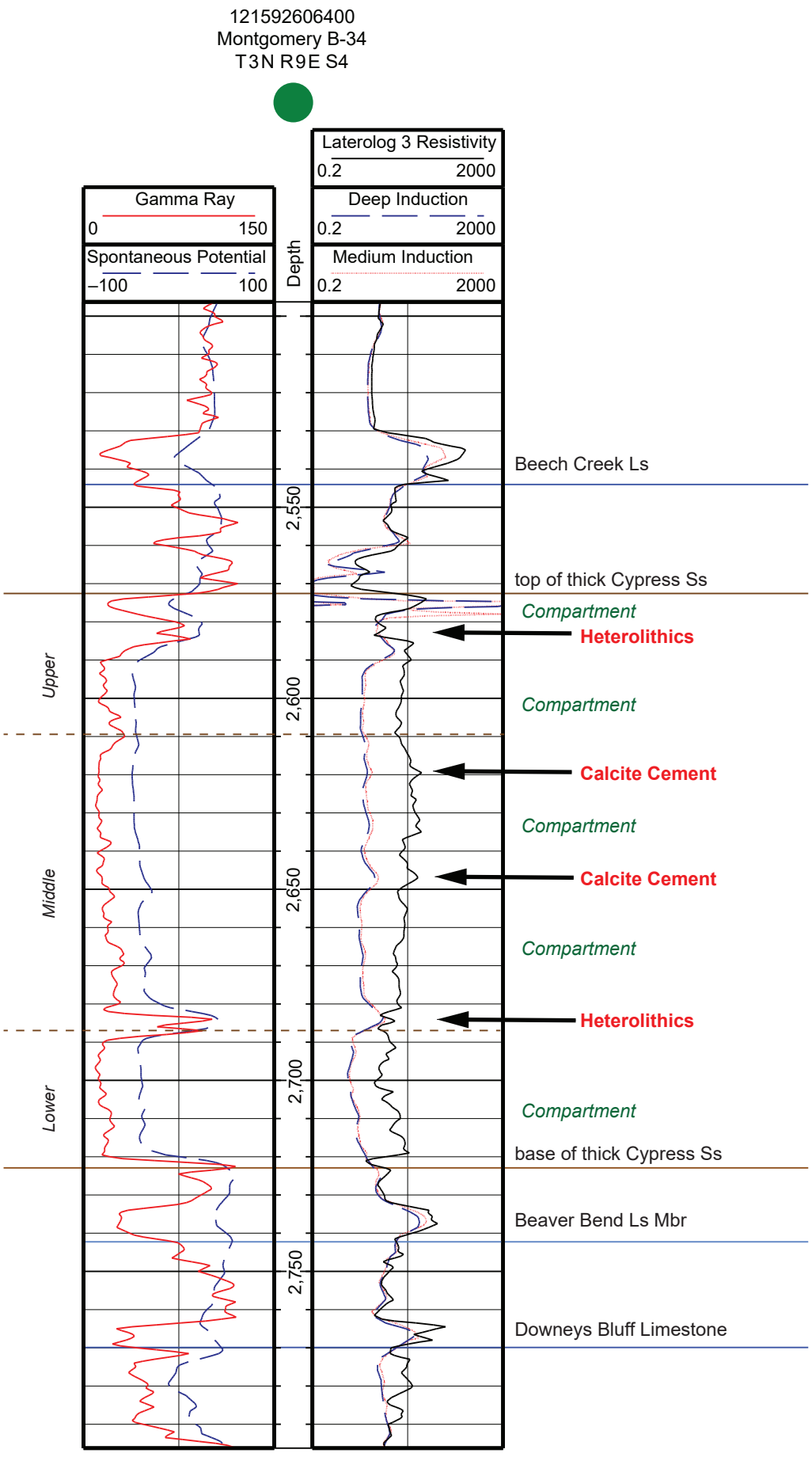

Figure 12 Geophysical log of the C.T. Montgomery B-34 well (API 121592606400, sec. 4, T3N, R9E) showing possible depositional and diagenetic features within the valley-fill Cypress Sandstone that create four potential baffles or boundaries to fluid flow (labeled in bold red). Possible compartments within the thick sandstone are labeled in green italics. The three main portions of the sandstone include a lower portion below a consistent shale break, as shown in Figure 8, a middle portion composed of a clean and blocky section, and an upper, more heterolithic and variable portion.

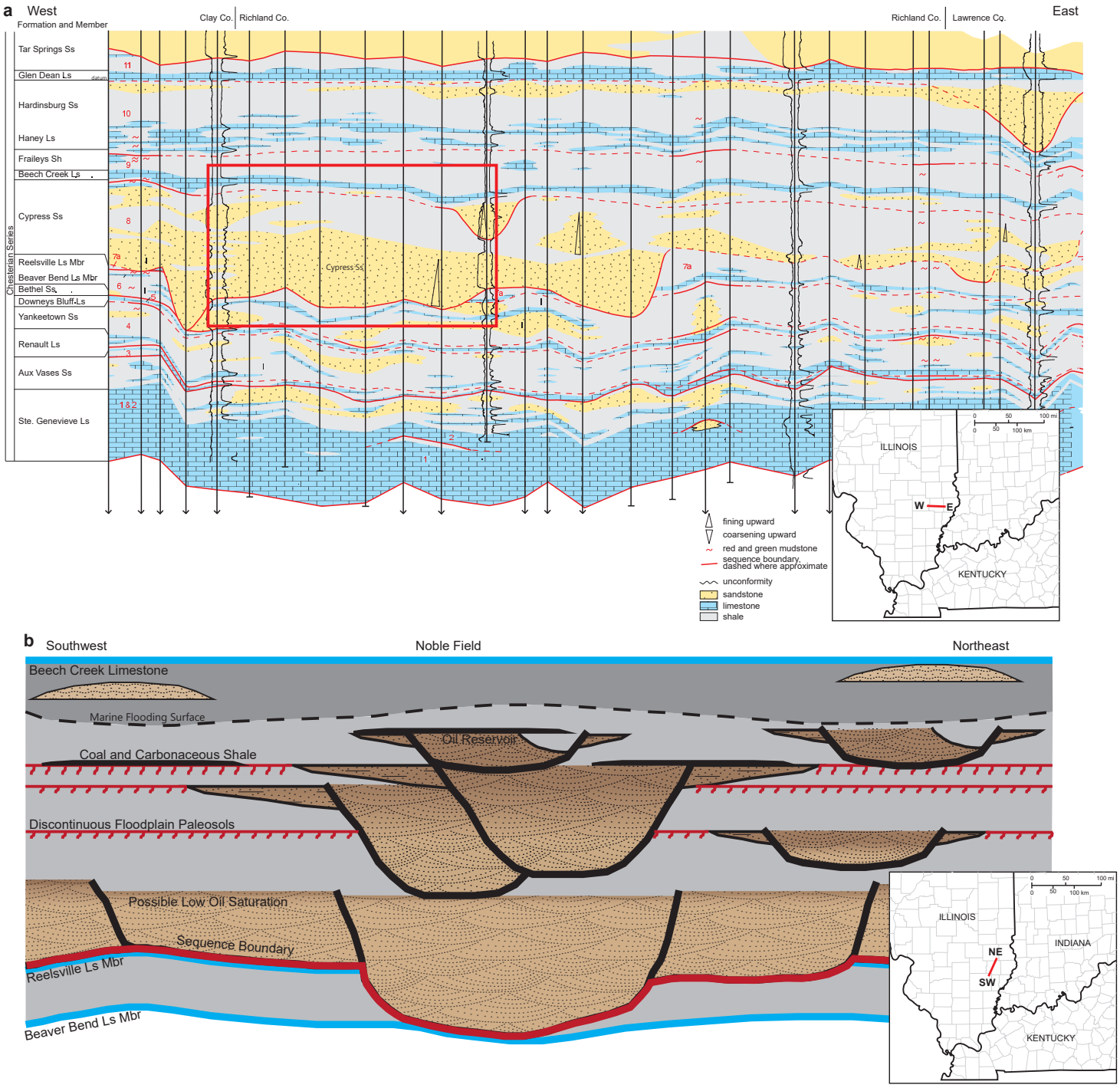

Figure 13 (a) Regional west-to-east cross section across Richland and adjoining counties (shown on inset map) showing the large-scale incised valley system occupied by the valley-fill Cypress Sandstone (modified from Nelson et al. 2002). The red box indicates the general location of (b) a simplified model of the internal architecture of the multistory Cypress Sandstone within the incised valley system at a much smaller scale in Noble Field, as shown in the hypothetical southwest-to-northeast cross section through the field. Darker brown shading within the sandstone represents the distribution of oil saturation.

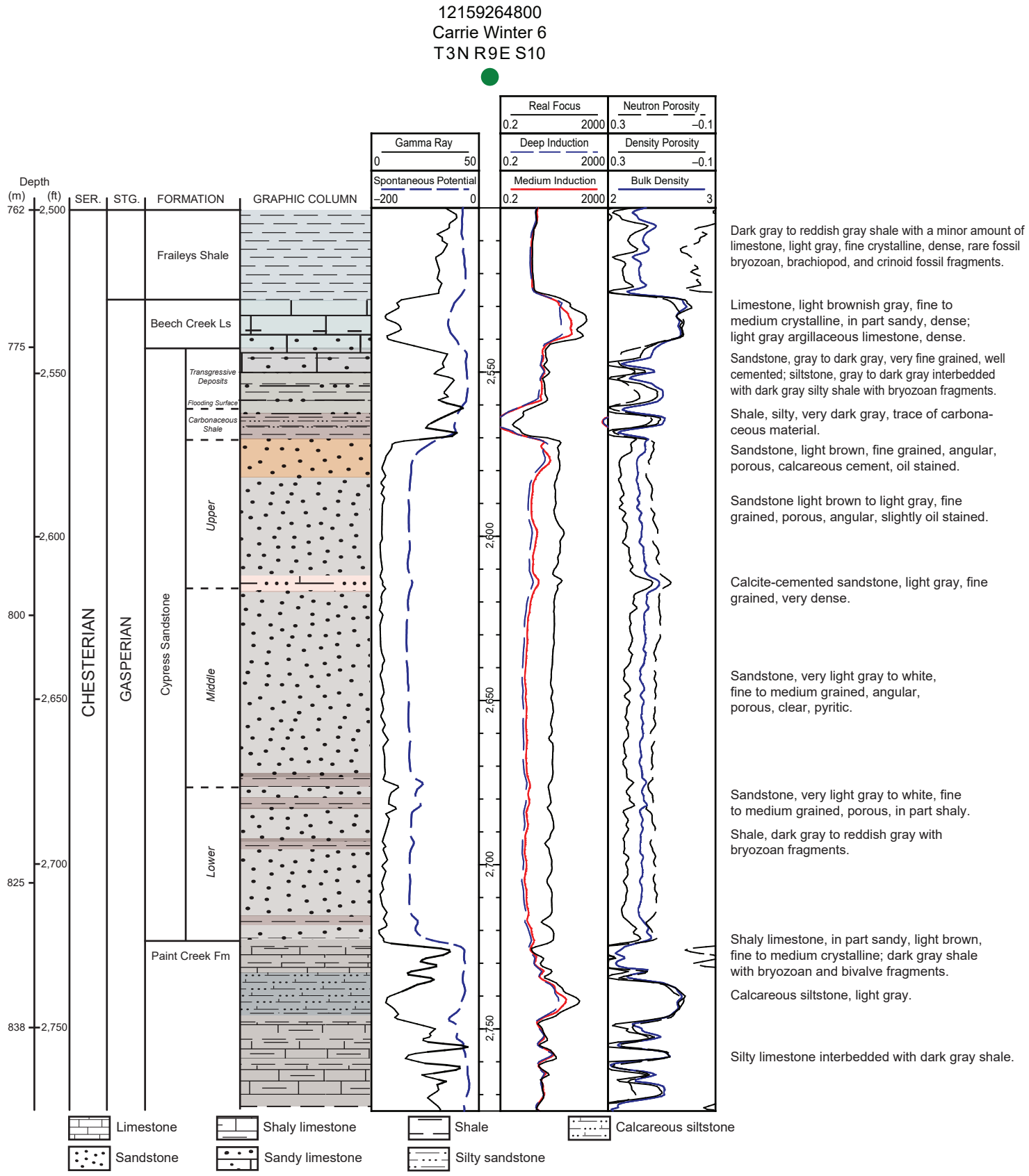

Figure 14 Graphical log and geologic description from a sample study of the Podolsky Oil Company, Winter 6 well (API 121592624800, NW¼NW¼ sec. 10, T3N, R9E), in Noble Field. Samples were studied in the 2,500 to 2,775 ft (762.0 to 845.8 m) interval. Samples indicate lithologic changes coincident with inflections in the spontaneous potential (SP) curve (reddish gray to dark gray shaley zones that can be fossiliferous), spikes in the resistivity curve within the sandstone (calcite-cemented zones), and low resistivity values above the sandstone (carbonaceous shales). Sample studies indicate oil-stained sandstone below the producing oil–water contact.

having a fluvial origin. Compared with the lower sandstone, the middle sandstone is thicker but less laterally persistent, with a greater degree of floodplain preservation, as indicated by the lateral transition to variegated and likely paleosol-bearing shale. The reduction in lateral reworking may reflect a rise in base level and a commensurate increase in accommodation. The sandstones above the lower sandstone are therefore likely fluvial deposits dominated by aggradation rather than lateral migration and reworking.

Upper Sandstone

The upper portion of the valley-fill Cypress Sandstone is the thinnest of the three subunits but has the most core data because it contains the oil reservoir (Figure 6). As described above, the general facies trend within the upper sandstone is somewhat transitional, from predominantly cross-bedded with associated ripple-bedded sandstone upward into more heterolithic strata before entering the shaley interval above the sandstone, as observed on geophysical logs. Clay laminations are found along some cross-bed foreset surfaces. Contorted cross bedding and convolute bedding are observed within this interval. These features formed because of soft sediment deformation of previously deposited cross beds, with deformation likely caused by compaction of the water-saturated sand, indicating rapid deposition.

As with the underlying sandstone units, the dominance of cross-bedded sandstone and lack of features indicating tidal influence (e.g., bidirectional bedding structures, tidal rhythmites) indicate that a fluvial interpretation is reasonable. The higher proportion of detrital clay within the cross-bedded facies as well as within the wavy- to flaser-bedded facies may indicate waning energy of the fluvial system or a lateral shift of the thalweg away from the cored area. This upper sandstone marks the uppermost fluvial sandstone body in Noble Field.

Together, the lower, middle, and upper sandstones in Noble Field constitute an amalgamated, multistory sandstone. These valley-fill sandstones of Sequence 8 are immediately overlain in places by a zone of low resistivity (e.g., Figure 10). A core description through this zone of the 1930s Arbuthnot 1 well (API 121590012100, NW¼NW¼ sec. 8, T3N, R9E) by L.E. Workman of the ISGS shows approximately 4 ft (1 m) of green to red mudstone that contains <0.08 in. (<2 mm) diameter calcite nodules, features indicative of a calcic vertisol (Mack et al. 1993). Samples described for the present study indicated a zone of carbonaceous material that also corresponds to a low-resistivity log signature and low-density signature on geophysical logs (Figures 10 and 14), which likely represent this paleosol horizon. Core from the Long 2 well through this interval confirmed the presence of <1 ft (<0.3 m) of carbonaceous shale overlying a dark gray shale with pervasive root marks. Approximately 6 mi (9.7 km) to the southwest in sec. 33, T3N, R8E, Chapman (1953) noted a 1 ft (0.3 m) thick seam of coal overlying the thick sand, providing further evidence of a paleosol horizon—in this case, a histosol (Mack et al. 1993). The paleosol horizon likely caps the valley-fill sequence except in places where active channels were flooded or where it may have been scoured by later marine transgression.

As a continued base-level rise began to overtake the sediment supply, the low gradient of the coastal plain and concomitant rivers would have been subject to marine inundation over great distances. Estuarine reworking of the upper portion of the fluvial sandstone succession may have occurred in some areas, whereas other areas may have experienced some minor transgressive scour.

Geophysical log cross sections show an inflection point, mainly on the gamma-ray log but also on the SP log, where the general profile of the log switches from retrogradational to progradational (Figure 8). This inflection may represent a significant marine-flooding surface above which some sandstone lenses may exist, but sample descriptions indicate they are very fine grained and well cemented (Figure 14). They may also be bioturbated, as has been observed in cores and outcrops (Cole and Nelson 1995).

Oil–Water Contact and Calcite Cement

The oil–water contact was identified on logs with resistivity curves at the inflection point where the decreasing resistivity values reached a more consistently flat, low-resistivity baseline. In nearly all the wells in the central part of Noble Field, a high-resistivity spike complicated identification of the oil–water contact (Figure 7). Sample studies have shown that the high-resistivity spikes correspond to zones of calcite-cemented sandstone (Figure 14). Porosity logs have also indicated that lower porosity coincides with the calcite-cemented zone observed in the samples. The spike of high resistivity and low porosity indicates a zone of calcite cement up to 4 ft (1.2 m) thick that commonly occurs near, or is coincident with, the oil–water contact and is persistent over a large portion of the field. A second calcite-cemented zone of similar thickness was also observed on logs; this zone occurred approximately 20 ft (6.1 m) below the calcite-cemented zone associated with the oil–water contact.

The coincidence of the oil–water contact with a dense calcite-cemented zone that occurs across much of the field may indicate a causal relationship. Calcite-cemented zones are known to form in association with the biodegradation of oil, a process that commonly occurs at the oil–water interface (Watson et al. 1995). The occurrence of a second calcite-cemented zone within the valley-fill Cypress Sandstone below the oil–water contact may reflect a relict, or paleo, oil–water contact. Although no core was available through this calcite-cemented zone, geophysical logs indicate that the low-porosity calcite-cemented zone occurs independently of any identified facies boundary. Thus, an oil–water interface would be a reasonable mechanism to explain the formation of the calcite-cemented zone. Such permeability and diagenetic boundaries have been noted elsewhere and have been attributed to paleo oil–water contacts (Heasley et al. 2000). The interpretation of a paleo oil–water contact would indicate its position before a postulated basinal tectonic tilting event reconfigured the reservoir hydrodynamics and shifted the oil–water contact, possibly forming an ROZ.

To understand the relationship between the calcite-cemented zones and the oil–water contact, further research is required. Specialized petrographic techniques, including cathodoluminescence, can provide information regarding the timing of cement development within the paragenetic sequence. Fluid inclusions contained within the cement can record

information about the fluids present at the time of cement formation and, if petroleum is present, would indicate an overlap between the timing of cementation and oil emplacement. Jensenius and Burruss (1990) used capillary gas chromatography to quantify the degree of biodegradation within oil in similar cements to provide a better understanding of both the microbial influence on cement formation and the conditions present at the time of oil migration, the latter of which would have important implications for identifying a suspected ROZ. Thus, future study of fluid inclusions within calcite-cemented zones of the Cypress could yield significant information about the relationship between petroleum migration and diagenesis.

The calcite-cemented zones may form baffles or boundaries to vertical fluid movement within the sandstone. The reduced porosity likely corresponds to a similar decrease in permeability in these zones; hence, the zones may contribute to compartmentalization (Figure 12). In addition, thin zones of shaley to heterolithic strata delineate compartments within the reservoir. The Montgomery B-34 core (Figures 5 and 6) showed an interval of heterolithic strata a few feet (<1 m) thick that separated a thin, reservoir-quality ripple-bedded sandstone from the underlying main sandstone, forming a thin compartment at the top of the valley-fill Cypress, as shown in Figure 12. The thin, laterally persistent shaley zone in the lower portion of the valley-fill Cypress observed on logs and in sample sets likewise creates a baffle. In all, the valley-fill Cypress Sandstone at Noble Field likely has numerous baffles that may either reduce or restrict vertical fluid movement within the reservoir.

Petrologic Properties

Sample Preparation

The Montgomery B-34 and Coen 120 cores in Noble Field were sampled for analysis of bulk and clay mineralogy and for petrographic thin sections. Samples were taken every 1 ft (0.3 m) at depths corresponding to existing core analysis data. Mineralogy samples were prepared by crushing and cleaning hydrocarbons. Micronized random powder packs (micronized bulk packs) were analyzed to make semiquantitative assessments of the bulk mineral composition by using established methods (Hughes and Warren 1989; Hughes et al. 1994). Air-dried <16 µm-oriented slides were also prepared for semiquantitative assessment of the relative abundance of clay mineral species relative to the total clay fraction (e.g. Glass and Killey 1987; Hughes and Warren 1989; Hughes et al. 1994). The complete bulk composition and the clay mineralogical composition are provided in Appendix B. Samples were sent to Wagner Petrographic (Lindon, Utah) for epoxy impregnation and mounting on standard 0.94 × 1.8 in. (24 × 46 mm) petrographic thin sections.

Mineralogy and Texture

The Cypress Sandstone in Noble Field is mainly quartz arenite, like the regional mineralogy of the Cypress (Pitman et al. 1998). Feldspar content of the samples is generally <10%. (Plagioclase is generally at least twice as abundant as orthoclase.) One percent to 2% calcite cement is also common in these samples.

A few trends emerged when the results of the mineralogical analysis were compared with observed sedimentary facies. First, cross-bedded sandstones, having been deposited in a higher energy regime than any other observed facies, had the lowest total clay volume in each sample (generally <2%; Figure 15). Ripple-bedded sandstone facies generally had >2% clays. Kaolinite was the dominant clay mineral throughout both cores, and it was the most prolific below the facies boundary separating the lower cross-bedded and ripple-bedded sandstone from the overlying heterolithic and bidirectionally ripple-bedded sandstones. The heterolithic facies contained the greatest abundance of illite and illite/smectite, whereas the bidirectionally ripple-bedded sandstone facies generally had 20% or more chlorite. The heterolithic facies showed a decline in quartz content; clays often made up 10% to 15% of the samples. A higher feldspar content and a small percentage of dolomite cement were noted in these samples as well.

Fine-grained sandstone was the most dominant texture, but medium-grained sandstone occurred rarely in the cross-bedded facies. In the reservoir facies, the grains were moderately well sorted and ranged from angular to rounded. Rounded grains were more prevalent. In general, the framework grains became more angular with depth from the top of the sandstone. These grains were angular as a result of the euhedral crystal faces of the quartz overgrowths found in sandstones with a lower clay content. Nonreservoir flaser-, wavy-, and lenticular-bedded sandstones were very fine grained.

Controls on Porosity and Permeability

Porosity and permeability data were available from 307 core plugs in 14 wells in Noble Field and are summarized in Table 2. The cores were generally collected from the oil reservoir in the top of the sandstone; none penetrated the entire valley-fill Cypress. Thus, the results described here are for the upper portion of the thick sandstone and may differ in the lower aquifer portion of the sandstone. The median porosity of the data set is only slightly higher than, and in good agreement with, the average. Low porosity values correspond to nonreservoir facies or well-cemented samples. The median permeability is somewhat lower than the average, and this discrepancy reflects the fact that a relatively small number of samples exhibited extremely high permeability of >1 D (0.986 μm^2).

Reservoir facies showed higher porosity and permeability values than did nonreservoir facies. Porosity values were similar for both the ripple-bedded and cross-bedded sandstones, but permeability values were much higher in the cross-bedded sandstones. Permeability differences between the two facies are likely due to factors related to depositional energy: in the horizontal core plugs, the ripple beds contained a greater number of bedding discontinuities and were relatively finer grained, whereas the cross-bedded facies were more continuous and relatively coarser grained. In addition, detrital clay minerals could have affected the reservoir by reducing vertical permeability. However, the vertical permeability values in the higher energy cross-bedded sandstone facies were nearly equal to the horizontal permeability values, demonstrating the limited amount of clay lamination found in this facies.

A portion of the porosity and permeability within the reservoir facies, especially the cross-bedded sandstone, could also be attributed to secondary porosity development. Elongated and oversized pores, as defined by Schmidt and McDonald (1979), were common (Figure 16) and reflected dissolution of the framework grains, likely feldspar, because dust rims outlined the former grain boundaries in some examples. Early diagenetic, most likely carbonate, cements may also have been dissolved. Syntaxial overgrowths of quartz also occurred. The result is a hybrid pore system of primary intergranular and secondary porosity. Long, well-connected pores that resulted from framework grain and cement dissolution likely contributed to the exceedingly high permeabilities observed.

The silt and clay in the nonreservoir facies were catalysts for compaction, which resulted in reduced porosity and permeability (Figures 17 and 18). Much of the porosity in the nonreservoir facies could be attributed to secondary dissolution of feldspar grains or carbonate cements. The increase in detrital clay content meant fine clay laminations compartmentalized the reservoir at a small scale. Thus, factors related to the original depositional energy in addition to secondary diagenetic dissolution and cementation affected the porosity and permeability of the nonreservoir facies.

The quartz content of all samples correlated well with the porosity and permeability of the samples; the inverse was true for clay content versus porosity and permeability (Figure 19). This relationship demonstrates the overall depositional controls on porosity and permeability. A comparison of the sedimentary facies observed with the porosity and permeability measurements in the Coen 120 and Montgomery B-34 cores showed the relative reservoir quality of the varying sandstone facies. In order of decreasing depositional energy, the primary facies observed in cores included higher energy cross-bedded and ripple-bedded reservoir sandstone facies and lower energy wavy-bedded and lenticular-bedded nonreservoir sandstone facies. The cross-bedded sandstones had the highest average porosity and permeability, at 18% and 755 mD (7.45×10^{-1} μm^2), respectively. Ripple-bedded sandstone was lower, at 16.6% and 31.9 mD (3.15×10^{-2} μm^2). Nonreservoir facies included wavy-bedded sandstone (11.6% and 3.3 mD, or 3.26×10^{-3} μm^2) and lenticular-bedded sandstone (7.8% and 0.3 mD, or 2.96×10^{-4} μm^2) that could form baffles within the reservoir.

A comparison of core data from the thick Cypress Sandstone in fields in other parts of the Basin (Figure 20) showed that a range of porosity and permeability values could be expected, depending on the location (Table 3). Average porosity values were typically 18% to 19%, except for Dale Field, which had an average porosity of 13%. Permeability values of the Cypress at Noble Field were higher than those at Loudon Field, as has been noted previously, and an inverse relationship between porosity and permeability was exhibited at those two fields (Piersol et al. 1940). This result suggests a diagenetic difference in the Cypress Sandstone across the Basin, if the texture and facies of the Cypress are consistent among the fields. Further investigation of the valley-fill Cypress Sandstone in other areas of the Basin is needed to understand whether the factors that control porosity and permeability in Noble Field can be observed elsewhere.

Structural Geology and Oil Trapping

A regional structure map contoured on the base of the Beech Creek Limestone shows the location of Noble Field with respect to major structural features in the Basin (Figure 21). Deformation of the Clay City Anticline occurred primarily in the early Pennsylvanian (Bell and Cohee 1938). Although Mississippian units were deformed over the anticline, Pennsylvanian strata generally lay flat and showed little effect of the movement of the anticline. Other structures in the vicinity, including the La Salle Anticlinorium, had persistent movement during and after the Pennsylvanian, causing Pennsylvanian units to thin over the structure (Jacobson 1985). The stratigraphy of Pennsylvanian rocks in Noble Field appears to be influenced more by the relief on the unconformity surface than by structural activity.

The structure of the Clay City Anticline was mapped on several formations in Noble Field; the map constructed on the base of the Beech Creek Limestone is shown in Figure 22. The Anticline is 4.5 mi (7.2 km) wide and plunges to the southwest at a dip of 0.3° (23.7 ft/mi, or 4.49 m/km). A narrow structural saddle trending northwest to southeast across the structure effectively delineates the boundary between Noble Field and Noble North Field. This saddle was also mapped in deeper horizons, including the Karnak Limestone Member and Downeys Bluff Limestone (not shown). Unique to the Beech Creek Limestone structure map is a small area of somewhat gentler dip to the southeast of the structural high that makes up Noble Field. The structural dip of this area appears to be subdued by an increase in thickness of the underlying Cypress Sandstone (Figure 9).

A structure map of the top surface of the valley-fill Cypress Sandstone shows the northeast–southwest-trending Clay City Anticline (Figure 23). The map shows a closure of 110 ft (33.5 m) with a reservoir spill plane at an elevation of approximately 2,165 ft (659.9 m) below mean sea level. As noted previously, a structurally high area into secs. 10, 11, 14, and 15 (T3N, R9E) coincides with the area of the thickest Cypress Sandstone (Figure 9).

The Cypress Sandstone is part of the New Albany–Chesterian petroleum system that is defined by source rocks in the Devonian–Mississippian New Albany Shale and areas of oil accumulation in reservoir rocks from Silurian through Pennsylvanian (Lewan et al. 2002). Oil expulsion began in the Middle Pennsylvanian and reached its peak in the Late Pennsylvanian–Early Permian, contemporaneous with extensive folding and faulting that resulted in many of the major traps in the system (Lewan et al. 2002).

Oil is trapped in the upper portion of the valley-fill Cypress Sandstone at Noble Field by a combination of structural and stratigraphic controls, and the oil column is thickest where the sandstone crosses the Clay City Anticline perpendicular to the crest of the Beech Creek Limestone structure. In fields where the structure is the only trapping mechanism, the oil–water contact follows a single elevation contour. Figure 24 illustrates several instances in Noble Field where the oil–water contact does not trace a constant elevation. First, in the northeast corner of the field, the oil–water contact is cut off abruptly along a generally northwest–southeast line, reflecting a stratigraphic

Figure 15 Graphs showing the relative abundance of different clay minerals within the clay mineral fraction. Samples were taken from (a) the Montgomery B-34 well (API 121592606400) and (b) the Coen 120 well (API 121592608300) for each depth shown along the left *y*-axis. Each segment of the bar graph represents the relative proportion of a certain clay mineral, color-coded to the legend. The *y*-axis labels on the right list the total clay percentage for each bulk sample. Annotations on the right reflect major facies changes in the core.

Table 2 Summary of core analysis data and statistics from Noble Field

	Minimum (P10)	Maximum (P90)	Median	Mean	Standard error
Porosity, %	13.5	20.3	17.4	17.0	0.18
Permeability, mD (μm²)	10.0 (0.01)	960.8 (0.95)	365.0 (0.36)	438.7 (0.43)	25.6

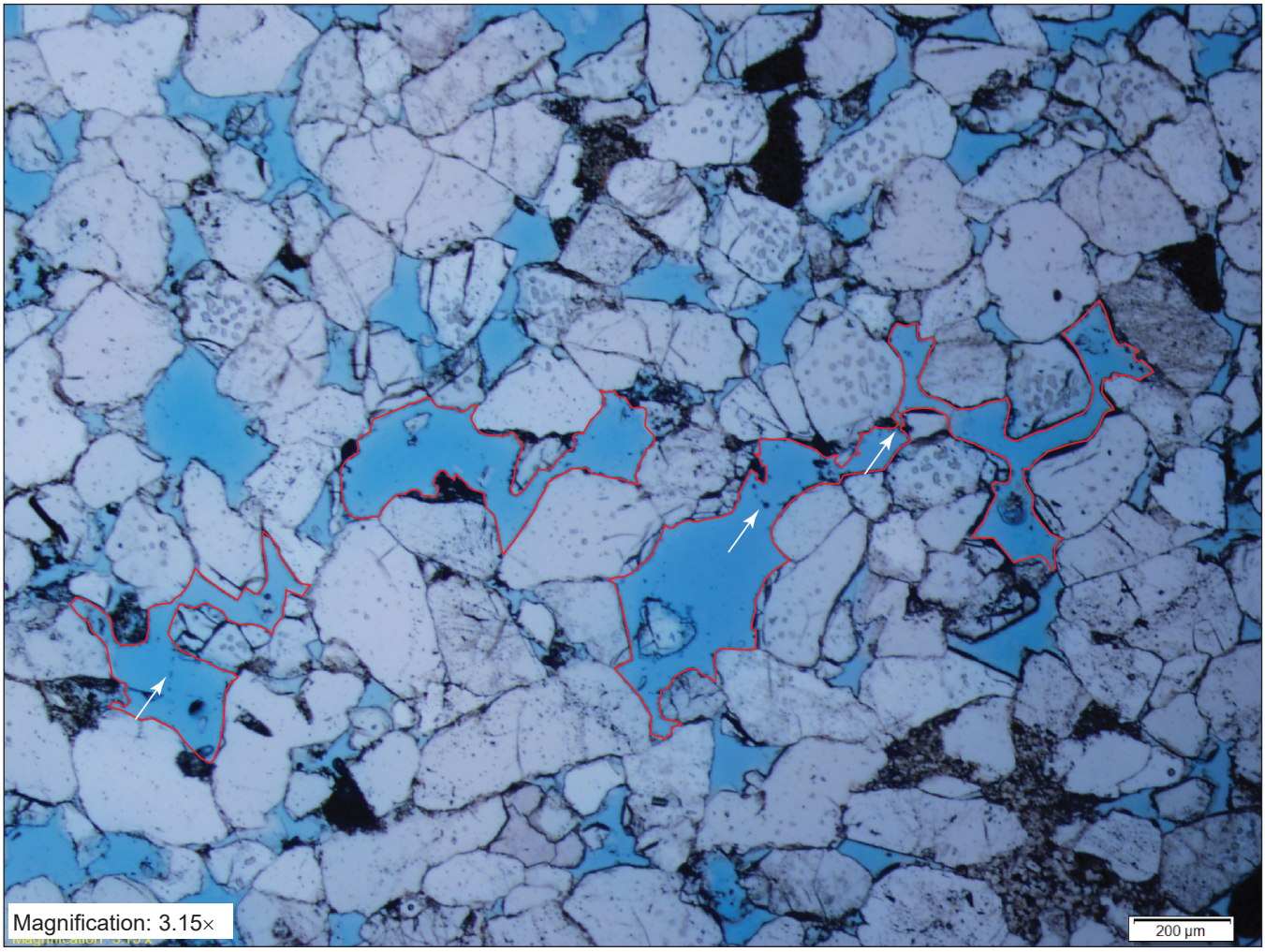

Figure 16 Example photomicrograph of cross-bedded sandstone from the Montgomery B-34 well at a depth of 2,597.5 ft (791.7 m). The scale bar in the lower right of the image is 200 μm. The quartz grains (white) are generally fine, with some medium and very fine grains, and are poorly sorted. Grains are mostly subangular to subrounded, and some grains are both angular and rounded. Dust rims (white arrows) can be observed in pore spaces outlining former grain boundaries. Large secondary pores (red patterns), likely caused by dissolution of the framework grains, carbonate cement, or both, are common. ϕ = 18.6%, k = 768 mD (0.758 μm²).

control on the trap. In this region of the field, the Cypress pinches downward and the top of the sandstone drops below the oil column (Figure 9). Second, at the southwestern nose of the anticline, the oil–water contact crosses several contours and drops approximately 60 ft (18.3 m) below its elevation within the main part of the field. This drop indicates that the oil–water contact tilts downward to the southwest (Figure 25) with a slope of roughly 20.6 ft/mi (3.9 m/km), or a dip angle of 0.2°. Tilted oil–water contacts may arise from several mechanisms, often hydrodynamic but also from tectonic or structural processes. Tilted oil–water contacts are significant in that they suggest the presence of ROZs below conventional oil reservoirs (Melzer et al. 2006). Whether an ROZ underlies the conventional reservoir at Noble Field is the subject of ongoing research.

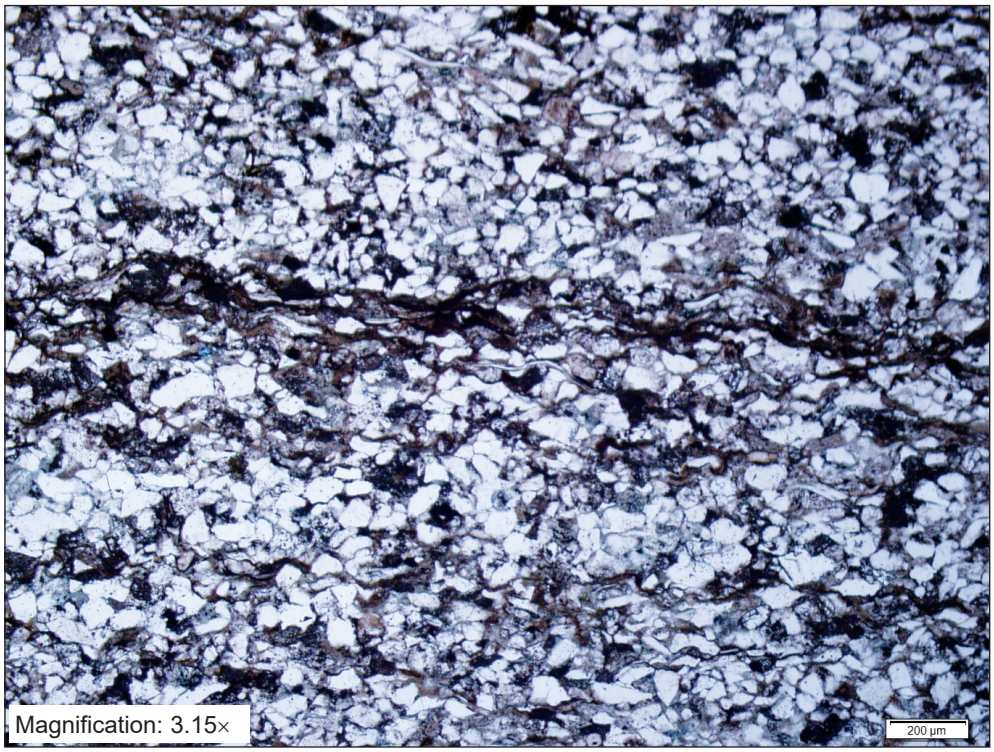

Figure 17 Example photomicrograph of wavy-bedded sandstone from the Montgomery B-34 well at a depth of 2,580.5 ft (786.5 m). The scale bar in the lower right of the image is 200 µm. Almost no pore spaces (blue) are visible in the image because the mostly fine quartz grains are well cemented by quartz and clay minerals. ϕ = 10.2%, k = 1.1 mD (0.001 µm).

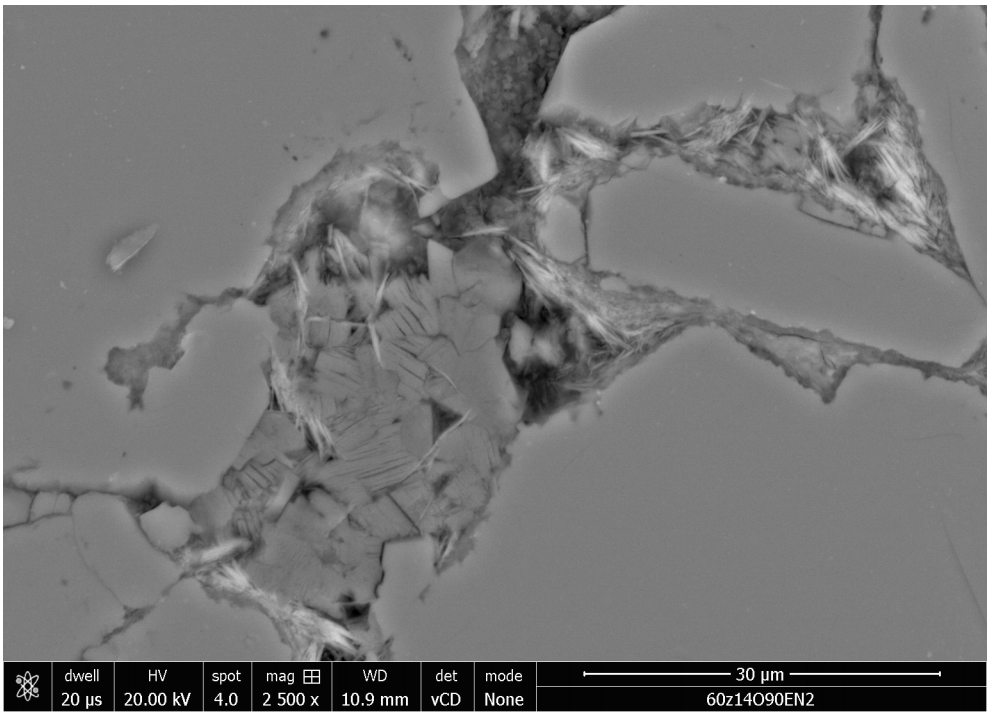

Figure 18 Example scanning electron backscatter photomicrograph from the ripple-bedded facies of the Montgomery B-34 well at a depth of 2,581.5 ft (786.8 m). The image shows fibrous illite and kaolinite booklets almost completely filling pore spaces between the quartz grains.

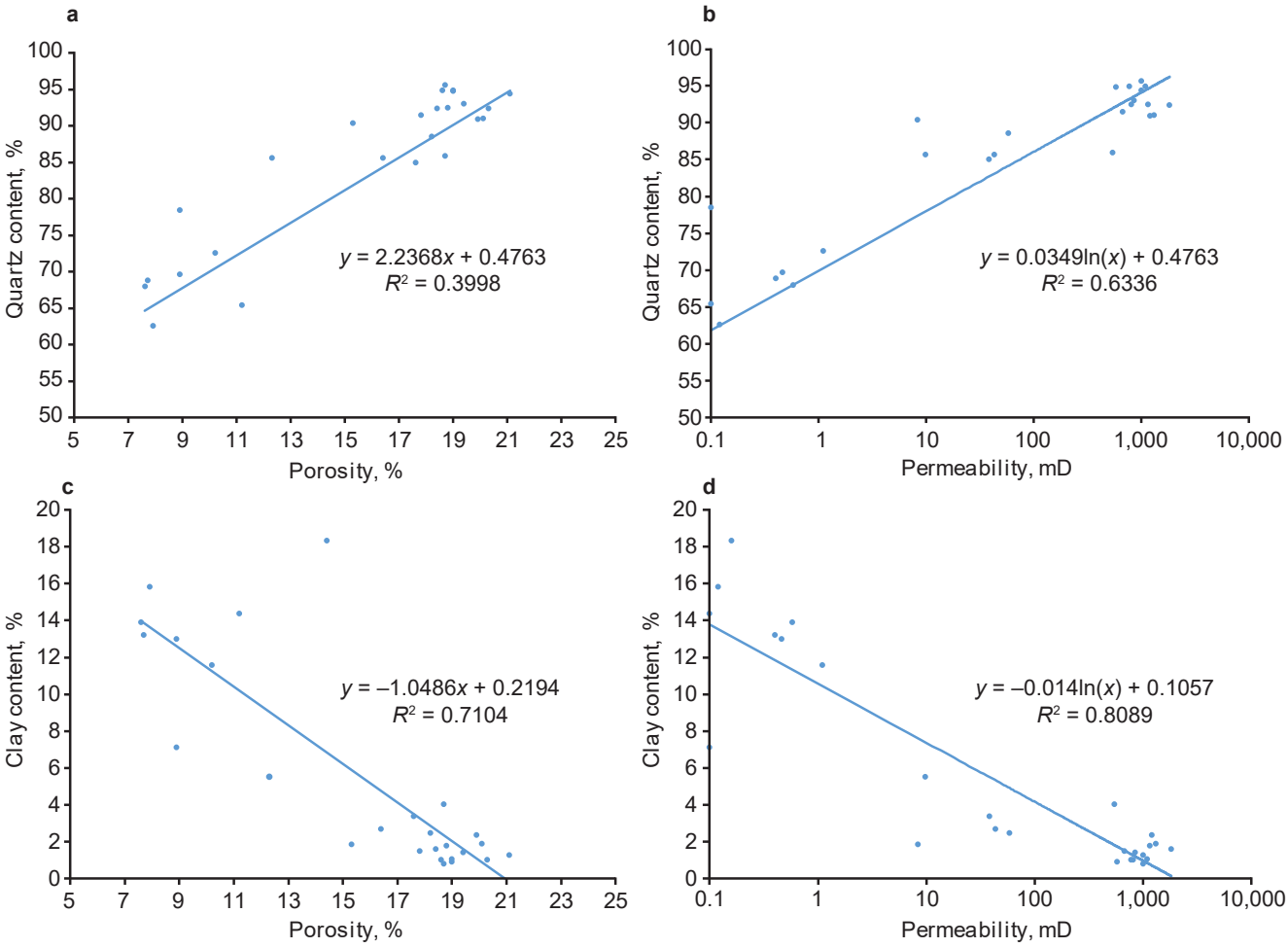

Figure 19 Reservoir properties of the Montgomery B-34 core plotted against mineralogy. (a, b) Increasing quartz content correlates directly with increasing porosity and permeability, whereas (c, d) increasing clay content has an inverse effect.

PRODUCTION CHARACTERISTICS

Production Data

Wells in Noble Field produce oil from several geologic formations, including the valley-fill Cypress Sandstone, and monthly pipeline production reports record commingled production from each lease. For this study, lease production data from the pipeline production reports were entered into a database to create cumulative and annual production curves for Noble Field (Figure 26). These curves were checked to ensure they followed typical oilfield production behavior, and the proportion of production attributed to the Cypress Sandstone was estimated.

All wells within the study area were assigned to a lease, and the behavior of the annual lease production curves was used to confirm the correct lease assignment (each new well resulted in an increase in production). Producing formations were assigned to each well by checking drilling permits and scout check tickets. In total, 239 (producing and injecting) wells within Noble Field were perforated in the valley-fill Cypress Sandstone between 1937 and 2015.

The number of wells perforated in the valley-fill Cypress Sandstone in each lease in each year was used to assign a portion of the total commingled production for that lease to the valley-fill Cypress Sandstone. First, each formation was assigned an even proportion of the production. For example, production from a lease with 10 wells that were all perforated in the valley-fill Cypress and two other formations was multiplied by a ratio (calculated by dividing the number of perforations in the valley-fill Cypress by all formations perforated, or 10/30) to assign a third of the total commingled production to the valley-fill Cypress. This ratio was updated for each year to ensure that old wells contributed proportionally less production and that spikes in production were attributed to new wells.

New cumulative and annual production curves were developed by using the production attributed to the valley-fill Cypress (Figure 26). Figure 27 shows that the valley-fill Cypress Sandstone made up 50% of the total field production over approximately 20 years from 1940 to 1960. The valley-fill Cypress Sandstone contrib-

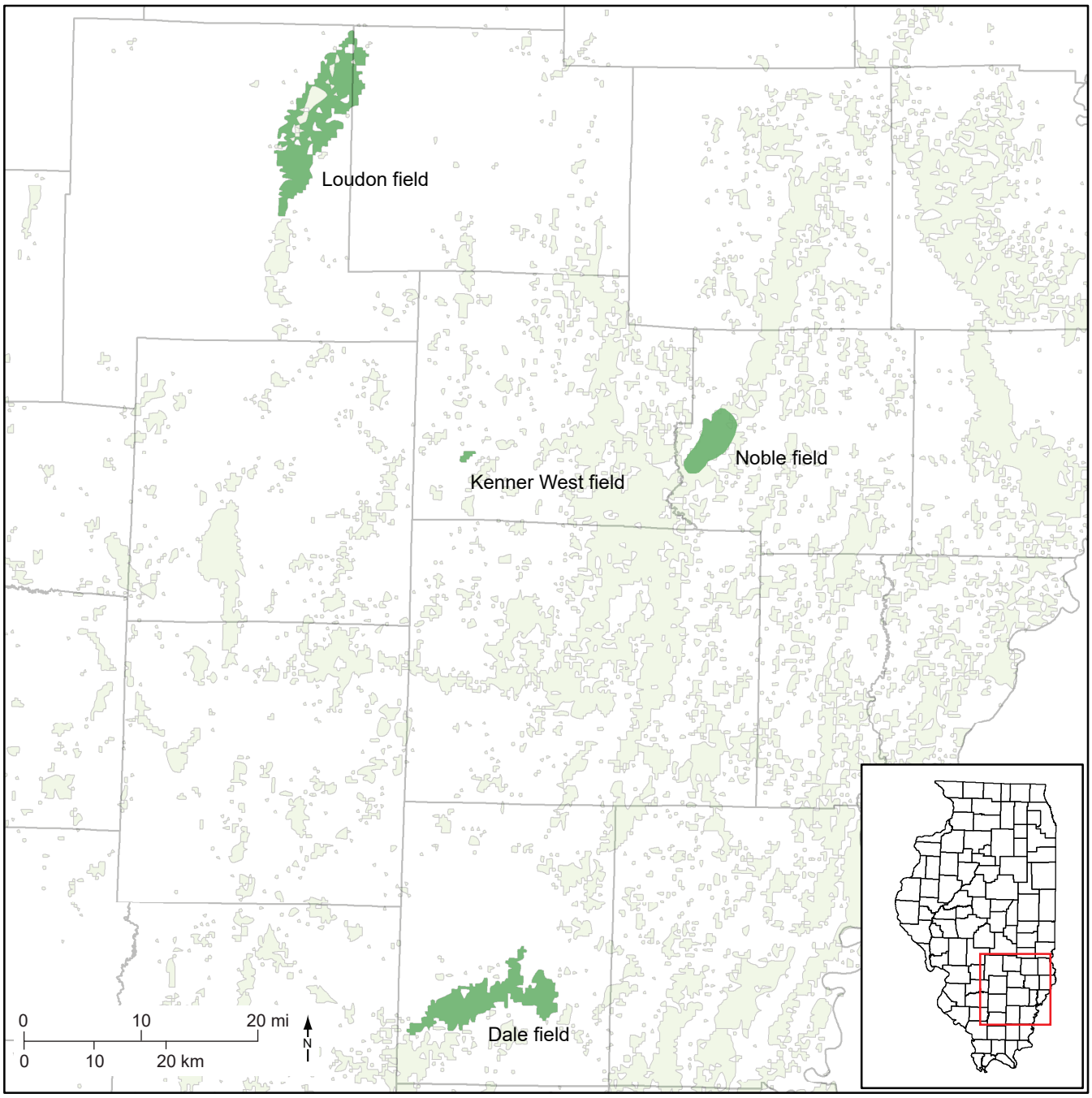

Figure 20 Map showing the locations of four fields in the Basin with core-measured porosity and permeability data from the valley-fill Cypress Sandstone.

Table 3 Typical core-measured porosity and permeability values observed in the valley-fill Cypress Sandstone in other fields in the Illinois Basin

Field	County	Depth to Cypress, ft (m)	Typical porosity, %	Typical permeability, mD (μm²)
Loudon	Eastern Fayette	1,600 (487.7)	19.2	80.9 (0.080)
Noble	Western Richland	2,600 (792.5)	18.0	482.0 (0.476)
Kenner West	Southwestern Clay	2,600 (792.5)	18.0	106.0 (0.105)
Dale	Southern Hamilton	2,900 (883.9)	13.5	62.5 (0.062)

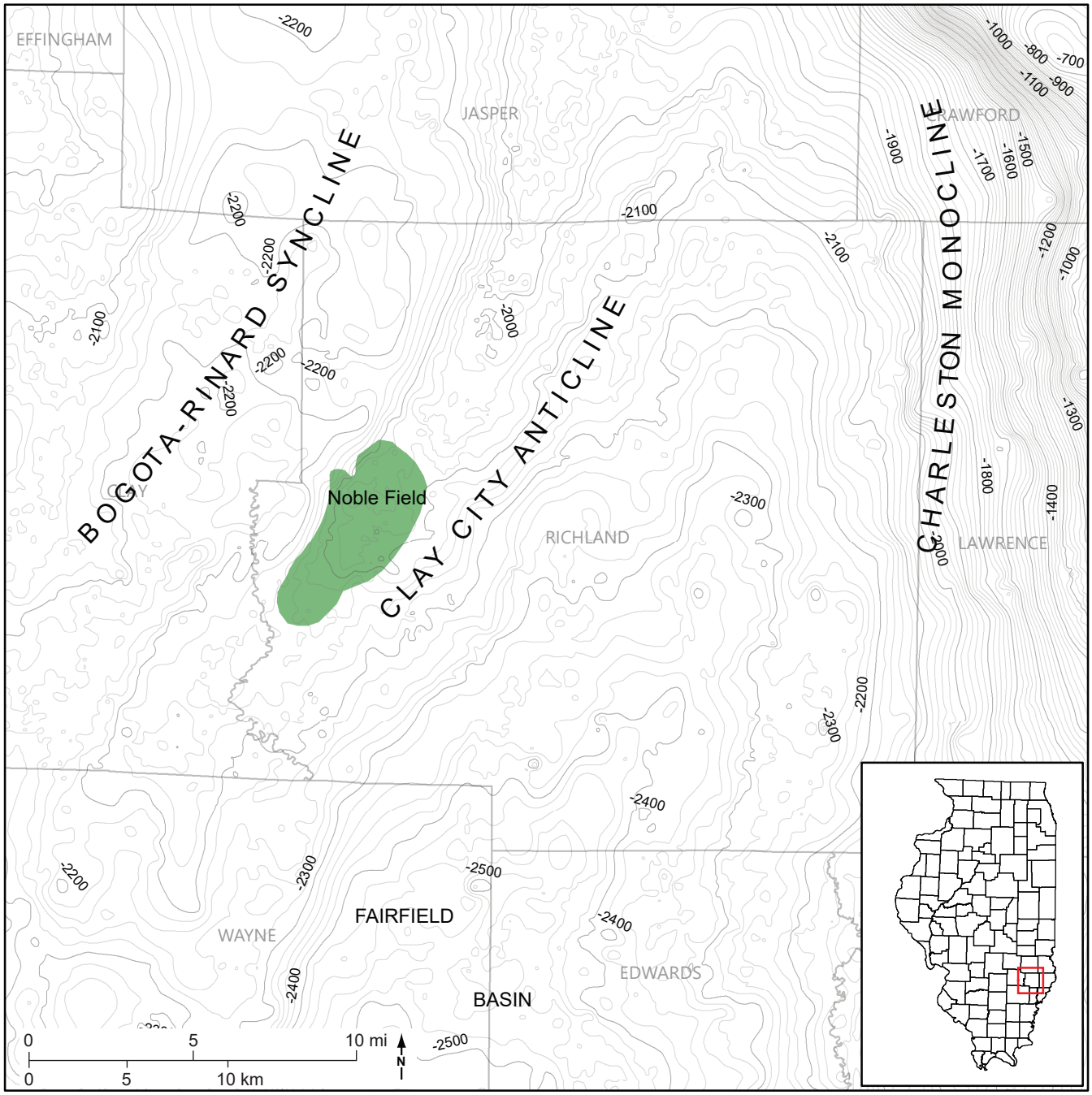

Figure 21 Structure map contoured on the subsea elevation of the base of the Beech Creek Limestone. The contour interval is 20 ft (6.1 m); index contours (darkened and labeled) are 100 ft (30.5 m). Noble Field (shaded in green) is located on the Clay City Anticline. Nearby structural features are labeled.

uted proportionally less after the mid-1990s as deeper formations were preferentially targeted. Using this method, we determined that the valley-fill Cypress Sandstone accounted for approximately 24 of the total 46 million barrels of oil (MMBO; 3.8 of 7.3 million m^3) of commingled cumulative production in Noble Field.

Well locations were used to define lease boundaries. The resulting lease map was checked against existing maps from waterflood reports and used to create a bubble map of the cumulative production from the valley-fill Cypress Sandstone normalized by the number of wells in a given lease (Figure 28). The cumulative valley-fill Cypress production for each lease was divided by the number of Cypress producing wells assigned to the lease to estimate the cumulative production per well. The bubble map shows the spatial distribution of production from the valley-fill Cypress Sandstone and a thickness map of the valley-fill Cypress

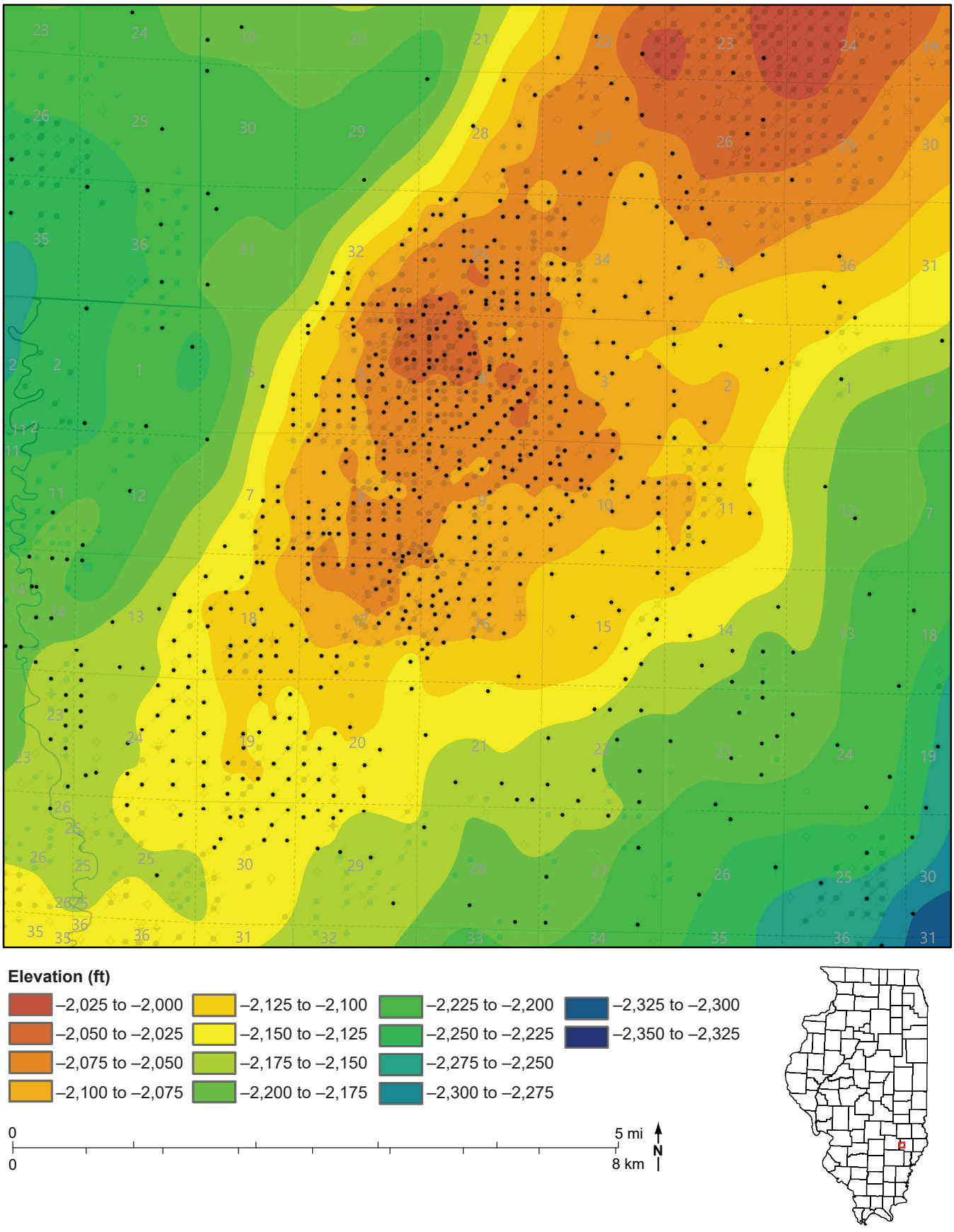

Figure 22 Map of Noble Field showing the structure at the base of the Beech Creek Limestone. Data points are shown as black dots. The contour interval is 25 ft (7.6 m), and contours are color-filled. The map shows the southwest-plunging Clay City Anticline. A northwest–southeast-trending saddle between structural highs may be related to a thinning trend in the valley-fill Cypress Sandstone (Figure 9).

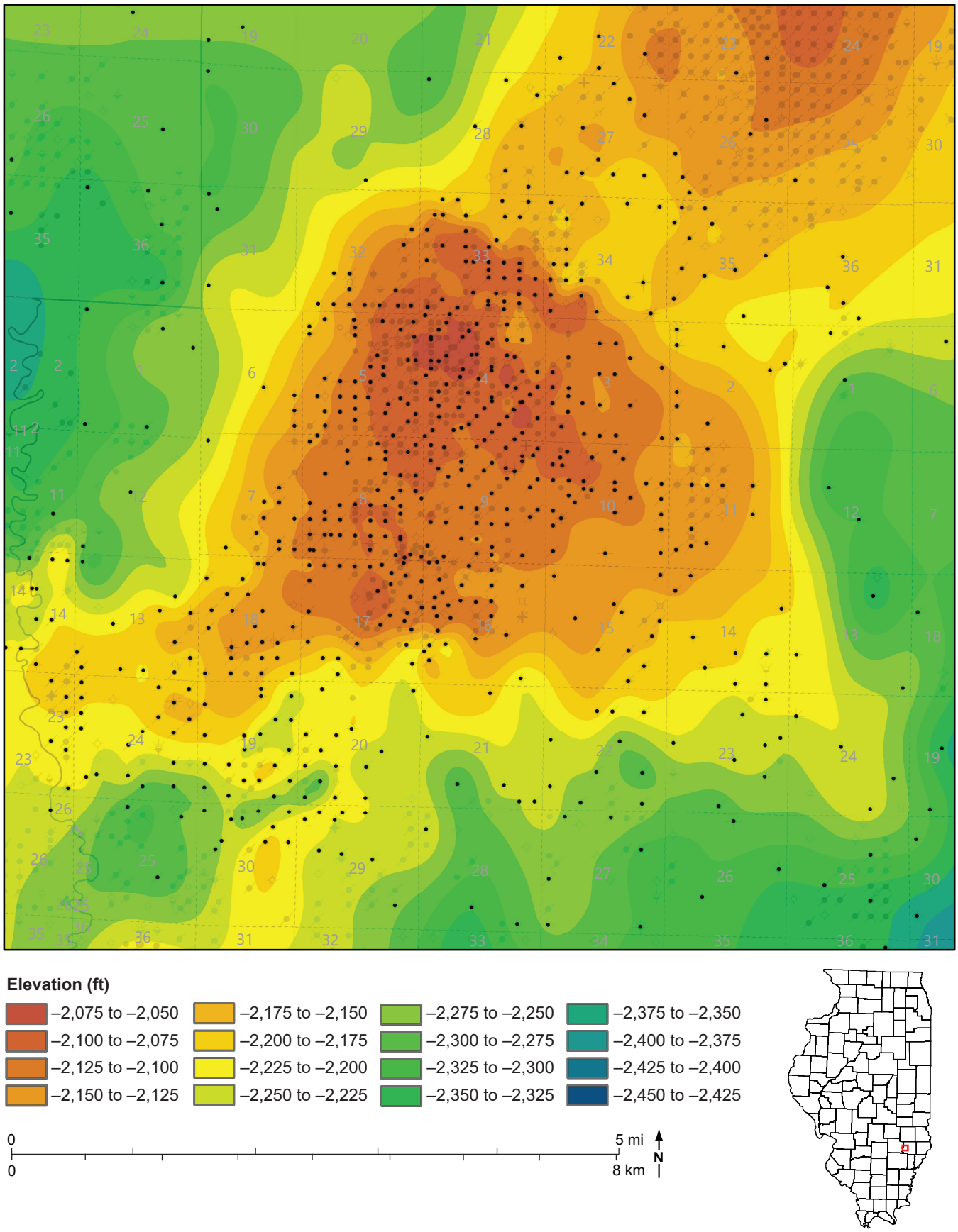

Figure 23 Map of Noble Field showing the structure of the top of the valley-fill Cypress Sandstone. The contour interval is 25 ft (7.6 m), and contours are color-filled. The map shows the northeast–southwest-trending and southwest-plunging Clay City Anticline similar to the structure map of the Beech Creek Limestone (Figure 22), but it also shows how the thickness of the Cypress Sandstone influences the structure by extending the structurally high area to the southeast and forming a nose with a gentler slope on the eastern flank of the anticline. A northwest–southeast-trending saddle between Noble and Noble North Fields is related to a thinning trend in the valley-fill Cypress Sandstone. Similarly, the northwest–southeast-trending structural high perpendicular to the Clay City Anticline coincides with the axis of thick sandstone (Figure 9). The data points are shown as black dots.

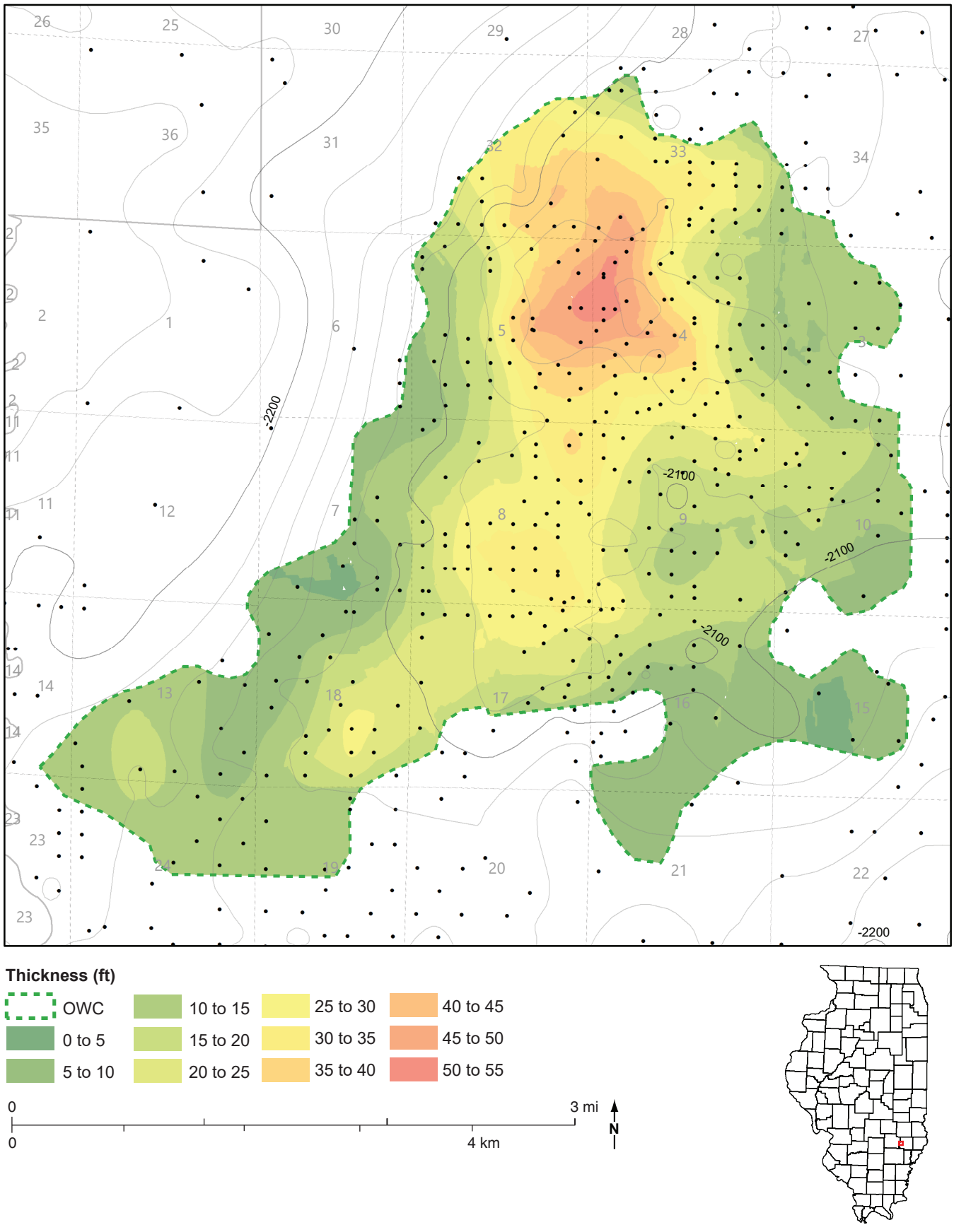

Figure 24 Isopach map of the oil reservoir developed in the top of the valley-fill Cypress Sandstone. The isopach contour interval is 5 ft (1.5 m) and the contours are color-filled. The green dashed line represents the oil–water contact (OWC) in Noble Field. The thickest oil column coincides with the peak of the structure, as can be seen in the overlaid structure contours of the Beech Creek Limestone. The structure contour interval is 20 ft (6.1 m). The data points are shown as black dots.

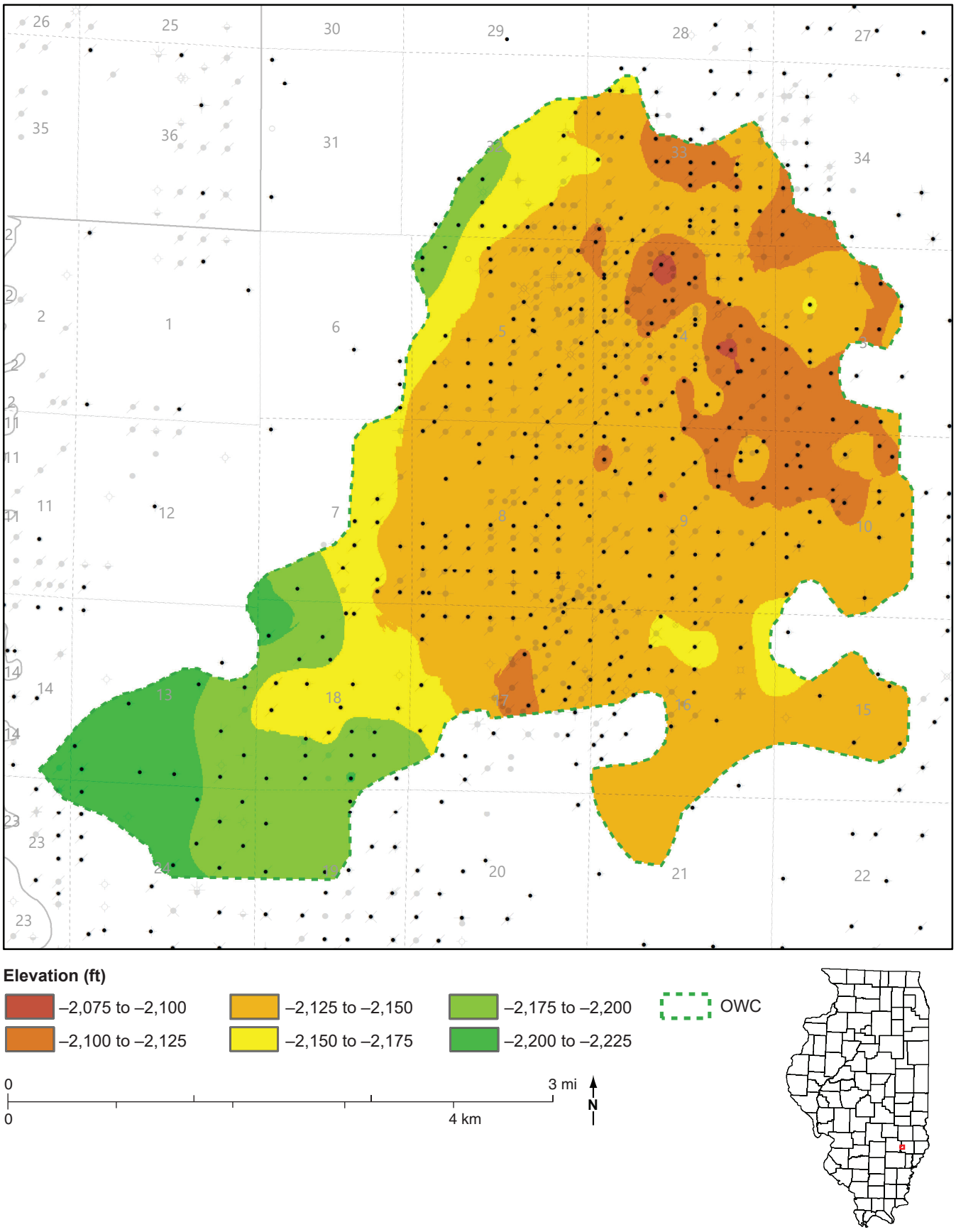

Figure 25 Structure map contoured on the oil–water contact (OWC) showing its southwestward tilt. The contour interval is 25 ft (7.6 m) and the contours are color-filled. The green dashed line represents the oil–water contact in Noble Field. The data points are shown as black dots.

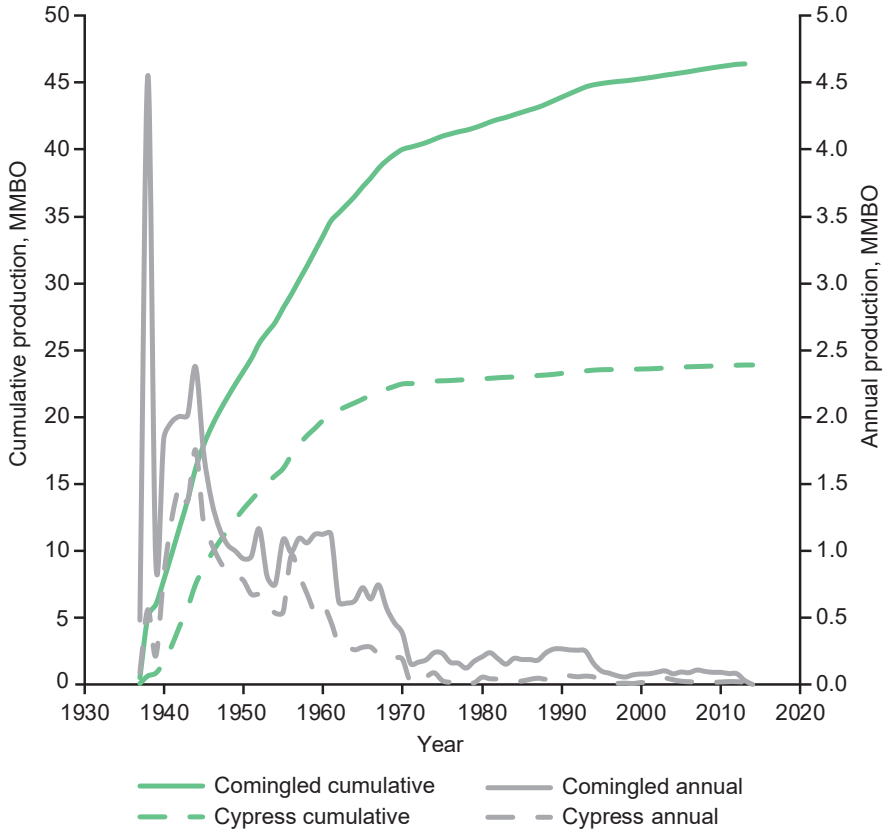

Figure 26 Graph of cumulative (green line) and annual (gray line) production data for all formations and all leases in Noble Field over the entire history of the field. The Cypress Sandstone accounts for approximately 50% of the cumulative production (green dashed line). MMBO, million barrels of oil.

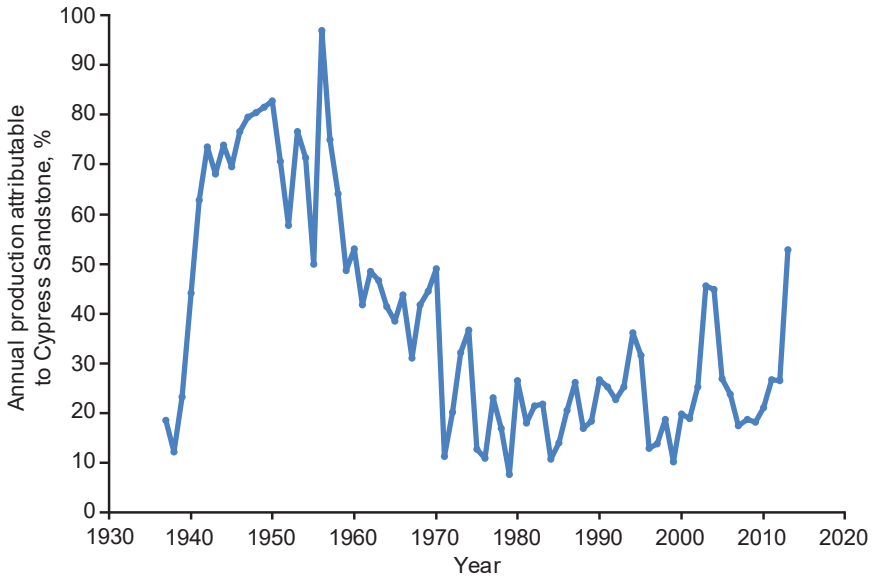

Figure 27 Graph showing the proportional contribution of the Cypress Sandstone to annual oil production in Noble Field. Cypress Sandstone annual production values are shown in Figure 26. The contribution of the Cypress Sandstone shown here is normalized to the annual cumulative production from all formations.

Sandstone oil column. The magnitude of production for each lease agrees well with the geologic interpretation; that is, with few exceptions, leases with a high production per well generally overlie areas of valley-fill Cypress with a thick oil column. The southeastern corner of sec. 8 has leases that have anomalously low production relative to the oil column thickness. This area is in downtown Noble, Illinois, and consists of very small leases that produced for only a few years, leading to low cumulative production volumes. Therefore, it is reasonable to assume that poor production in this area is due to completion practices instead of a geologic control.

Production History

Production from the valley-fill Cypress Sandstone occurred over most of Noble Field. The greatest concentration of Cypress producing wells occurred in sec. 4, T3N, R9E (Figure 29). Most wells that specifically targeted the valley-fill Cypress Sandstone had open-hole, natural completions. Many other wells were initially drilled to deeper target formations and later plugged back and perforated in the oil reservoir in the top of the valley-fill Cypress Sandstone. Initial production values from wells producing only from the Cypress Sandstone commonly showed 100 to 300 barrels of oil per day (BOPD; 15.9 to 47.7 m^3/d) with 0 to 300 barrels of water per day (47.7 m^3/d). The highest initial production recorded was 1,896 BOPD (301.5 m^3/d) from the C.T. Montgomery B-2 well (API 121590139100) in northwestern sec. 4, T3N, R9E (Figure 30).

The production history of Noble Field was analyzed to determine the contribution of production from the Cypress Sandstone relative to the cumulative production from all formations and to understand factors influencing rapid peaks and declines in annual production (Figure 26). Oil production from Noble Field in 1937 was 947,340 bbl (150,627 m^3), with a daily average of 10,033 BOPD (1,595 m^3/d) from 47 wells over 470 acres (190 ha; Bell 1938). The field underwent rapid development. Annual production peaked in 1938, when more than 4.5 MMBO (0.72 million m^3) was being produced. By July 1939, 162 wells were producing from 2,920 developed acres (1,182 ha; Lee 1939). A rapid decline to annual

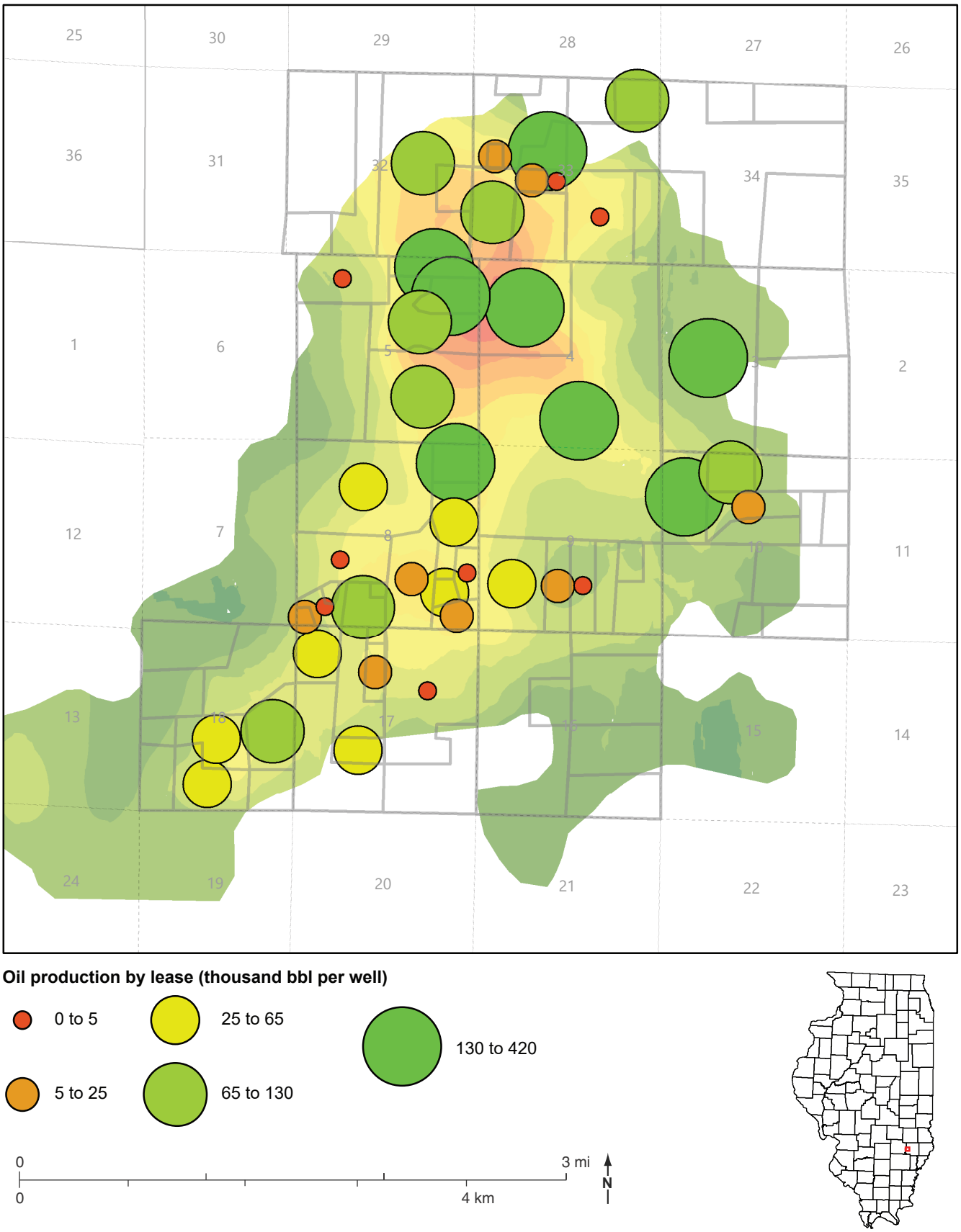

Figure 28 Bubble map showing the cumulative lease production of the valley-fill Cypress Sandstone normalized by the number of wells in each lease. The bubble map is overlain on an isopach map of the oil reservoir (see Figure 24). Lease boundaries were defined from well data and waterflood reports, and bubbles were created by evenly dividing the production from the 40 leases with valley-fill Cypress production into five groupings. Each bubble size group includes eight leases. The northernmost bubble outside the mapped oil thickness shows Cypress production from Noble North Field. bbl, barrels.

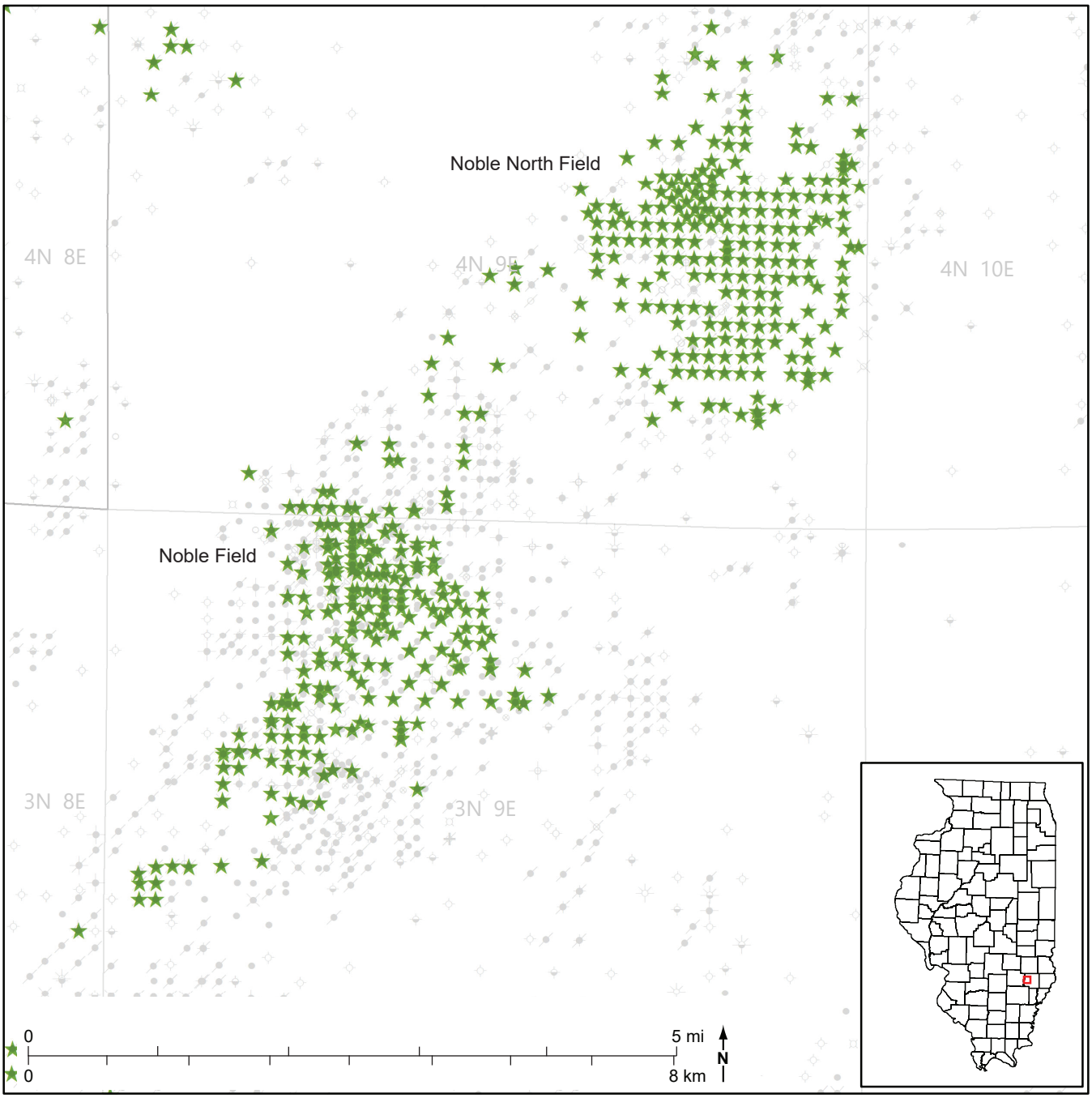

Figure 29 Map showing wells producing from a relatively thin oil reservoir in the valley-fill Cypress Sandstone in Noble Field, mainly in T3N, R9E. Northeast of Noble Field, in Noble North Field, the valley-fill Cypress breaks up into thinner sandstone bodies and production comes from an upper 6 to 30 ft (1.8 to 9.1 m) thick oil-saturated sandstone separated from an underlying thick, brine-saturated sandstone by 20 ft (6.1 m) of shale (Lee 1939; MGSC 2005). Green stars indicate wells with oil production attributed to the Cypress Sandstone.

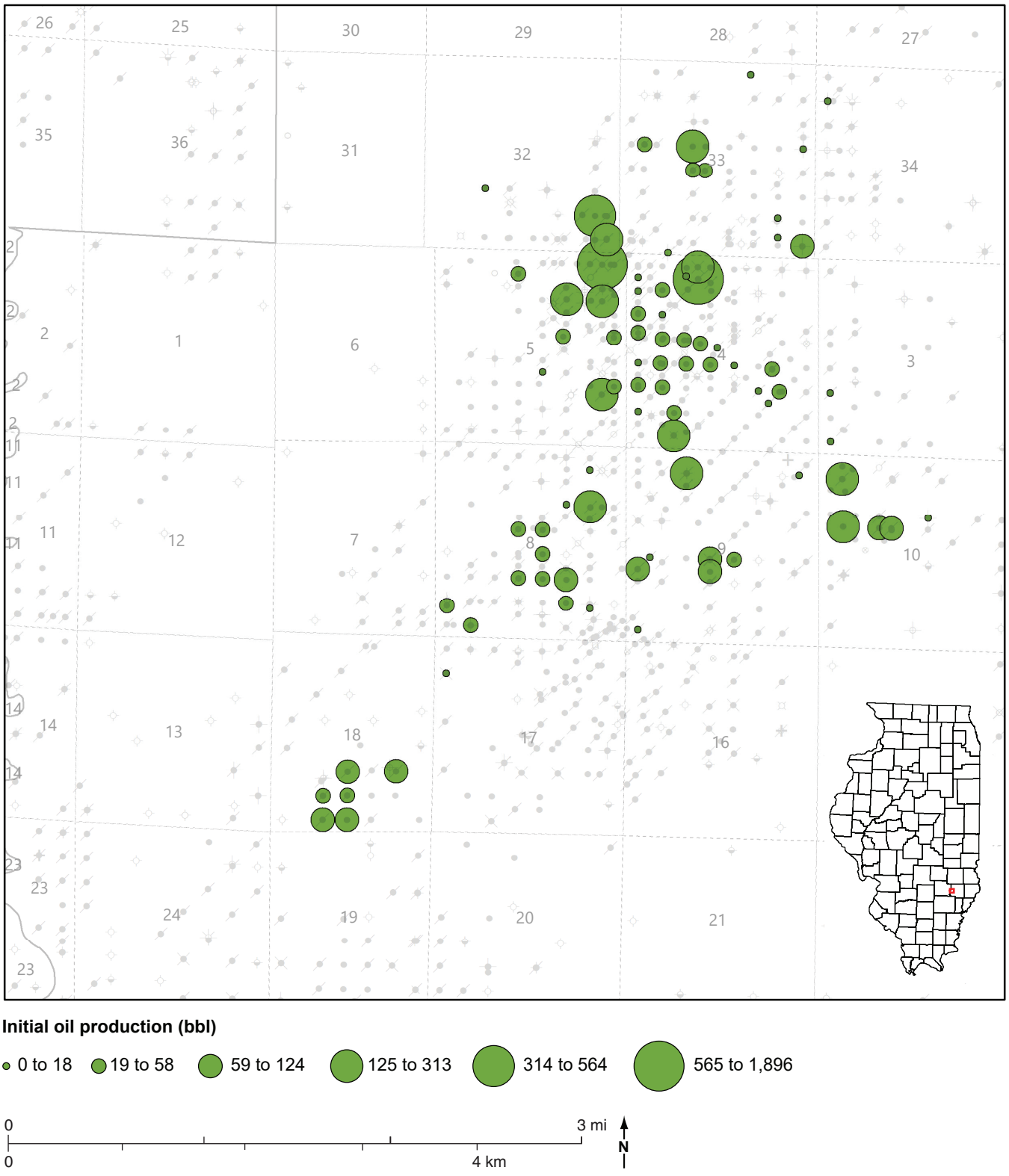

Figure 30 Map of initial oil production rates for wells in Noble Field where data were available. The size of a circle is scaled to the magnitude of oil production attributed to the Cypress Sandstone. bbl, barrels.

Table 4 Waterfloods conducted in Noble Field

Waterflood unit	Waterflood unit ID number	Section (township)	Start year	End year	Target formation	Water source formation
East Noble	3403	2, 10, 11 (3N, 9E)	1955	1969	Spar Mountain ("Rosiclare")	Cypress
Old Noble	3404	4, 5, 8, 9 (3N, 9E) 32, 33, 34 (4N, 9E)	1954	2009	Fredonia ("McClosky")	Cypress
Noble Coop	3416	8 (3N, 9E)	1954	1975	Fredonia ("McClosky")	Produced and Cypress
Hog Run	3431	17, 20 (3N, 9E)	1965	2001	Aux Vases, Fredonia ("McClosky")	Cypress
Colborn	3446	4, 5, 8, 9 (3N, 9E)	1976	2006	Aux Vases, Fredonia ("McClosky"), St. Louis, Salem	Produced
Foss–Bowers	3450	8 (3N, 9E)	1979	2006	Cypress	Produced
Clark–Grubb–Evans	3449/3451	18 (3N, 9E)	1962	2006	Cypress	Produced

production rates of 1 to 2 MMBO (0.16 to 0.32 million m^3) occurred throughout the 1940s (Figure 26). Annual production continued to decline steeply throughout the 1950s and 1960s before a more gradual decline after 1970, when annual production averaged slightly more than 200 thousand barrels of oil (MBO; 31.8 thousand m^3) until 1995. Since 1995, annual production has rarely exceeded 100 MBO (15.9 thousand m^3). Cumulative oil production from Noble Field exceeds 45 MMBO (7.2 million m^3). Additional details about Noble Field oil production are discussed in the Production Characteristics section.

Waterflooding

Waterflooding in Noble Field began in August 1954 as operators attempted to return energy to small, compartmentalized "McClosky" reservoirs (Witherspoon and Jackson 1955). The valley-fill Cypress Sandstone served as a water source for waterfloods in deeper formations (Table 4). Deeper formations were the primary target, but the valley-fill Cypress Sandstone was the target of two waterfloods, one beginning in 1962 and one beginning in 1979. Waterflood information is on file at the ISGS and is available via the Illinois Oil & Gas Resources (ILOIL) website (https://www.isgs.illinois.edu/illinois-oil-and-gas-resources-interactive-map).

Completion Techniques

Oil production from the valley-fill Cypress Sandstone at Noble Field has historically led to water coning and excessive water production. Operators have attempted to minimize water production by setting casing within the first few feet (<1 m) of the oil-saturated sandstone and then completing the well open hole, but this has generally not been successful, as described in a Core Laboratories, Inc. report on the John O. Coen 23 well (API 121590138200, sec. 4, T3N, R9E; scanned and available from https://www.isgs.illinois.edu/illinois-oil-and-gas-resources-interactive-map). Squeeze jobs (i.e., injecting cement slurry into a zone, generally for pressure-isolation purposes) to cement off the water-producing part of the sandstone before perforating the upper half of the oil reservoir can help slow the infiltration of water, but the Core Laboratories, Inc. report indicated most wells still have a 50% or greater water cut (i.e., ratio of water produced to the volume of total liquids produced). Many wells in Noble Field targeted deeper formations first, generally the "McClosky," and the wells were plugged back and perforated in the Cypress Sandstone upon depletion of the original target.

Since 1993, five horizontal wells have been drilled into the valley-fill Cypress Sandstone at Noble Field (Table 5). These wells have targeted the top of the valley-fill Cypress Sandstone approximately 20 to 50 ft (6.1 to 15.2 m) above the oil–water contact. Two of them (Montgomery wells in Table 5), in the northwest quarter of sec. 4, targeted the thickest oil column in the field (Figure 24); however, the Montgomery B-26 well was drilled too high, resulting in poor oil production, and the well was ultimately plugged. The Coen and Runyon wells were drilled in areas of thinner oil columns. Because of lease-based production reporting, the long-term productivity of these wells is not known, but the initial production records for all wells indicate significant water production.

RESERVOIR CHARACTERISTICS

Temperature, Pressure, and Formation Fluid

The reservoir temperature for the Cypress Sandstone at Noble Field was determined to be 89 °F (31.7 °C), in agreement with the expected temperature (88 °F at 2,675 ft, or 31.1 °C at 815.3 m) based on the standard geothermal gradient for the Illinois Basin (at 100 ft, 62 °F + 1 °F per 100 ft depth, or at 30.5 m, 16.7 °C + 0.56 °C per 30.5 m depth). Appendix C details the data and calculations used to determine the reservoir temperature. Reservoir pressure, as recorded in several

Table 5 The five horizontal wells drilled into the top of the valley-fill Cypress Sandstone in Noble Field[1]

Well name	API number	Location	Year drilled	Initial production	Status
C.T. Montgomery B-26	121592547600	NW sec. 4, T3N, R9E	1993	No data	Plugged as of 2007
C.T. Montgomery B-27	121592548100	NW sec. 4, T3N, R9E	1993	34 bbl (5.4 m^3) of oil/121 bbl (19.2 m^3) of water	Producing
John O. Coen 1H	121592629100	NE sec. 9, T3N, R9E	2009	No data	Producing
John O. Coen 3H	121592629800	SE sec. 4, T3N, R9E	2010	103 bbl (16.4 m^3) of oil/2,200 bbl (349.8 m^3) of water	Producing
Runyon 1-HOR-10	121592644800	NW sec. 10, T3N, R9E	2015	20 bbl (3.2 m^3) of oil/55 bbl (8.7 m^3) of water	Producing

[1]The year drilled and status of the well area are also listed when available. bbl, barrels.

drill stem tests from the 2000s, is roughly 1,200 psi (8.27 mPa). The standard hydrostatic pressure gradient of 0.433 psi/ft (9.79 kPa/m) for the normally pressured Illinois Basin gives an expected pressure of 1,104 psi (7.61 mPa) for an average reservoir depth of 2,550 ft (777.2 m), which makes the Cypress at or slightly above hydrostatic pressure. The primary reservoir-drive mechanism for the Cypress Sandstone is likely a combination of solution gas drive (i.e., gas dissolved in the fluid that provides the energy to transport and produce reservoir fluids) and bottom water drive (i.e., an aquifer below the oil field that provides the reservoir's drive energy).

Records of oil analyses from the John O. Coen 23 well (API 121590138200, SW¼SE¼ of the southeast quarter of sec. 4, T3N, R9E) from 1942 indicate an API gravity of 37.5°. A waterflood summary for the Grubb–Evans waterflood unit listed an API gravity of 31.8°. A new oil sample from a Cypress Sandstone-only tank battery yielded an API gravity of 33.3° and a viscosity of 7.1 cP. Density of the oil was 0.492 and 0.491 oz/in^3 (0.851 to 0.850 g/mL) at temperatures of 76.5 and 88.7 °F (24.7 and 31.5 °C), respectively. The wells contributing Cypress oil to the battery included the John O. Coen 90, 91, 92, 94, 98, 100; Palmer–Taylor 26; and C.L. Wilson 4 (SW¼ sec. 4 [Coen], SE¼ sec. 5 [Palmer–Taylor], and NE¼ sec. 8 [Wilson], T3N, R9E).

The disparity in oil gravity from the various samples likely relates to the original setting of the oil within the reservoir. The Coen 23 well was drilled in the early development of the field, perforated in the upper 4 ft (1.2 m) of the reservoir, and sampled shortly after completion, resulting in a higher API gravity. Oil gravity commonly increases from the base to the top of the reservoir because higher volatiles naturally migrate upward over geologic time. The later waterflood unit and tank battery oil samples, which were collected farther down the production curve and likely have a lower gas content, may reflect oil that was originally lower in the reservoir that had migrated up over time with development and production in the field, particularly as water coning moved oil from lower in the reservoir upward.

An operator in Noble Field reported that biodegradation has increased the viscosity of the oil produced from the Cypress, as evidenced by chunks of paraffin and "slime balls" recovered from produced oil. Operators must circulate biocide through equipment every few months to prevent corrosion and biomass from plugging the reservoir permeability. The brine–oil interactions responsible for biodegradation of the oil may not be limited to the oil–water contact and may reflect the incursion of brine into the reservoir from water coning, which is associated with the production or disposal of formation waters into the Cypress over several decades.

Meents et al. (1952) recorded a brine composition of 98,182 parts per million (ppm) of total dissolved solids (TDS) from an unspecified well in sec. 8, T3N, R9E. An analysis by Demir (1995) of a brine sample from a well northeast of Noble Field had slightly more than 101,000 ppm of TDS. A new brine sample that was collected from the John O. Coen 92 well (API 121592607500, NW¼SW¼ sec. 4, T3N, R9E) yielded 98,121 ppm of TDS, consistent with the previous findings. The complete cation and anion brine analyses are provided in Appendix D.

Water resistivity values for the Cypress Sandstone can be calculated by using Equation 3 from Demir (1995):

$$R_{w(T)} = 957 \Big/ \left[(\mathrm{TDS})^{0.778} \times (1.017)^{T} \right], \quad (1)$$

where $R_{w(T)}$ is water resistivity (in ohm-m) at temperature T (°C), and TDS is the total dissolved solids concentration (in mg/L or ppm). With a reservoir temperature of 89 °F (31.7 °C) and a TDS value of 98,121, the R_w for the brine is 0.073.

Volumetric Analysis of the Oil Reservoir

Original oil in place (OOIP) was calculated for the Cypress Sandstone reservoir at Noble Field by using a modified volumetric formula:

$$\mathrm{OOIP} = \left(\frac{7{,}758 \times \phi \times (1 - S_w) \times A \times h}{B_{oi}} \right) \times \mathrm{net}, \quad (2)$$

where 7,758 is barrels of oil per acre foot, ϕ is porosity, S_w is water saturation, A is area, h is height, B_{oi} is a formation volume factor, and net is the average net/gross ratio within the reservoir as derived from normalized SP logs.

Three different approaches were taken to calculate the OOIP to compare traditional methods of calculating the OOIP with a model-based approach. The first two used methods based on the traditional volumetric formula, whereas the third

Table 6 Volumetric characteristics of the Cypress Sandstone at Noble Field[1]

Reservoir volumetric characteristic[1]	Production, MMBO (million m^3)
OOIP (traditional volumetrics, average porosity, 87% net/gross)	94.5–110.2 (15.0–17.52)
OOIP (traditional volumetrics, porosity gradient)	93.3–108.8 (14.8–17.30)
OOIP (geocellular model-based volumetrics, average porosity)	88.7–103.5 (14.1–16.46)
Mobile OOIP (to water, assuming 25% S_{or})	54.6–70.1 (8.68–11.1)
Cumulative production	23.9 (3.80)
Recovery efficiency	26.3%–22.5%
Remaining mobile oil	30.7–46.2 (4.88–7.35)

[1]Calculations are described on pages 40, and 41. OOIP, original oil in place; S_{or}, residual oil saturation; MMBO, million barrels of oil.

Table 7 Area, volume, and average porosity for each 5 ft (1.5 m) slice of the valley-fill Cypress Sandstone oil reservoir used to calculate the original oil in place[1]

Iso contour	Area, acres (ha)	Volume, acre ft (ha m)	Average porosity, %
5	6,915.8 (2,798.8)	34,579.0 (4,265.3)	11.4
10	6,841.9 (2,768.9)	34,209.3 (4,219.7)	14.0
15	5,149.3 (2,083.9)	25,746.6 (3,175.8)	15.5
20	3,498.5 (1,415.8)	17,492.7 (2,157.7)	17.8
25	2,458.0 (994.8)	12,290.1 (1,516.0)	18.3
30	1,663.6 (673.3)	8,318.2 (1,026.0)	17.3
35	1,025.6 (415.1)	5,127.8 (632.5)	17.8
40	566.4 (229.2)	2,832.2 (349.4)	16.5
45	295.2 (119.5)	1,475.8 (182.0)	16.8
50	139.8 (56.6)	699.1 (86.2)	17.8
55	33.9 (13.7)	169.3 (20.9)	17.1

[1]The iso contour column indicates the base of the slice, measured in feet below the top of the reservoir.

used values taken from a three-dimensional geocellular model of the valley-fill Cypress Sandstone in Noble Field (Grigsby and Webb, 2020).

For the traditional approaches, the reservoir area (A) was the area within the line that represented the oil–water contact (Figure 24), and height (h) was the average thickness of the reservoir from the oil–water contact to the top of the Cypress Sandstone. An average porosity of 17.3% had been determined previously. Because of the blocky nature of the Cypress Sandstone on geophysical logs, the entire thickness was considered of equal reservoir quality. Data from 385 normalized SP logs across the field indicated that the average net/gross ratio within the valley-fill Cypress Sandstone was 87%. Thus, the calculated OOIP was multiplied by 87% to obtain the final OOIP (Table 6). Two typical values for water saturation (S_w), 30% and 40%, were used to give a range of possible OOIP values.

The Cypress Sandstone reservoir is influenced by its variable shale content and calcite cement, so a second approach was used to apply a porosity gradient to obtain a refined value for OOIP that would perhaps better represent the heterogeneity of the reservoir. The reservoir was divided into 5 ft (1.5 m) thick slices, and the volume and average porosity (from porosity logs) were calculated for each slice (Table 7). The OOIP was calculated for each slice and summed to determine the final OOIP, as reported in Table 6.

A third alternative calculation of OOIP was conducted by using values of the reservoir volume (reservoir area [A] × reservoir height [h]) and average porosity ($\varnothing$) determined from a three-dimensional geocellular model created in Isatis software by Geovariances (https://www.geovariances.com/en/software/isatis-geostatistics-software/). The surface elevations for the top of the valley-fill Cypress Sandstone and the oil–water contact used in the geocellular model were the same as those used in the traditional volumetric calculations. This permitted comparison of the modeling and traditional approaches to determine the OOIP. See Grigsby and Webb (2020) for further details on the modeling.

The formation volume factor (B_{oi}) of 1.06 for an oil sample from the John O. Coen 23 well (API 121590138200, sec. 4, T3N, R9E) was used to convert the volume of oil in the reservoir to the volume of produced oil at the surface. Volume loss was attributable to degassing of the oil at atmospheric pressure. As with the traditional volumetric calculations, two typical values for S_w, 30% and 40%, were used in the model calculations to give a range of OOIP values.

The resulting OOIP values are listed in Table 6. The OOIP calculated by the modeling approach yielded a lower value, likely because of the ability of the model to better incorporate localized,

log-indicated zones of low-quality reservoir (e.g., shaley or cemented sandstone zones that were not represented in the core plug data). In other words, the model approach better honored all the data, whereas the traditional approaches tended to generalize the data and, in this case, were probably overly optimistic. The average reservoir porosity calculated from the geocellular model was 12.6%, which is nearly 5% lower than the core plug data used in the traditional calculations.

Mobile OOIP is a calculation of the portion of oil that can be removed above residual oil saturation (S_{or}). The mobile OOIP value was calculated by using the standard volumetric formula:

$$\text{Mobile OOIP} = \left\{7{,}758 \times \phi \times \left[1 - (S_o - S_{or})\right] \times A \times h\right\} / B_{oi}, \quad (3)$$

where A, h, and B_{oi} are defined the same as in the OOIP equation, S_o is oil saturation, and S_{or} is residual oil saturation.

Recovery efficiency was calculated by using the average of the two OOIP values derived from the porosity gradient method and the geocellular model method. Residual oil saturation (S_{or}) into water was assumed to be 25% (MGSC 2005). The remaining mobile oil was the difference in cumulative production from mobile OOIP.

The results of the volumetric calculations showed that the three methodologies for calculating OOIP produced comparable results, with an average estimated OOIP of 100 MMBO (15.9 million m^3) of Cypress oil. With a cumulative production of 23.9 MMBO (3.80 million m^3), more than 75 MMBO of oil remains in the reservoir, of which an estimated 30.7 to 46.2 MMBO (4.88 to 7.35 million m^3) is movable oil.

CONCLUSIONS

Detailed geologic characterization of Noble Field yielded several findings pertinent to the geology and reservoir properties of the valley-fill Cypress Sandstone:

1. The valley-fill Cypress Sandstone is interpreted as being composed of multistory fluvial sandstone deposited during lowstand and transgression, with evidence of a change to estuarine conditions near the top. Despite some internal heterogeneity, where multiple sandstone stories amalgamate (as in Noble Field), they create thick, relatively widespread sandstone bodies that have characteristics favorable for CO_2 storage, such as high lateral and vertical permeability, limited compartmentalization, and large pore volumes.
2. The valley-fill Cypress Sandstone in Noble Field has some of the highest permeability values known from the Cypress anywhere in the Illinois Basin. Petrographic analysis of the cross-bedded sandstone revealed a hybrid pore system of primary intergranular and secondary porosity. Facies deposited in high-energy environments that are relatively coarser grained and that have long, well-connected pores resulting from carbonate cement dissolution likely contribute to the high permeability values.
3. The valley-fill Cypress Sandstone accounts for approximately 50% of oil production in Noble Field. Roughly 24 MMBO (3.8 million m^3) of the approximately 46 MMBO (7.3 million m^3) produced in the field is from the Cypress.
    a. Volumetric calculations indicate an average OOIP of 100 million barrels (MMbbl; 15.9 m^3) in the valley-fill Cypress Sandstone at Noble Field.
    b. More than 75 MMbbl (12 million m^3) of oil remains in the reservoir, of which 30.7 to 46.2 MMbbl (4.88 to 7.35 million m^3) is estimated to be moveable.
4. A southwesterly tilted oil–water contact and the occurrence of a persistent, parallel calcite-cemented zone beneath the oil–water contact led to the hypothesis than an ROZ may be present within the valley-fill Cypress Sandstone.
    a. Two persistent, thin calcite-cemented zones occur within the sandstone, one coincident with the oil–water contact and a second, lower zone that is parallel to the oil–water contact.
    b. The lower of these two zones may indicate a paleo oil–water contact, which may have implications for the former position of the oil–water contact before it became tilted.

The following areas are suggested for additional research to better understand the reservoir properties and petroleum system of the valley-fill Cypress Sandstone:

1. Future research is needed on the paragenetic sequence of each facies to address specific questions pertaining to reservoir quality: What are the controls on primary and secondary porosity and permeability (texture, sorting, diagenetic factors)? Do calcite cements pre- or postdate other cements? Could calcite cement have been a framework cement that preserved initial porosity?
2. Further investigation is necessary to determine the relationship between the calcite-cemented zones and the oil–water contact. This should include cathodoluminescence petrography and analysis of fluid inclusions, which can provide information regarding the timing of cement development within the paragenetic sequence and information about the fluids present at the time of cement formation. Such details may indicate an overlap between the timing of cementation and oil emplacement that may shed light on their relationship, with important implications for identifying a suspected ROZ.
3. To provide conclusive evidence of an ROZ, further study is suggested, including petrophysical analysis to determine the water saturation profile, cased-hole pulsed-neutron logging in existing wells to determine oil saturation through the entire valley-fill Cypress Sandstone, and measurements of oil saturation from physical samples of fresh core.
4. Further research, including three-dimensional modeling and reservoir simulation, will be required to design and implement a CO_2-EOR and storage program. This research should include determination of the well pattern, injection, and conformance scenarios needed to make CO_2-EOR and storage economical and successful.

ACKNOWLEDGMENTS

This research was funded in part by the U.S. Department of Energy under contract number DE-FE0024431. Portions of the mapping were conducted with IHS Petra software as part of the University

Grants Program. Citation Oil and Gas Corp. is acknowledged for donating two whole cores to the ISGS collection for detailed study and permanent storage. CountryMark Energy Resources, LLC worked in partnership with the ISGS to collect new cores from their Long 2 well in Noble Field; specifically, Malcolm Booth, production engineer for CountryMark, coordinated the logistics of coring and logging the well. Podolsky Oil Company provided valuable insight into oil production characteristics of the Cypress Sandstone in Noble Field. Kalin Howell provided descriptions, photographs, and graphical logs of the available core. Zohreh Askari analyzed well cuttings and provided sample descriptions and graphical logs. Shane Butler and Eve Mason conducted the processing and analysis of samples for identification of bulk and clay mineralogy via X-ray diffraction. Leo Giannetta provided scanning electron photomicrographs and mineral identification. Jaclyn Daum described, photographed, and conducted point counts on petrographic thin sections. Scott Frailey and Mackenzie Smith provided the reservoir temperature analysis. Peter Berger collected oil and brine samples from Noble Field and provided the results of oil and brine analyses. The authors extend thanks to John Grube, Beverly Seyler, Hannes Leetaru, Kalin Howell, and Steve Whittaker for their contributions to and review of this manuscript. Daniel Klen and Susan Krusemark provided technical editing of this manuscript. Michael Knapp revised the figures and provided the final layout of the circular.

REFERENCES

Bell, A.H., 1938, Oil and gas development in Illinois in 1937: Illinois State Geological Survey, Illinois Petroleum 31, 20 p.

Bell, A.H., and G.V. Cohee, 1938, Recent petroleum development in Illinois: AAPG Bulletin, v. 22, no. 6, p. 649–658.

Blatchley, R.S., 1913, The oil fields of Crawford and Lawrence Counties: Illinois State Geological Survey, Bulletin 22, 442 p.

Blum, M., J. Martin, K. Milliken, and M. Garvin, 2013, Paleovalley systems: Insights from Quaternary analogs and experiments: Earth-Science Reviews, v. 116, p. 128–169.

Bristol, H.M., and R.H. Howard, 1971, Paleogeologic map of the Sub-Pennsylvanian Chesterian (Upper Mississippian) surface in the Illinois Basin: Illinois State Geological Survey, Circular 468, 14 p.

Cady, G.H., H.A. Lowenstam, H.L. Smith, M.W. Pullen, M.B. Rolley, and R. Siever, 1951, Subsurface geology and coal resources of the Pennsylvanian system in certain counties of the Illinois Basin: Illinois State Geological Survey, Report of Investigations 148, 151 p.

Chapman, J.J., 1953, Sand distribution in the Cypress Formation, Clay County and vicinity, Illinois: University of Illinois at Urbana-Champaign, 47 p.

Cole, R.D., and W.J. Nelson, 1995, Stratigraphic framework and environments of deposition of the Cypress Formation in the outcrop belt of Southern Illinois: Illinois State Geological Survey, Illinois Petroleum 149, 47 p.

Demir, I., 1995, Formation water chemistry and modeling of fluid–rock interaction for improved oil recovery in Aux Vases and Cypress Formations, Illinois Basin: Illinois State Geological Survey, Illinois Petroleum 148, 60 p.

Glass, H., and M. Killey, 1987, Principles and applications of clay mineral composition in Quaternary stratigraphy: Examples from Illinois, USA, *in* J.J.M. van der Meer, ed., Tills and glaciotectonics: Rotterdam, A.A. Balkema, p. 117–125.

Grigsby, N.P., and N.D. Webb, 2020, Assessing the Cypress Sandstone for carbon dioxide-enhanced oil recovery and carbon storage: Part II—Leveraging geologic characterization to develop a representative geocellular model for Noble Oil Field, western Richland County, Illinois: Illinois State Geological Survey, Circular 602, 19 p.

Grube, J.P., 1992, Reservoir characterization and improved oil recovery from multiple bar sandstones, Cypress Formation, Tamaroa and Tamaroa South Fields, Perry County, Illinois: Illinois State Geological Survey, Illinois Petroleum 138, 49 p.

Grube, J.P., and W.T. Frankie, 1999, Reservoir characterization and its application to improved oil recovery from the Cypress Formation (Mississippian) at Richview Field, Washington County, Illinois: Illinois State Geological Survey, Illinois Petroleum 155, 39 p.

Heasley, E.C., R.H. Worden, and J.P. Hendry, 2000, Cement distribution in a carbonate reservoir: Recognition of a palaeo oil–water contact and its relationship to reservoir quality in the Humbly Grove field, onshore, UK: Marine and Petroleum Geology, v. 17, no. 5, p. 639–654.

Holbrook, J.M., 1996, Complex fluvial response to low gradients at maximum regression: A genetic link between smooth sequence-boundary morphology and architecture of overlying sheet sandstone: Journal of Sedimentary Research, v. 66, no. 4, p. 713–722.

Holbrook, J.M., R.W. Scott, and F.E. Oboh-Ikuenobe, 2006, Base-level buffers and buttresses: A model for upstream versus downstream control on fluvial geometry and architecture within sequences: Journal of Sedimentary Research, v. 76, no. 1, p. 162–174.

Huff, B.G., and B. Seyler, 2010, Oil and gas geology, *in* D.R. Kolata and C.K. Nimz, eds., Geology of Illinois: Champaign, Illinois State Geological Survey, p. 283–298.

Hughes, R.E., D.M. Moore, and H.D. Glass, 1994, Qualitative and quantitative analysis of clay minerals in soils, *in* J.E. Amonette, L.W. Zelazny, and R.J. Luxmoore, eds., Quantitative Methods in Soil Mineralogy: Madison, Wisconsin, Soil Science Society of America, p. 330–359.

Hughes, R., and R. Warren, 1989, Evaluation of the economic usefulness of earth materials by X-ray diffraction, *in* R.E. Hughes, and J.C. Bradbury, eds., Proceedings of the 23rd Forum on the Geology of Industrial Minerals: Illinois State Geological Survey, Illinois Minerals Notes 102, p. 47–57.

Jacobson, R.J., 1985, Stratigraphic correlations of the Seelyville, Dekoven and Davis Coal Members—Spoon Formation (Illinois), Staunton Formation (Indiana), or beds—Carbondale Formation (Western Kentucky): University of Illinois at Urbana-Champaign, master's thesis, 79 p.

Jensenius, J., and R.C. Burruss, 1990, Hydrocarbon–water interactions during brine migration: Evidence from hydrocarbon inclusions in calcite cements from Danish North Sea oil fields: Geochimica et Cosmochimica Acta, v. 54, no. 3, p. 705–713.

Lee, L.K., 1939, Geology of basin fields in southeastern Illinois: AAPG Bulletin, v. 23, no. 10, p. 1493–1506.

Leetaru, H.E., 2000, Sequence stratigraphy of the Aux Vases Sandstone: A major oil producer in the Illinois Basin: AAPG Bulletin, v. 84, no. 3, p. 399–422.

Leetaru, H.E., K. Mize, and J.S. Cokinos, 2005, The Benoist (Yankeetown) Sandstone play in the Illinois Basin: Illinois State Geological Survey, Circular 568, 46 p.

Lewan, M.D., M.E. Henry, D.K. Higley, and J.K. Pitman, 2002, Material-balance assessment of the New Albany–Chesterian petroleum system of the Illinois Basin: AAPG Bulletin, v. 86, no. 5, p. 745–777.

Mack, G.H., W.C. James, and H.C. Monger, 1993, Classification of paleosols: Geological Society of America Bulletin, v. 105, p. 129–136.

Maples, C., and J. Waters, 1987, Redefinition of the Meramecian/Chesterian boundary (Mississippian): Geology, v. 15, p. 647–651.

Meents, W.F., A.H. Bell, O.W. Rees, and W.G. Tilbury, 1952, Illinois oil-field brines: Their geologic occurrence and chemical composition: Illinois State Geological Survey, Illinois Petroleum 66, 38 p.

Melzer, L.S., G.J. Koperna, and V.A. Kuuskraa, 2006, The origin and resource potential of residual oil zones, *in* Proceedings—SPE Annual Technical Conference and Exhibition: Richardson, Texas, Society of Petroleum Engineers, p. 3507–3511.

Midwest Geological Sequestration Consortium (MGSC), 2005, An assessment of geological carbon sequestration options in the Illinois Basin: Illinois State Geological Survey, technical report for U.S. Department of Energy contract DE-FC26-03NT41994 (issued December 31, 2005), 478 p.

Morad, S., K. Al-Ramadan, J.M. Ketzer, and L.F. De Ros, 2010, The impact of diagenesis on the heterogeneity of sandstone reservoirs: A review of the role of depositional facies and sequence stratigraphy: AAPG Bulletin, v. 94, no. 8, p. 1267–1309.

Nelson, W.J., 1995, Structural features in Illinois: Illinois State Geological Survey, Bulletin 100, 144 p.

Nelson, W.J., L.B. Smith, J.D. Treworgy, L.C. Furer, and B.D. Keith, 2002, Sequence stratigraphy of the Lower Chesterian (Mississippian) strata of the Illinois Basin: Illinois State Geological Survey, Bulletin 107, 70 p.

Phillips, S.H., 1954, Subsurface studies of the Cypress Formation, Richland County Area, Illinois: University of Illinois at Urbana-Champaign, 18 p.

Piersol, R.J., L.E. Workman, and M.C. Watson, 1940, Porosity, total liquid saturation, and permeability of Illinois oil sands: Illinois State Geological Survey, Report of Investigations 67, 72 p.

Pitman, J.K., M. Henry, and B. Seyler, 1998, Reservoir quality and diagenetic evolution of Upper Mississippian rocks in the Illinois Basin: Influence of a regional hydrothermal fluid-flow event during late diagenesis: U.S. Geological Survey, Professional Paper 1597, 25 p.

Potter, P.E., 1962, Late Mississippian sandstones of Illinois: Illinois State Geological Survey, Circular 340, 36 p.

Schmidt, V., and D.A. McDonald, 1979, Texture and recognition of secondary porosity in sandstones, *in* P.A. Scholle, and P.R. Schluger, eds., Aspects of diagenesis: Tulsa, Oklahoma, Society of Economic Paleontologists and Mineralogists, p. 209–225.

Seyler, B., 1986, Aux Vases and Ste. Genevieve Formations: A core workshop and field trip guidebook: Carbondale, Southern Illinois University, Petroleum Technology Transfer Council workshop guidebook , 67 p.

Shanley, K.W., and P.J. McCabe, 1994, Perspectives on the sequence stratigraphy of continental strata: AAPG Bulletin, v. 78, no. 4, p. 544–568.

Wasson, T., 1938, Recent oil discoveries in southeastern Illinois: AAPG Bulletin, v. 22, no. 1, p. 71–78.

Watson, R.S., N.H. Trewin, and A.E. Fallick, 1995, The formation of carbonate cements in the Forth and Balmoral Fields, northern North Sea: A case for biodegradation, carbonate cementation and oil leakage during early burial: Geological Society, London, Special Publications, v. 94, no. 1, p. 177–200.

Whitaker, S.T., and A.K. Finley, 1992, Reservoir heterogeneity and potential for improved oil recovery within the Cypress Formation at Bartelso Field, Clinton County, Illinois: Illinois State Geological Survey, Illinois Petroleum 137, 40 p.

Willman, H.B., E. Atherton, T.C. Buschbach, C. Collinson, J.C. Frye, M.E. Hopkins, J.A. Lineback, and J.A. Simon, 1975, Handbook of Illinois stratigraphy: Illinois State Geological Survey, Bulletin 95, 261 p.

Witherspoon, P.A., and E.G. Jackson, 1955, Summary of water flood operations in Illinois oil pools during 1954: Illinois State Geological Survey, Illinois Petroleum 73 , 63 p.

Workman, L.E., and A.H. Bell, 1937, Correlation problems in the new Illinois Basin fields: Illinois State Geological Survey, Circular 22, 3 p.

Wright, V.P., and S.B. Marriott, 1993, The sequence stratigraphy of fluvial depostional systems: The role of floodplain sediment storage: Sedimentary Geology, v. 86, no. 3–4, p. 203–210.

Xu, J., and B.G. Huff, 1995, The Cypress Sandstone (Mississippian) reservoir and its recovery potential at Xenia East Oil Field, Clay County, Illinois: Illinois State Geological Survey, Illinois Petroleum 147, 47 p.

APPENDIX A—CORE DESCRIPTIONS

Elysium Energy, L.L.C.
NW NE Sec. 4, T3N, R9E, Lat. 38.727132N, Long. 88.214030W
Richland County, Illinois
Elevation: 473 Kelly Bushing, Landowner: Coen, John O., Hole No. 120, API 121592608300
Described by Kalin Howell and Nathan Webb, Date: June 24, 2015

Description	Thickness, ft (m)	Top, ft (m)	Bottom, ft (m)
Sandstone: light pale brown, oil stained, very fine grained, ripple cross laminated with rare planar laminations in bottom half, ripples are defined by clay laminations that are commonly on foresets, calcite and iron oxide mottling throughout, calcite mottles are larger than iron oxide mottles, ripples are not well defined but abundant—may display bifurcations in places, ripples may be bidirectional?, bottom ~1.3 ft (0.4 m) resembles subtle flaser bedding with ripples, gradational lower contact	9.7 ft (3.0 m)	2,583.0 ft (787.3 m)	2,592.7 ft (790.3 m)
Sandstone: whitish gray, very fine grained, wavy flaser bedded to ripple cross laminated, mainly wavy flaser bedded with high sand-to-shale ratio throughout, very slightly calcareous throughout—slightly more at ~2,596.3 ft (791.4 m), iron oxide mottling (limonite?) throughout, dark gray sulfurous rippled to wavy heterolithic sections at the base of the section, 2,596.0 (791.3 m), and 2,595.3 ft (791.0 m), rare rip-up chips (~0.3 in. [0.8 mm]) at base, sharp lower contact	4.3 ft (1.3 m)	2,592.7 ft (790.3 m)	2,597.0 ft (791.6 m)
Sandstone: brown, oil stained, fine to very fine grained—fining upward, moderately angled cross bedded to ripple cross bedded, slight calcite mottling throughout (mottles are very reactive), subtle iron oxide mottling (limonite?) throughout, iron oxide mottles are typically smaller than calcite mottles, heavily unidirectional rippled section (~2 in. [5.1 cm]) at base showing bifurcations, cross-bed sets are ~6 in. (15.2 cm), wavy-bedded sections at ~2,597.7 and 2,598.7 ft (~791.8 and 792.1 m) with sharp lower and upper contacts—sandy parts are very fine grained and whitish gray, shows few unidirectional? ripples, above lower wavy-bedded section (2,598.7 ft [792.1 m]) is an oil-stained section with ripple cross laminations superimposed on what appear to be cross beds, gradational lower contact	1.8 ft (0.5 m)	2,597.0 ft (791.6 m)	2,598.8 ft (792.1 m)
Sandstone: brown, oil stained, fine grained, relatively steep angle cross-bedded (angle of repose ~20° to 30°) planar laminations increase in abundance upward, intense calcite mottling in bottom ~2.5 ft (0.8 m) where bedding planes are less apparent, slight calcareous mottling throughout the rest of the section (calcite mottles are very reactive), cross-bed sets are typically ~6 in. (15.2 cm), bedding surfaces are condensed at truncation surfaces, clay laminations on cross-bed foresets are moderately dispersed throughout and appear to be rhythmic	12.5 ft (3.81 m)	2,598.8 ft (792.1 m)	2,611.3 ft (795.9 m)

Elysium Energy L.L.C.
NE NW Sec. 4, T3N, R9E, Lat. 38.727821N, Long. 88.217885W
Richland County, Illinois
Elevation: 473 Kelly Bushing, Landowner: C.T. Montgomery, Hole No. B-34, API 121592606400
Described by Kalin Howell and Nathan Webb, Date: June 24, 2015

Description	Thickness, ft (m)	Top, ft (m)	Bottom, ft (m)
Sandstone: light brown gray, very fine grained, ripple cross laminated but becoming less apparent upward, noncalcareous, bedding in top ~1 ft (0.3 m) is slightly distorted, iron oxide mottling throughout (limonite?), few fine-grained heavy mineral flecks throughout (producing mottling?), at 2,577.4 to 2,577.6 ft (785.6 to 785.7 m) is a whitish gray section with wavy flaser bedding and some ripple cross laminations showing subtle bidirectionality, sharp lower contact	2.1 ft (0.6 m)	2,576.0 ft (785.2 m)	2,578.1 ft (785.8 m)
Heterolithic strata: generally transitions upward from lenticular to condensed wavy to wavy flaser bedding 2,580.8 to 2,578.1 ft (786.6 to 785.8 m) is wavy flaser bedded with few bifurcations, overall sandy parts are very fine grained, overall orangish white in appearance (iron oxide staining?), iron oxide mottled at ~2,579.2 ft (786.1 m), some ripple cross laminations throughout—subtle bidirectionality, rare horizontal burrows, top ~2 in. (5.1 cm) is wavy lenticular bedded with few ripple cross laminations and horizontal burrows—similar to bottom of section, gradational lower contact 2,580.8 to 2,583.3 ft (786.6 to 787.4 m) is primarily yellow in appearance (limonite staining?) and wavy bedded with a few sections of highly condensed wavy bedding (1 to 2 in. [2.5 to 5.1 cm] thick), ~2,581.3 and 2,582.8 ft (~786.8 and 787.2 m) are moderately condensed wavy-bedded sections, noncalcareous, subtle bidirectionality throughout, minor load casts at section base, contains rare horizontal to vertical (more rare) burrows, at ~2,581.8 ft (786.9 m) is a ~2 in. (5.1 cm) sigmoidal cross-bed set with shale drapes defining bed surfaces, ~2 in. (5.1 cm) below this is a very yellow section (~1.5 in. [3.8 cm]) that is likely limonite abundant, 2,582.5 ft (787.1 m) contains ~2 in. (5.1 cm) section with abundant iron oxide mottling, in general iron oxide mottling is constrained to sections that are relatively free of shaley lenses or drapes, gradational lower contact 2,583.3 to 2,584.7 ft (787.4 to 787.8 m) is lenticular bedded, sand is very fine grained and whitish gray, noncalcareous, horizontal burrows at 2,883.8 ft (879 m), shaley parts are very fine grained micaceous and gray, ripple cross laminations within lenses show subtle bidirectionality—specifically at the base of section, sharp lower contact	6.0 ft (1.8 m)	2,578.1 ft (785.8 m)	2,584.7 ft (787.8 m)
Sandstone: brown, oil stained, very fine grained, unidirectional ripple cross laminated, noncalcareous, tabular rip-up chip at base (~2,589 ft [789.1 m]) ranging from a few millimeters to 1 in. (2.5 cm), ~1 in. (3 cm) gray shaley parting at 2,588.6 ft (789.0 m), some iron oxide mottling (limonite?) at ~2,588.5 ft (789.0 m), distorted bedding at 2,588 ft (788.8 m), some planar bedding approximately 2,587.3 (788.6 m), upper ~5 in. (12.7 cm) contains iron oxide mottling and pyrite, gradational lower contact	4.1 ft (1.2 m)	2,584.7 ft (787.8 m)	2,588.5 ft (789.0 m)
Sandstone: brown, oil stained, fine grained, planar to moderately angled cross bedded with moderate clay drapes defining foresets, becomes very slightly calcareous upward, some calcite mottling throughout, truncation surfaces are typically 2 to 4 in. (5.1 to 10.2 cm) apart, bedding planes are typically more condensed at truncation surfaces, distorted bedding at ~2,599.3 ft (792.3 m), soft sediment deformation at ~2,601.5 ft (792.9 m), top ~5 in. (12.7 cm) contains heavier iron oxide mottling and top ~1 in. (2.5 cm; depth, 2,588.8 ft [789.1 m]) is sulfurous and swelling/disintegrating.	13.2 ft (4.0 m)	2,588.8 ft (789.1 m)	2,602.0 ft (793.1 m)

APPENDIX B—X-RAY DIFFRACTION MINERALOGY RESULTS

Table B1 John O. Coen 120 well (API 121592608300)[1]

	Clay minerals relative to each other, %					Bulk mineral data, %					
			If either mineral is indistinguishable	If kaolinite is present	If chlorite is present						
Depth, ft	Illite/smectite	Illite	Kaolinite + chlorite	Kaolinite	Chlorite	Clay	Quartz	k-Feldspar	p-Feldspar	Calcite	Pyrite/ marcasite
2,583.5	1	13	86	48	38	2	89	1	7	1	0
2,584.5	4	11	85	64	21	6	81	4	9	0	0
2,585.5	5	8	86	55	31	3	86	3	7	0	0
2,586.5	0	9	91	68	23	3	85	3	6	1	0
2,587.5	1	12	87	62	25	6	83	3	7	0	0
2,588.5	1	10	89	68	21	3	85	4	8	0	0
2,589.5	2	16	82	60	22	5	82	3	9	0	0
2,590.5	1	11	88	65	23	4	91	3	2	1	0
2,592.5	0	16	84	60	24	3	85	3	8	1	0
2,593.5	6	10	84	64	20	4	84	3	8	1	0
2,594.5	4	18	78	47	31	12	74	4	9	0	0
2,595.5	4	14	82	64	18	3	85	2	8	0	1
2,596.5	4	13	84	59	25	5	82	3	8	0	0
2,597.5	4	6	90	85	5	9	76	2	4	0	7
2,598.5	1	5	94	86	8	2	87	3	5	2	1
2,599.5	0	9	90	81	9	5	84	2	6	1	1
2,600.5	6	2	92	86	6	3	88	2	5	1	1
2,601.5	4	12	84	77	7	4	87	2	5	1	0
2,602.5	0	45	55	39	16	2	91	1	3	2	1
2,603.5	1	5	94	86	7	1	94	1	3	0	0
2,604.5	2	4	94	89	5	1	94	0	4	0	1
2,605.5	1	2	97	92	5	1	95	1	3	0	0
2,606.5	1	7	93	81	11	2	91	1	5	0	0
2,607.5	3	2	95	90	5	1	94	1	3	0	1
2,608.5	2	3	95	87	8	1	94	1	3	0	0
2,609.5	9	8	83	60	23	1	95	1	3	0	0
2,610.5	11	1	88	75	12	2	86	2	4	6	0

[1]6A708/4658 final results. Processed by Eve Mason and Shane Butler on 5/12/2016.

Table B2 C.T. Montgomery B-34 well (API 121592606400)[1]

	Clay minerals relative to each other, %					Bulk mineral data, %							
			If either mineral is indistinguishable	If kaolinite is present	If chlorite is present								
Depth, ft	Illite/ smectite	Illite	Kaolinite + chlorite	Kaolinite	Chlorite	Clay	Quartz	k-Feldspar	p-Feldspar	Calcite	Dolomite	Siderite	Pyrite/ marcasite
2,576.5	2	5	93	68	25	2	90	1	5	1	0	1	0
2,577.5	5	16	79	45	34	18	22	13	35	2	2	6	3
2,578.5	17	18	66	32	34	14	65	5	9	1	1	3	1
2,579.5	7	16	78	29	49	7	79	2	9	0	1	2	1
2,580.5	7	14	78	28	50	12	73	2	11	0	1	2	0
2,581.5	17	27	55	27	28	13	70	4	8	0	1	3	1
2,582.0	8	25	67	55	12	2	84	2	6	0	0	2	4
2,582.5	13	25	62	40	22	14	68	4	9	1	1	3	1
2,583.5	21	20	59	44	15	13	69	4	9	1	1	2	1
2,584.5	13	26	62	48	14	16	63	5	10	1	1	4	0
2,585.5	6	10	84	67	17	3	85	3	6	1	0	1	0
2,586.5	7	10	83	59	24	2	89	2	4	0	0	2	1
2,587.5	7	12	81	61	20	3	86	2	7	0	0	1	1
2,588.5	4	7	89	83	7	6	86	1	4	2	0	1	0
2,589.5	2	5	93	86	8	4	86	1	3	2	0	1	2
2,590.5	0	17	83	58	25	2	91	1	2	1	0	1	1
2,591.5	0	8	92	80	12	2	93	1	3	0	0	1	0
2,592.5	3	32	65	47	18	2	91	2	3	1	0	1	1
2,593.5	1	43	55	43	12	1	94	1	2	0	0	1	0
2,594.5	0	2	98	90	7	1	93	1	2	1	0	1	1
2,595.5	3	8	89	75	14	1	92	2	3	0	0	1	1
2,596.5	2	2	95	92	3	2	92	1	2	1	0	0	1
2,597.5	0	4	96	87	9	1	95	1	2	0	0	0	0
2,598.5	1	3	97	90	6	1	95	1	2	0	0	0	0
2,599.5	3	2	95	90	5	1	96	1	2	0	0	0	0
2,600.5	1	5	94	85	9	1	95	1	2	0	0	0	0
2,601.5	0	8	93	79	14	1	92	2	3	0	0	0	0

[1]6A707/4657 final results. Processed by Eve Mason, Samuel Noethe, and Shane Butler on 10/23/2015.

APPENDIX C—RESERVOIR TEMPERATURE CALCULATIONS

Reservoir temperature data were downloaded from the National Geothermal Data System (http://azgs.arizona.edu/energy/national-geothermal-data-system), a database of bottomhole temperatures digitized from geophysical logs. Bottomhole temperatures are recorded for 84 wells within the Noble Field. Most of these wells were drilled into the St. Louis or Salem Limestone (~3,200 or 3,700 ft [~975.4 or 1,127.8 m], respectively). An average temperature gradient was calculated for each of the wells from a datum depth of 100 ft (30.5 m), below the influence of seasonal temperature fluctuations, at a temperature of 62 °F (16.7 °C). The average depth to the center of the Cypress Sandstone is 2,675 ft (815.3 m), based on 335 wells in Noble Field for which the top and bottom of the valley-fill Cypress Sandstone were identified. Temperatures were calculated for the Cypress Sandstone in each of the 84 wells by using the calculated geothermal gradient and the average depth to the middle of the valley-fill Cypress Sandstone of 2,675 ft (815.3 m). The resulting temperature data were grouped by season and plotted on histograms to identify outliers in the data (Figures C1–C7). The mode of the data across all seasons (Figure C1) indicated a temperature of 89 °F (31.7 °C) for the Cypress Sandstone, in agreement with the temperature expected based on the standard geothermal gradient for the Illinois Basin (at 100 ft, 62 °F + 1 °F/100 ft depth = 88 °F at 2,675 ft [or at 30.5 m, 16.7 °C + 0.56 °C/30.5 m depth = 31.1 °C at 815.3 m]).

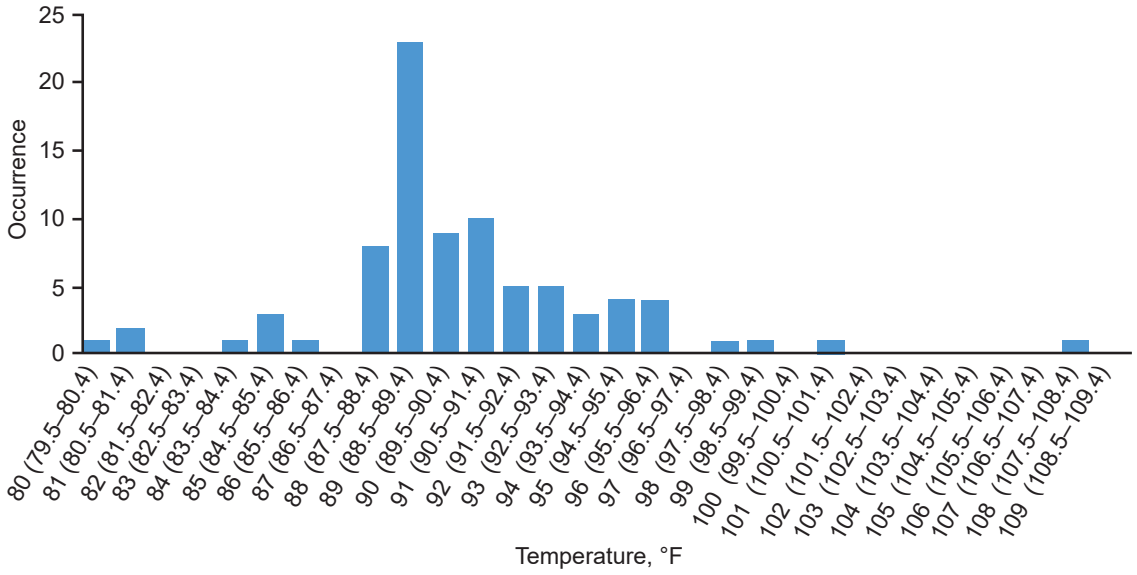

Figure C1 Reservoir temperatures for the Cypress Sandstone at a depth of 2,675 ft (815.3 m), calculated by using all data across all seasons.

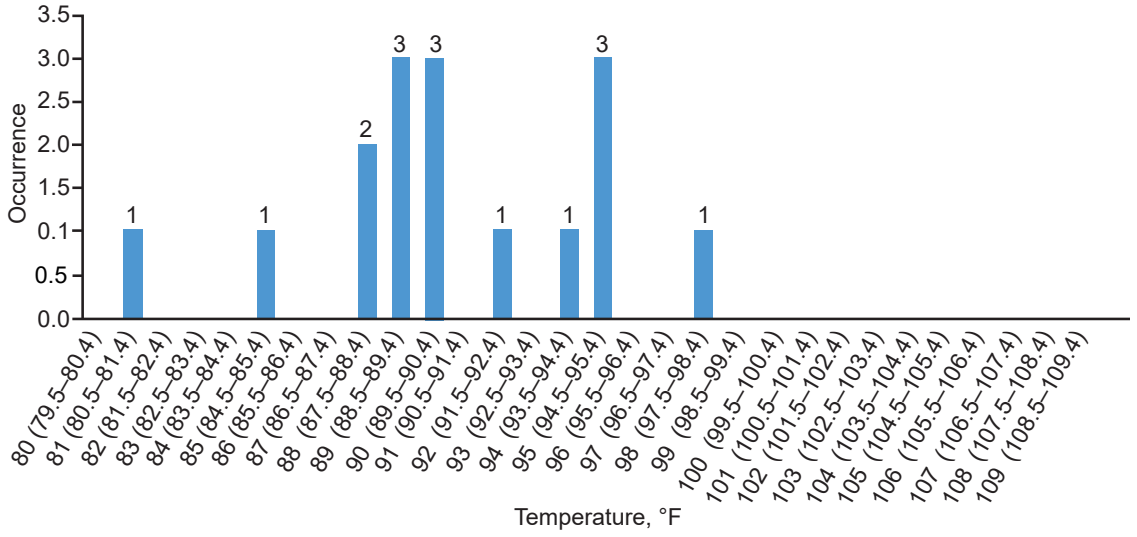

Figure C2 Reservoir temperatures for the Cypress Sandstone at a depth of 2,675 ft (815.3 m), calculated by using data from wells drilled during the fall season.

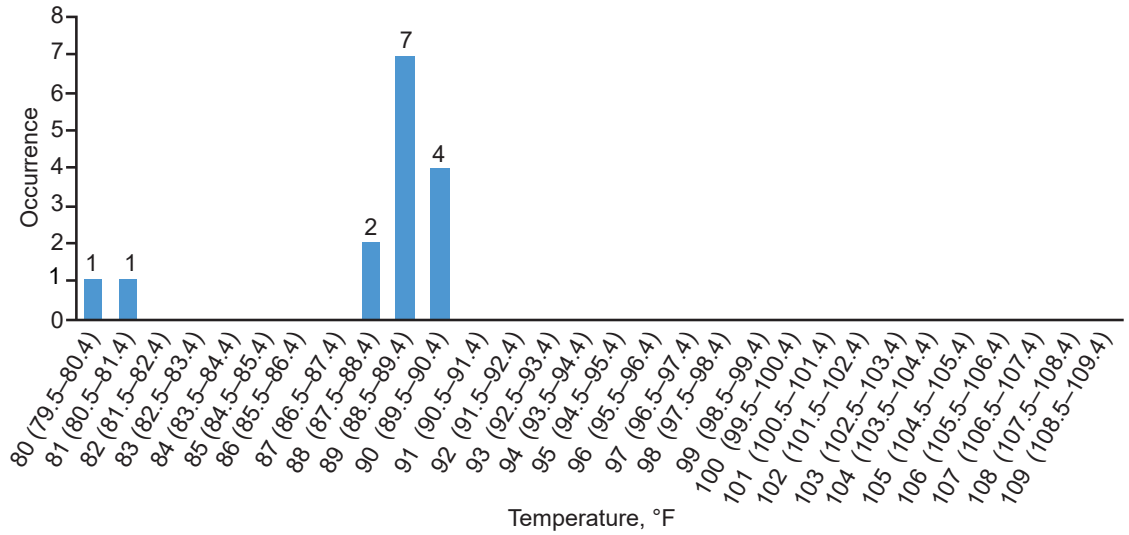

Figure C3 Reservoir temperatures for the Cypress Sandstone at a depth of 2,675 ft (815.3 m), calculated by using data from wells drilled during the winter season.

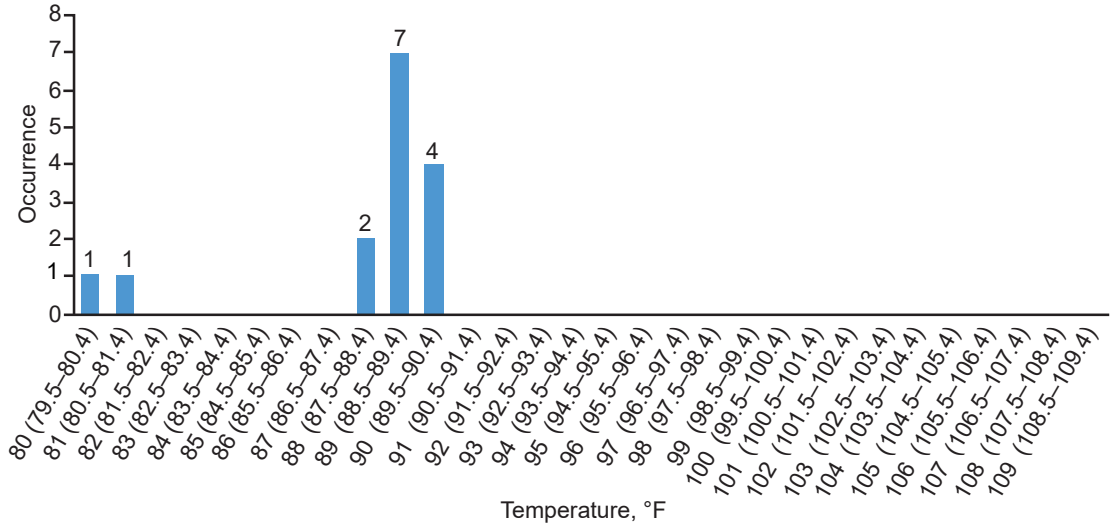

Figure C4 Reservoir temperatures for the Cypress Sandstone at a depth of 2,675 ft (815.3 m), calculated by using data from wells drilled during the spring season.

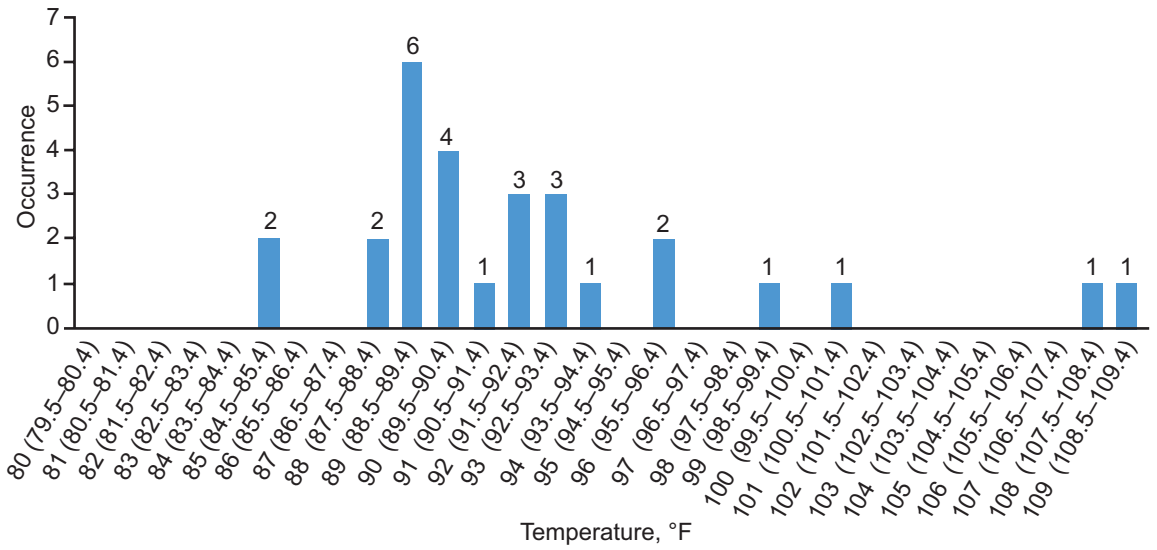

Figure C5 Reservoir temperatures for the Cypress Sandstone at a depth of 2,675 ft (815.3 m), calculated by using data from wells drilled during the summer season.

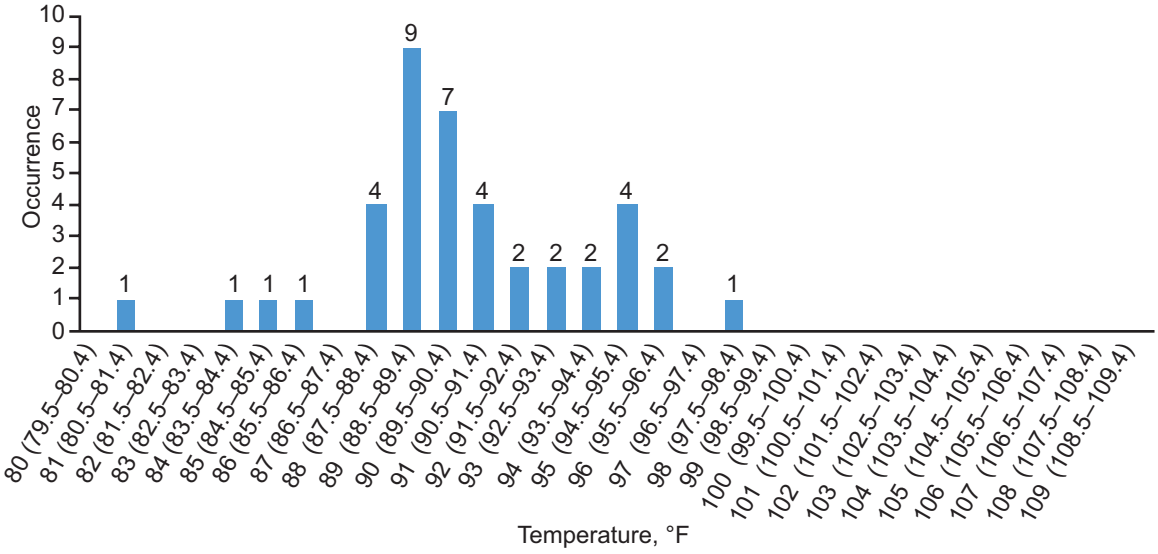

Figure C6 Reservoir temperatures for the Cypress Sandstone at a depth of 2,675 ft (815.3 m), calculated by using data from wells drilled during the fall and spring seasons.

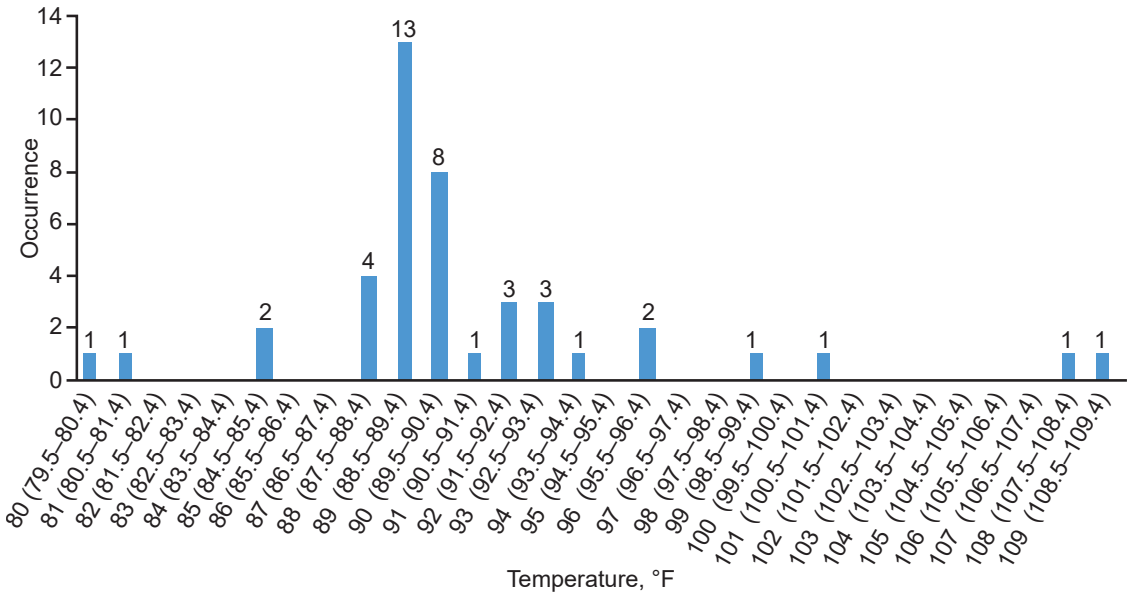

Figure C7 Reservoir temperatures for the Cypress Sandstone at a depth of 2,675 ft (815.3 m), calculated by using data from wells drilled during the winter and summer seasons.

APPENDIX D—RESERVOIR FLUID PROPERTIES

Table D1 Anion analysis conducted at the ISGS for Cypress brine samples from the John O. Coen 92 well (API 121592607500, Sec. 4, T3N, R9E) showing a Cl^- concentration of 58,744.6 mg/L, a Br^- concentration of 460.2 mg/L, and a SO_4^- concentration of 1,115.31 mg/L[1]

	Sample name										
Sample type	Al	As	B	Ba	Be	Ca	Cd	Co	Cr	Cu	
MDL	0.93‡	1.1‡	0.58‡	0.021‡	0.0055‡	0.29‡	0.12‡	0.13‡	0.058‡	0.040‡	
Cypress brine	<0.93‡	<1.1‡	6.91	0.208	<0.0055‡	2,730	<0.12‡	<0.13‡	<0.058‡	<0.040‡	
	Fe	K	Li	Mg	Mn	Mo	Na	Ni	P	Pb	
MDL	0.24‡	0.40‡	2.8‡	0.27‡	0.015‡	0.22‡	0.26‡	0.43‡	0.73‡	0.41‡	
Cypress brine	<0.24‡	214	11.1	1,307	0.198	<0.22‡	32,516	<0.43‡	<0.73‡	<0.41‡	
	S	Sb	Se	Si	Sn	Sr	Ti	Tl	V	Zn	Zn
MDL	2.2‡	1.5‡	1.3‡	1.7‡	0.86‡	0.0037‡	0.0056‡	0.43‡	0.47‡	0.097‡	0.097‡
Cypress brine	919	<1.5‡	<1.3‡	5.3	<0.86‡	81.8	<0.0056‡	0.67	<0.47‡	<0.097‡	<0.097‡

[1]Inductively coupled plasma analyses by the Illinois State Water Survey. Samples received 10/20/2015. Samples analyzed 10/23/2015. Report date 11/06/2015. All concentrations are in milligrams per liter (mg/L). Cation analyses for the same sample are listed in the table. A dagger (‡) indicates the method detection limit (MDL) was elevated and was estimated because of a difficult matrix.